Reformulation of the Hermitean 1-Matrix Model as an Effective Field Theory

Dissertation
zur
Erlangung des Doktorgrades (Dr. rer. nat.)
der
Mathematisch-Naturwissenschaftlichen Fakultät
der
Rheinischen Friedrich-Wilhelms-Universität Bonn

vorgelegt von

Alexander Klitz

aus
Lünen

Bonn 2009

Diese Dissertation ist auf dem Hochschulschriftenserver der ULB Bonn unter
`http://hss.ulb.uni-bonn.de/diss_online` elektronisch publiziert.

Erscheinungsjahr: 2009

Angefertigt mit Genehmigung der Mathematisch-Naturwissenschaftlichen Fakultät
der Rheinischen Friedrich-Wilhelms-Universität Bonn

Referent: Prof. Dr. Rainald Flume
Korreferent: Prof. Dr. Albrecht Klemm
Tag der Promotion: 20. Juli 2009

Abstract

The formal Hermitean 1-matrix model is shown to be equivalent to an effective field theory. The correlation functions and the free energy of the matrix model correspond directly to the correlation functions and the free energy of the effective field theory. The loop equation of the field theory coupling constants is stated. Despite its length, this loop equation is simpler than the loop equations in the matrix model formalism itself since it does not contain operator inversions in any sense, but consists instead only of derivative operators and simple projection operators. Therefore the solution of the loop equation could be given for an arbitrary number of cuts up to the fifth order in the topological expansion explicitly. Two different methods of obtaining the contributions to the free energy of the higher orders are given, one depending on an operator H and one not depending on it.

Für Margrit

Danksagung

Ich bedanke mich bei Prof. R. Flume für die Betreuung meiner Dissertation. Des weiteren danke ich Prof. J. B. Zuber für seinen Hinweis auf die Formel zur Berechnung der Anzahl der Summanden in der Lagrangefunktion (Anhang A). Für das Korrekturlesen der Arbeit bedanke ich mich bei Dr. K. E. Williams.

Contents

Chapter 1

Introduction

1.1 Hermitean matrix model

Matrix models were introduced in physics in 1951 by Wigner [1]. Many narrow resonances were observed in the scattering of slow neutrons by heavy nuclei. It was a hopeless task to explain each excited state of the nucleus individually. Wigner proposed a theory which described the statistical behaviour of these levels by a random matrix model. For an arbitrary specific energy level the probability of finding the neighbouring level at a given energy distance is described by the spacing distribution. For a random matrix model, the spacing distribution is the probability of finding an arbitrary eigenvalue at a given distance from the neighbouring eigenvalue. Wigner proposed the equality of the slow neutron energy spacing distribution and the eigenvalue spacing distribution of the matrix model. Since the quality of the experimental distribution could only be improved by gathering more data, i.e. measuring more resonances, it took until 1982 to gather enough data to conclusively show that both distributions agree. This approach was then successfully applied to the spacings of atomic and molecular energy levels.
Other applications were found in chaotic systems—One example of this kind is the hydrogen atom in a strong magnetic field, a second is the modelling of the game 'billiards'. The distribution of the zeros of the Riemann zeta function can be approximated to great accuracy with a random matrix model. Matrix models are applied to topological string theory, to the chiral phase transition in QCD, to disordered mesoscopic systems and to counting knots and links.
This list is far from being complete.
The loop equations for matrix models were given in 1983 [36]. The Her-

mitean multi-point functions for genus zero and a method to derive higher order contributions were given in [37], [38], [39]. For several cuts the solution was given in 1996 by Akemann [5]. For matrix models with fixed filling fractions, substantial progress was made in 2004 by Eynard [6]. By utilising loop equations of higher degree, it was possible to write a recursion formula for the correlation functions. Since this formula contains one residue, a single term of one specific correlation function is given by a system of nested residues. A diagrammatic representation for these terms was developed in [6] and subsequent work [7], [13]. These diagrams were initially claimed to be Feynman diagrams [7]. Later this assertion was revoked [13], [14]. To get a good overview see [34], [24] or [35].

1.2 Motivation for the reformulation of the Hermitean matrix model as an effective field theory

The contributions to the correlation functions and free energies of a well-known matrix model, the Hermitean 1-matrix model, appear to be well ordered in the field theory approach. It is valid for all numbers of cuts. The field theory scheme mainly applies to the formal model with fixed filling fractions, but for the one cut case no filling fraction has to be specified and hence the model is identical with the 'energy-minimized' model. This model has been known for a long time.
The correlation functions and the free energy appear in the field theory together with all their higher genus corrections in a consistent, new and beautiful way. There have been several incentives to construct a field theory underlying Eynard's formalism. The first of these comes from Kostov's (unfinished) program [40] to fit matrix models into 2-dimensional conformal field theories. An effective Lagrangian sets a benchmark of what has to be achieved in such an undertaking. Another motivation is provided by the manifold connections of matrix models with string theories, in particular topological string theories. A specially neat link between the two fields has been discovered by Dijkgraaf and Vafa [9], who observed that recursion relations derived in matrix models via loop equations are identical with certain Ward identities of a two dimensional field theory related to Kodaira-Spencer theory of Calabi-Yau threefolds. Our construction will make clear that an effective Lagrangian is hiding behind the structure of the recursion relations.

In addition to the calculation of the correlators themselves, one can use the

approach to deal with topological string theory [27], [28], [29] and [9].
Since the matrix model is applied to the enumeration of discrete surfaces ([21], [2], [14]) it becomes possible to apply the field theory version to the same problem. The calculation of Weil-Petersson volumes [22] and [30] could be repeated in terms of the field theory. Critical phenomena related to matrix models ([15], [16], [17], [18]) can be explored by the renormalization group of the field theory.

1.3 Outline

Starting from Eynards work [6] the three point function for genus zero is derived.
Higher loop multipoint functions are not, in contrast to [6], calculated by more complex loop equations which contain smaller multipoint functions of the same or smaller genus. Instead the new function is calculated from the action of the loop operator to the multipoint function of the same genus with one point less. Surprisingly, it turns out that the structure of the new terms in the four point function is very similar to the structure of the contributions to the three point function. By defining propagators $B_i^f(p)$ and $B_{i,j}^{f,g}$, as well as vertex factors $y_{f,i}$ with $f, g = 0, 1, 2$, all terms of the three point function and the four point function are covered. For the higher multipoint functions the generalization to $f, g = 0, 1, 2, \ldots$, is sufficient, i.e. the loop operator, acting on these quantities, produces again only such quantities. In chapter 4 the recursion step to the first correction in $1/N^2$ is done with the recursion equation of [6] which is determined by the loop equations. Fortunately, the correlators emerging from the application of the loop equation can still be expressed in the quanatities $B_i^f(p)$, $B_{i,j}^{f,g}$ and $y_{f,i}$.
For the three point function a Lagrangian is found which leads to the same three point function as the matrix model. The loop operator is then applied to the three point function to obtain the four point function. The field theory tailored to describe the three point function is compared with the four point function of the matrix model. All contributions respective Feynman diagrams of the field theory appear with the correct weight but, in addition to these contributions, the matrix model four point function contains more diagrams. These additional diagrams correspond in a field theory to four point interactions. In an effective ansatz these additional interactions are inscribed into the Lagrangian. By this, the Lagrangian already describes two correlation functions correctly. Using the recursion formula from the loop equation, the one point function is determined in first order approximation in $1/N^2$. Again, the matrix model correlator contains more diagrams than predicted by the

Lagrangian $\mathcal{L}_3^{(0)} + \mathcal{L}_4^{(0)}$. The Lagrangian is enhanced by a contribution $\mathcal{L}_1^{(1)}$ in such a way that the correlators coincide. The enlargement of the Lagrangian can be generalized. The hypothesis that the Lagrangian constructed in this way describes all matrix model correlators in any order in $1/N^2$ correctly, suggests itself. This assertion is proven by induction on the number of points of the multipoint functions in chapter 8 and by induction on the genus in chapter 9.

1.4 List of preprints and publications

1. R. Flume, J. Grossehelweg, A. Klitz, *A Lagrangean formalism for Hermitean matrix models,* Nucl. Phys. B812 (2009) 322 (doi:10.1016/j.nuclphysb.2008.10.008), arXiv:0805.3078 [hep-th]

2. R. Flume, A. Klitz, *A new type of critical behaviour in random matrix models,* J. Stat. Mech. 2008: N10001 (2008) (doi:10.1088/1742-5468/2008/10/N10001), arXiv:0901.2424 [math-ph]

3. A. Klitz, *Proof of the Lagrangean formalism of Hermitean 1-matrix models to all orders,* Preprint Bonn-TH-09-02, arXiv:0904.0753 [math-ph]

Chapter 2

The Hermitean 1-matrix model

2.1 Definitions

The partition function $Z_N(t)$ and the free energy $\mathcal{F}$ of the matrix model are given by an integral over all Hermitean matrices:

$$\mathcal{Z}_N(t) = \int e^{-N \operatorname{tr} V(M)} \, dM = e^{\mathcal{F}} \ . \tag{2.1}$$

The Lebesgue measure dM consists of all real diagonal entries and of the real and the imaginary parts of the entries in the upper triangle:

$$dM = \prod_i dM_{ii} \prod_{i<j} Re \ dM_{ij} \prod_{i<j} Im \ dM_{ij}.$$

The entries in the lower triangle are also determined by these variables since the $N \times N$ matrix M is Hermitean. The potential is defined as

$$V(M) = \sum_{n \geq 1} t_n M^n, \tag{2.2}$$

where $t_n \in \mathbb{C}$ for $n \in \mathbb{N}$. The usual method to associate a field theory with a matrix model is to consider M in this equation as a field φ. That route is not followed in this work. Later, a Lagrangian will be defined which is only indirectly connected to the potential V. The expansion of the free energy is given by

$$\mathcal{F} = \sum_{h=0}^{\infty} N^{2-2h} \, \mathcal{F}^{(h)}. \tag{2.3}$$

The resolvent is defined as

$$W(z) = \frac{1}{N} tr \frac{1}{z - M} \ , \tag{2.4}$$

and the averaging operation for a function f is

$$\Big\langle f(M) \Big\rangle = \frac{1}{\mathcal{Z}_N(t)} \int f(M)\, e^{-N \,\mathrm{tr}\, V(M)}\, dM. \tag{2.5}$$

Now the correlation functions for $n \geq 1$ can be defined:

$$W_n(z_1, \ldots, z_n) = N^{2n-2} \Big\langle W(z_1) \ldots W(z_n) \Big\rangle_{\mathrm{conn}} \tag{2.6}$$

The $1/N^2$ expansion of the free energy results in an expansion for the correlators

$$W_n(z_1, \ldots, z_n) = \sum_{h=0}^{\infty} N^{-2h} W_n^{(h)}(z_1, \ldots, z_n). \tag{2.7}$$

The zeroth correlator is introduced for reasons of effective notation:

$$W_0^{(h)} = \mathcal{F}^{(h)} \quad \text{and} \quad W_0 = \mathcal{F}/N^2. \tag{2.8}$$

As will be shown in the solution of the correlator $W_1^{(0)}$ in section 2.4, there appear so-called branch points a_i, $i = 1, \ldots, 2s$, which are grouped to contours A_l surrounding the interval $[a_{2l-1}, a_{2l}]$, $l = 1, \ldots, s$ in the complex plane. The eigenvalues concentrate between these branch points. The fraction of eigenvalues which concentrates around the l-th interval, is denoted the filling fraction ε_l. These filling fractions are given parameters of the matrix model:

$$\varepsilon_l = \frac{1}{2} \oint_{A_l} \frac{dx}{2\pi i}\, y(x) \text{ for } l = 1, \ldots, s-1. \tag{2.9}$$

The sum of the relative weights gives one:

$$\sum_{l=1}^{s} \varepsilon_l = 1. \tag{2.10}$$

These additional $s-1$ parameters fix, as is shown in section 2.4, the solution completely.

2.2 Algebraic geometry

A hyperelliptic Riemann surface of genus $s-1$ is defined by the equation

$$y^2 = M^2(x)\sigma(x), \tag{2.11}$$

where M is a polynomial in x and

$$\sigma(x) = \prod_{i=1}^{2s}(x - a_i). \tag{2.12}$$

A_l denotes a contour, which encircles counterclockwise only the l-th cut $[a_{2l-1}, a_{2l}]$. The Abelian differential of the third kind dS belonging to a Riemann surface is determined uniquely by the following properties:

$$\oint_{A_j} dS(x, x') = 0 \quad \forall\, j = 1, \ldots, s-1. \tag{2.13}$$

and

$$dS(x, x') \underset{x \to x'}{=} \frac{dx}{x - x'} + \text{ finite}, \tag{2.14}$$

$$dS(x, x') \underset{x \to \overline{x'}}{=} -\frac{dx}{x - x'} + \text{ finite} \tag{2.15}$$

($\overline{x}$ denotes the hyperelliptic involution of x). The singularities appearing in eqs. (2.14) and (2.15) are the only ones. An explicit representation for dS in the case of a hyperelliptic Riemann surface can be given by

$$dS(x, x') = \frac{\sqrt{\sigma(x')}}{\sqrt{\sigma(x)}} \left(\frac{1}{x - x'} - \sum_{j=1}^{s-1} C_j(x') L_j(x) \right) dx, \tag{2.16}$$

where

$$C_j(x') = \frac{1}{2\pi i} \oint_{A_j} \frac{dx}{\sqrt{\sigma(x)}} \frac{1}{x - x'}. \tag{2.17}$$

The $s-1$ polynomials $L_j(x)$ of degree $s-2$ are uniquely determined by the conditions

$$\oint_{A_l} \frac{L_j(x)}{\sqrt{\sigma(x)}} dx = 2\pi i \delta_{jl} \text{ for } \; l, j = 1, \ldots, s-1. \tag{2.18}$$

Reciprocally, every polynomial P of degee $s-2$ can be projected on the basis of the L_j and written as

$$P(x) = \sum_{j=1}^{s-1} L_j(x) \frac{1}{2\pi i} \oint_{\mathcal{A}_j} \frac{P(x')\, dx'}{\sqrt{\sigma(x')}}. \tag{2.19}$$

Closely connected to the Abelian differential of the third kind is the Bergmann kernel $B(p,q)$ of a Riemann surface, which is uniquely determined by the following statement: B is a bidifferential at the Riemann surface with only one single pole of order two at $p=q$, $B(p,q)=(\frac{dp\,dq}{(p-q)^2}+\text{finite})$ for $p\to q$, which fulfills the normalization equations

$$\oint\limits_{q\in A_j} B(p,q)=0,\ j=1,\ldots,s-1. \tag{2.20}$$

The Bergmann kernel is symmetric. It is related to the Abelian differential of the third kind:

$$B(p,q)=\frac{1}{2}\frac{\partial}{\partial q}\left(\frac{dp}{p-q}+dS(p,q)\right)dq. \tag{2.21}$$

2.3 Loop equations

The reparametrisation invariance of the integral in eq. (2.1) for the substitution $M\to M+\delta M$ with

$$\delta M=\varepsilon\frac{1}{z-M} \tag{2.22}$$

leads to the loop equation

$$(W_1(z))^2+\frac{1}{N^2}W_2(z,z)=\frac{1}{N}\Big\langle \mathrm{tr}\frac{V'(M)}{z-M}\Big\rangle. \tag{2.23}$$

The l.h.s. of this equation originates from the variation of the integral measure dM and the r.h.s. of the variation of the integrand $\exp(-N\ \mathrm{tr}\,V(M))$. The more complex variation

$$\delta M=\varepsilon\frac{1}{z_1-M}\mathrm{tr}\frac{1}{z_2-M} \tag{2.24}$$

yields the loop equation for the two point function:

$$2W_1(x_1)W_2(x_1,x_2)+\frac{1}{N^2}W_3(x_1,x_2,x_3)+\frac{\partial}{\partial x_2}\frac{W_1(x_2)-W_1(x_1)}{x_2-x_1} \tag{2.25}$$

$$=V'(x_1)W_2(x_1,x_2)-\Big\langle \mathrm{tr}\frac{V'(x_1)-V'(M)}{x_1-M}\ \mathrm{tr}\frac{1}{x_2-M}\Big\rangle_{conn}. \tag{2.26}$$

2.4 The correlator $W_1^{(0)}$

For the planar approximation, i.e. in the lowest order in $1/N^2$, the loop equation (2.23) simplifies to

$$(W_1^{(0)}(z))^2 - V'(z)W_1^{(0)}(z) + \frac{1}{N}\Big\langle \mathrm{tr}\frac{V'(z)-V'(M)}{z-M}\Big\rangle = 0. \tag{2.27}$$

As can be seen easily, the last term is a polynomial in z, which is renamed $f(z)$ for this reason. For the quadratic equation two solutions are possible:

$$W_1^{(0)}(p) = \frac{1}{2}V'(p) \pm \frac{1}{2}\sqrt{(V'(p))^2 + 4f(p)}. \tag{2.28}$$

One has to choose the solution with the minus sign, since this reproduces the asymptotic behaviour $W_1^{(0)}(p) \sim \frac{1}{p}$ for $p \to \infty$ predicted by the definition of the correlation functions (2.6). The square root in the correlator gives a direct connection to the hyperelliptic Riemann surface. The general algebraic equation (2.11) which describes the Riemann surface becomes in the Hermitean matrix model

$$y^2 = (V'(\lambda))^2 + 4f(\lambda). \tag{2.29}$$

Thus

$$W_1^{(0)}(x_1) = \frac{1}{2}V'(x_1) - \frac{1}{2}M(x_1)\sqrt{\sigma(x_1)}. \tag{2.30}$$

The assumption that the support of the eigenvalue density is compact, as it is for example used in [41] to write the correlator as an integral, is already contained in the definition (2.9) of the matrix model with fixed filling fractions. One can show [5] that the polynomial $M(\lambda)$ can be expressed in the following way:

$$M(\lambda) = \oint_{\mathcal{C}_\infty} \frac{d\omega}{2\pi i}\frac{1}{\omega-\lambda}\frac{V'(\omega)}{\sqrt{\prod_{i=1}^{2s}(\omega-a_i)}}. \tag{2.31}$$

$\mathcal{C}_\infty$ denotes a contour which encircles counterclockwise all branch points a_i , $i = 1, \ldots, 2s$ and λ. Then $W_1^{(0)}(\lambda)$ can be rewritten as

$$W_1^{(0)}(\lambda) = \frac{1}{2}\oint_{\mathcal{C}} \frac{d\omega}{2\pi i}\frac{V'(\omega)}{\lambda-\omega}\sqrt{\frac{\prod_{i=1}^{2s}(\lambda-a_i)}{\prod_{j=1}^{2s}(\omega-a_j)}}. \tag{2.32}$$

The contour $\mathcal{C}$ encircles counterclockwise all branch points, but not λ.
To determine the $2s$ branch points a_i from the coefficients t_n of the potential

V the equation (2.32) is compared to the definition (2.6) for $x_1 \to \infty$. Exactly $s+1$ equations are obtained. The asymptotic behaviour found in (2.6) is $W_1^{(0)}(x_1) \to 1/x_1$. The equation (2.32) is expanded in powers of x_1 which gives $W_1^{(0)}(x_1) \to c_{s-1}x_1^{s-1} + c_{s-2}x_1^{s-2} + \ldots$. The $s+1$ equations $c_j = \delta_{-1,j}$ with $j \in \{s-1, \ldots, -1\}$ leave $s-1$ degrees of freedom undetermined. These $s-1$ degrees of freedom can be fixed by assuming some conditions of stability against tunneling of eigenvalues between different cuts as in [42], [5]. In this work (as for example in [6], [7]) instead of imposing these conditions of stability, the remaining $s-1$ equations are given by the fixed filling fractions (2.9).

2.5 The loop operator

The loop operator is defined as

$$\frac{\partial}{\partial V(z)} = -\sum_{j=1}^{\infty} \frac{1}{z^{j+1}} \frac{\partial}{\partial t_j}. \tag{2.33}$$

The n-point function then can be rewritten as

$$W_n(z_1, \ldots, z_n) = \frac{1}{N^2} \frac{\partial}{\partial V(z_1)} \cdots \frac{\partial}{\partial V(z_n)} \mathcal{F} \tag{2.34}$$

for $n \in \mathbb{N}_0$. The filling fractions ε_l are fixed constants of the model. They do not change by application of the loop operator. The replacement of y with $W_1^{(0)}$ in (2.9) and subsequent application of the loop operators $\frac{\partial}{\partial V(x_k)} \cdots \frac{\partial}{\partial V(x_2)}$ results therefore in

$$\oint_{\mathcal{A}_l} W_k^{(0)}(x_1, x_2, \ldots, x_k)\, dx_1 = 0 \text{ for } k \geq 2. \tag{2.35}$$

From a similar argument, since eigenvalues only accumulate within the cuts, for any point m in the complex plane away from the cuts follows

$$\oint_m W_1^{(0)}(x_1)\, dx_1 = 0. \tag{2.36}$$

Application of the loop operator gives

$$\oint_m W_2^{(0)}(x_1, x_2)\, dx_1 = 0. \tag{2.37}$$

2.6 The correlator $W_2^{(0)}$

The discussion in this section closely follows the aguments in [6]. The leading order in $1/N^2$ of the loop equation (2.25) is given by

$$2W_1^{(0)}(x_1)W_2^{(0)}(x_1,x_2) + \frac{\partial}{\partial x_2}\frac{W_1^{(0)}(x_2)-W_1^{(0)}(x_1)}{x_2-x_1} = V'(x_1)W_2^{(0)}(x_1,x_2) - U_2^{(0)}(x_1,x_2) \tag{2.38}$$

with

$$U_2^{(0)}(x_1,x_2) = \lim_{N\to\infty}\Big\langle \mathrm{tr}\frac{V'(x_1)-V'(M)}{x_1-M}\ \mathrm{tr}\frac{1}{x_2-M}\Big\rangle_{conn}. \tag{2.39}$$

Inserting the solution for $W_1^{(0)}$ one finds

$$M(x_1)\sqrt{\sigma(x_1)}W_2^{(0)}(x_1,x_2) - U_2^{(0)}(x_1,x_2) = \frac{\partial}{\partial x_2}\frac{W_1^{(0)}(x_2)-W_1^{(0)}(x_1)}{x_2-x_1} \tag{2.40}$$

$$= \frac{1}{2}\frac{\partial}{\partial x_2}\frac{V'(x_2)-V'(x_1)}{x_2-x_1} - \frac{1}{2}\frac{\partial}{\partial x_2}\frac{M(x_2)\sqrt{\sigma(x_2)}-M(x_1)\sqrt{\sigma(x_1)}}{x_2-x_1} \tag{2.41}$$

$$= \frac{1}{2}\frac{\partial}{\partial x_2}\frac{V'(x_2)-V'(x_1)}{x_2-x_1} - \frac{1}{2}\frac{\partial}{\partial x_2}\Big(\sqrt{\sigma(x_2)}\frac{M(x_2)-M(x_1)}{x_2-x_1}\Big) - \frac{1}{2}\frac{\partial}{\partial x_2}\Big(M(x_1)\frac{\sqrt{\sigma(x_2)}-\sqrt{\sigma(x_1)}}{x_2-x_1}\Big). \tag{2.42}$$

Some terms are combined to $R_2(x_1,x_2)$, which is a polynomial in x_1, giving

$$\sqrt{\sigma(x_1)}W_2^{(0)}(x_1,x_2) = -\frac{1}{2}\frac{\partial}{\partial x_2}\Big(\frac{\sqrt{\sigma(x_2)}-\sqrt{\sigma(x_1)}}{x_2-x_1}\Big) + \frac{R_2(x_1,x_2)}{M(x_1)}. \tag{2.43}$$

The l.h.s. of eq. (2.43) has no poles at the zeros of M because of (2.37). That implies that

$$P_2(x_1,x_2) = \frac{R_2(x_1,x_2)}{M(x_1)} \tag{2.44}$$

is a polynomial in x_1. Then we have

$$W_2^{(0)}(x_1',x_2) = \frac{1}{2\sqrt{\sigma(x_1')}}\frac{\partial}{\partial x_2}\frac{\sqrt{\sigma(x_2)}}{x_1'-x_2} - \frac{1}{2}\frac{1}{(x_1'-x_2)^2} + \frac{P_2(x_1',x_2)}{\sqrt{\sigma(x_1')}}. \tag{2.45}$$

In order to apply eq. (2.19) (which we will need for the next step in the calculation) one has to show that the degree of $P_2(x_1,x_2)$ in x_1 is at most

$s-2$.
Let V be a polynomial of degree $d+1$.

$$\frac{V'(x_1)-V'(x_2)}{x_1-x_2}=\sum_{k=0}^{d-1}c_k x_1^k \tag{2.46}$$

is a polynomial in x_1 of degree $d-1$. Since, for the highest coefficient c_{d-1}, the condition $\frac{\partial}{\partial x_2}c_{d-1}=0$ holds, one can conclude that

$$\frac{\partial}{\partial x_2}\frac{V'(x_1)-V'(x_2)}{x_1-x_2} \tag{2.47}$$

is a polynomial in x_1 of degree at most $d-2$.
$U_2^{(0)}$ is a polynomial in x_1. An expression (in x_1) can in general be divided into a polynomial part and a principal part (consisting of inverse powers of x_1). The quantity

$$\Big\langle \mathrm{tr}\frac{-V'(M)}{x_1-M}\mathrm{tr}\frac{1}{x_2-M}\Big\rangle_{\mathrm{conn}} \tag{2.48}$$

has no polynomial part in x_1. Therefore $U_2^{(0)}$ is equal to the polynomial part of $V'(x_1)W_2^{(0)}(x_1,x_2)$. The asymptotic behaviour $W_2^{(0)} \underset{x_1\to\infty}{\sim} \frac{1}{x_1^n}$ with $n\geq 2$ follows from eq. (2.37). Therefore the degree of $U_2^{(0)}$ in x_1 is at most $d-2$. From eq. (2.30) and $W_1^{(0)}(x_1) \underset{x_1\to\infty}{\sim} \frac{1}{x_1}$ (which follows from the definition (2.6)) follows $d=m+s$ where m is the degree of M.
To determine the degree of $R_2(x_1,x_2)$ in x_1, one takes the maximal degree of the three terms in eq. (2.42), which are $d-2$, $m-1$ and $d-2$ for $U_2^{(0)}$. $m-1$ is equal to $d-s-1$ which is less or equal to $d-2$. Therefore the degree of $R_2(x_1,x_2)$ in x_1 is, at most, $d-2$. From that follows that the degree of $P_2(x_1,x_2)$ in x_1 is, at most, $d-2-m=s-2$.

Utilizing this maximal degree, the operator

$$\sum_{j=1}^{s-1}L_j(x_1)\oint\limits_{\mathcal{A}_j}\frac{dx_1'}{2\pi i}\cdot \tag{2.49}$$

is applied to both sides of equation (2.45) and the relations (2.35) and (2.19) are used resulting in

$$0=\frac{1}{2}\sum_{j=1}^{s-1}L_j(x_1)\frac{\partial}{\partial x_2}\sqrt{\sigma(x_2)}C_j(x_2)+P_2(x_1,x_2). \tag{2.50}$$

Inserting the result for the polynomial $P_2(x_1, x_2)$ from eq. (2.50) in eq. (2.45) and using the explicit representation of dS from eq. (2.16) and the relation to $B(p, q)$ from eq. (2.21) one finds

$$\begin{aligned} W_2^{(0)}(x_1, x_2) &= \frac{1}{2}\frac{\partial}{\partial x_2}\sqrt{\frac{\sigma(x_2)}{\sigma(x_1)}}\frac{1}{x_1 - x_2} - \frac{1}{2}\frac{1}{(x_1 - x_2)^2} \\ &\quad -\frac{1}{2}\frac{\partial}{\partial x_2}\sqrt{\frac{\sigma(x_2)}{\sigma(x_1)}}\sum_{j=1}^{s-1} L_j(x_1)C_j(x_2) \\ &= \frac{B(x_1, x_2)}{dx_1\, dx_2} - \frac{1}{(x_1 - x_2)^2}. \end{aligned} \tag{2.51}$$

2.7 Recursion equation

The equation (2.23) is expanded in powers of $1/N^2$. One obtains an equation involving $W_1^{(m)}$ with $m = 1, \ldots, h$ and $W_2^{(h-1)}$. As in the previous section 2.6, a part of the equation is identified as polynomial part and this polynomial is computed by the same methods used in section 2.6. This leads to a formula containing in addition to the aforementioned correlators the Abelian differential of the third kind $dS(p, x)$ and eventually leads to the recursion [6]

$$W_1^{(h)}(p) = \sum_{i=1}^{2s} \operatorname*{Res}_{x \to a_i} \frac{dS(p, x)}{dp}\frac{1}{y(x)}\left(\sum_{m=1}^{h-1} W_1^{(h-m)}(x)W_1^{(m)}(x) + W_2^{(h-1)}(x, x)\right). \tag{2.52}$$

for $h \geq 1$.

Chapter 3

Planar diagrams

3.1 The correlator $W_3^{(0)}$

The three point function in [6] is derived from a loop equation. As described in [6], such a loop equation emerges from a reparametrisation invariance with a variation similar to (2.22) and (2.24). In this work, as in [3] and [4], no further loop equation is used. Instead, the three point function is determined by eq. (2.34), i.e. by the action of the loop operator on $W_2^{(0)}$.
For the consideration of the asymptotic behaviour of $B(p,q)$ for $q \to a_j$ the quantity $B(p,[a_j])$ is introduced:

$$B(p,[a_j]) = 2\frac{\sqrt{q-a_j}B(p,q)}{dq}\bigg|_{q\to a_j}. \tag{3.1}$$

One of the variational formulas of Rauch [11] describes the behaviour of the Bergmann kernel (2.21) as the branch points a_j are varied:

$$\delta B(p,q) = \frac{1}{2}\sum_j B(p,[a_j])B(q,[a_j])\delta a_j. \tag{3.2}$$

To apply the loop operator to $W_2^{(0)}$, one also has to determine $\frac{\delta a_j}{\delta V(p)}$. For this purpose, $\frac{\delta y(q)}{\delta V(p)}$ is first calculated. From eq. (2.30) it follows that

$$y(q) = -2W_1^{(0)}(q) + V'(q). \tag{3.3}$$

The statement of eq. (2.34)

$$\frac{\delta}{\delta V(p)}W_1^{(0)}(q) = W_2^{(0)}(q,p) \tag{3.4}$$

is combined with the result from eq. (2.51). Eq. (2.33) is then utilized to calculate

$$\frac{\delta}{\delta V(p)} V'(q) = -\frac{1}{(q-p)^2}. \tag{3.5}$$

With the definition

$$\widetilde{B}(p,q) = \frac{B(p,q)}{dp\, dq} - \frac{1}{2}\frac{1}{(p-q)^2} \tag{3.6}$$

one obtains [7]

$$\frac{\delta y(q)}{\delta V(p)} = -2\widetilde{B}(p,q). \tag{3.7}$$

The behaviour of the algebraic curve $y(q)$ close to a_i is described by

$$y(q) = y([a_i])\sqrt{q-a_i} + \mathcal{O}((q-a_i)^{3/2}). \tag{3.8}$$

An integral representation of $y([a_i])$ is given by

$$y_{1,i} = y([a_i]) = \oint\limits_{a_i} \frac{dz}{2\pi i} \frac{y(z)}{(z-a_i)^{3/2}}. \tag{3.9}$$

For $q \to a_i$ we have

$$\left.\frac{\delta y(q)}{\delta V(p)}\right|_{q\to a_i} = -\frac{1}{2} y([a_i]) \frac{1}{\sqrt{q-a_i}} \frac{\delta a_i}{\delta V(p)} + \mathcal{O}(\sqrt{q-a_i}). \tag{3.10}$$

In analogy to the relation of $y(x)$ to $y([a_i])$ we define a quantity related to $\widetilde{B}(p,z)$ which does not vary in z for $z \to a_i$:

$$B_j^0(p) = 2 \oint\limits_{a_j} \frac{dz}{2\pi i} \frac{\widetilde{B}(p,z)}{(z-a_j)^{1/2}}. \tag{3.11}$$

Comparing the eqs. (3.7) and (3.10) results in

$$\frac{\delta a_i}{\delta V(p)} = \frac{2B_i^0(p)}{y([a_i])}. \tag{3.12}$$

Combining this with eq. (3.2) one obtains

$$W_3^{(0)}(p_1,p_2,p_3) = \frac{\delta}{\delta V(p_3)} W_2^{(0)}(p_1,p_2) = \sum_{i=1}^{2s} \frac{B_i^0(p_1) B_i^0(p_2) B_i^0(p_3)}{y([a_i])}. \tag{3.13}$$

3.2 A field theory which describes the matrix model correlator $W_3^{(0)}$

The three point function of a field theory is given by (e.g.[19])

$$\left\langle 0 \middle| \varphi(p_1)\varphi(p_2)\varphi(p_3)\; e^{\int dx\, \mathcal{L}_{\rm int}(x)} \middle| 0 \right\rangle. \tag{3.14}$$

We assume a cubic interaction Lagrangian

$$\mathcal{L}_{\rm int}(x) = \lambda(x)\frac{\varphi(x)\varphi(x)\varphi(x)}{3!} = \lambda\frac{\varphi^3}{3!} \tag{3.15}$$

with a coupling $\lambda(x)$. For the moment we are only interested in the lowest order in perturbation theory given by tree graphs. The projection of the expression $< 0|\ldots|0 >$ to graphs with l loops is denoted by the subscript 'l loops'. It turns out that the Wick contractions (their number compensates the 1/3! from the coupling) lead to only one diagram:

$$\begin{aligned} &\left\langle 0 \middle| \varphi(p_1)\varphi(p_2)\varphi(p_3)\; e^{\int dx\, \mathcal{L}_{\rm int}(x)} \middle| 0 \right\rangle_{0 \text{ loops}} \\ &= \int dx\, \lambda(x)\, \overbrace{\varphi(x)\; \varphi}(p_1)\; \overbrace{\varphi(x)\; \varphi}(p_2)\; \overbrace{\varphi(x)\; \varphi}(p_3). \end{aligned} \tag{3.16}$$

This function bears a great resemblance to (3.13). The propagator is specified as

$$\overbrace{\varphi(a_i)\; \varphi}(p) = B_i^0(p). \tag{3.17}$$

and as a coupling we choose

$$\lambda(x) = \sum_{i=1}^{2s} \delta(x - a_i)\frac{1}{y([x]_i)} \tag{3.18}$$

where

$$y([x]_i) = \frac{y(x)}{\sqrt{x - a_i}}. \tag{3.19}$$

Then the three point function of the matrix model from eq. (3.13) is equal to the three point function of the field theory from eq. (3.16).

Instead of dealing with the delta functions in a complex one-dimensional integral over the Riemann surface with the variable x one can integrate this out and obtain a replacement of the integration with a sum over the branch points:

$$\int dx \to \sum_{i=1}^{2s} \Big|_{x=a_i}. \tag{3.20}$$

The Lagrangian is defined as

$$\mathcal{L}_3^{(0)}(a_i) = \lambda_{(3),i}^{(0)} \frac{\varphi_i^3}{3!} \tag{3.21}$$

where φ_i denotes $\varphi(a_i)$. The coupling $\lambda_{(3)}^{(0)} = \lambda^{(0)}$ is given by

$$\lambda^{(0)} = \frac{1}{y_1}. \tag{3.22}$$

The upper index of $\lambda^{(h)}$ refers to the order of this interaction in the topological expansion and is hence denoted as topological index h. To determine $\lambda_{(3),i}^{(0)}$ one only has to add the lower index i to all quantities on the r.h.s. of eq. (3.22). Then the matrix model correlator is given by

$$W_3^{(0)}(p_1,p_2,p_3) = \left\langle 0 \middle| \varphi(p_1)\varphi(p_2)\varphi(p_3)\, e^{\sum_{i=1}^{2s} \mathcal{L}_3^{(0)}(a_i)} \middle| 0 \right\rangle_{0 \ loops}. \tag{3.23}$$

The only Feynman diagram appearing in the tree graph order in the three point function is depicted in figure 3.1.

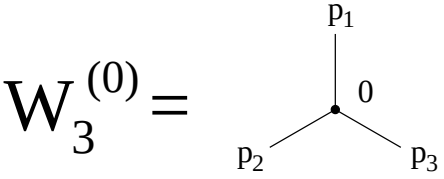

Figure 3.1: Three point function $W_3^{(0)}(p_1,p_2,p_3)$. The zero situated close to the vertex refers to the upper index of $\lambda^{(0)}$. The vertex factor is $\lambda^{(0)} = 1/y_1$.

3.3 The loop operator in propagator notation

As a prerequisite to determining the four point function, the loop operator is applied to the quantities $B_i^0(p)$ and $y_{1,i}$. This results in

$$\begin{aligned} \frac{\delta}{\delta V(q)} B_i^0(p) &= 3\frac{B_i^0(q)}{y_{1,i}} 2 \oint\limits_{a_i} \frac{dz}{2\pi i} \frac{\widetilde{B}(p,z)}{(z-a_i)^{3/2}} \\ &\quad + \sum_{j=1}^{2s} \frac{B_j^0(p)B_j^0(q)}{y_{1,j}} 4 \oint\limits_{a_i} \frac{dz}{2\pi i} \oint\limits_{a_j} \frac{dz'}{2\pi i} \frac{\widetilde{B}(z,z')}{(z-a_i)^{1/2}(z-a_j)^{1/2}}. \end{aligned} \tag{3.24}$$

The first new integral is a generalization of $B_i^0(p)$, where the power of the denominator in eq. (3.11) is 3/2 instead of 1/2. The second new integral requires a new definition which is given as

$$B_{i,j}^{0,0} = 4 \oint\limits_{a_i} \frac{dz}{2\pi i} \oint\limits_{a_j} \frac{dz'}{2\pi i} \frac{\widetilde{B}(z,z')}{(z-a_i)^{1/2}(z-a_j)^{1/2}}. \tag{3.25}$$

In general, we define

$$B_i^f(p) = 2 \oint\limits_{a_i} \frac{dz}{2\pi i} \frac{\widetilde{B}(p,z)}{(z-a_i)^{f+1/2}} \tag{3.26}$$

$$B_{i,j}^{f,g} = 4 \oint\limits_{a_i} \frac{dz}{2\pi i} \oint\limits_{a_j} \frac{dz'}{2\pi i} \frac{\widetilde{B}(z,z')}{(z-a_i)^{f+1/2}(z-a_j)^{g+1/2}} \tag{3.27}$$

$$y_{f,i} = \oint\limits_{a_i} \frac{dz}{2\pi i} \frac{y(z)}{(z-a_i)^{f+1/2}}. \tag{3.28}$$

with $f, g \in \mathbb{N}_0$ in eqs. (3.26), (3.27) and $f \in \mathbb{N}$ in eq. (3.28). When the loop operator is applied to such expressions it can be reformulated as

$$\frac{\partial}{\partial V(q)} = \sum_{k,i,f} \frac{\delta B_i^f(p_k)}{\delta V(q)} \frac{\partial}{\partial B_i^f(p_k)} + \sum_{f,g,i,j} \frac{\delta B_{i,j}^{f,g}}{\delta V(q)} \frac{\partial}{\partial B_{i,j}^{f,g}} + \sum_{f,i} \frac{\delta y_{f,i}}{\delta V(q)} \frac{\partial}{\partial y_{f,i}}. \tag{3.29}$$

In this way the loop operator can be subdivided into the following seven parts [4]:

$$\frac{\delta y_{f,i}}{\delta V(q)} = \big(\Delta_1(q) + \Delta_2(q)\big)(y_{f,i}) \tag{3.30}$$

$$\big(\Delta_1(q)\big)(y_{f,i}) = (2f+1)\frac{y_{f+1,i}}{y_{1,i}} B_i^0(q)$$

$$\big(\Delta_2(q)\big)(y_{f,i}) = -B_i^f(q)$$

$$\frac{\delta B_i^f(p)}{\delta V(q)} = \big(\Delta_3(q)+\Delta_4(q)\big)(B_i^f(p)) \tag{3.31}$$

$$\big(\Delta_3(q)\big)(B_i^f(p)) = (2f+1)\frac{B_i^{f+1}(p)B_i^0(q)}{y_{1,i}}$$

$$\big(\Delta_4(q)\big(B_i^f(p)) = \sum_{j=1}^{2s}\frac{B_{i,j}^{f,0}B_j^0(p)B_j^0(q)}{y_{1,j}}$$

$$\frac{\delta B_{i,j}^{f,g}}{\delta V(q)} = \big(\Delta_5(q)+\Delta_6(q)+\Delta_7(q)\big)(B_{i,j}^{f,g}) \tag{3.32}$$

$$\big(\Delta_5(q)\big)(B_{i,j}^{f,g}) = (2f+1)\frac{B_{i,j}^{f+1,g}B_i^0(q)}{y_{1,i}}$$

$$\big(\Delta_6(q)\big)(B_{i,j}^{f,g}) = (2g+1)\frac{B_{i,j}^{f,g+1}B_j^0(q)}{y_{1,j}}$$

$$\big(\Delta_7(q)\big)(B_{i,j}^{f,g}) = \sum_{k=1}^{2s}\frac{B_{i,k}^{f,0}B_{j,k}^{g,0}B_k^0(q)}{y_{1,k}}.$$

Applying $\Delta_1(q)$ to $B_i^0(p)$ instead of $y_{f,i}$ gives zero. More generally, applying $\Delta_j(q)$, $j=1,\ldots,7$ to an expression not noted above gives zero.

Assume that a correlator $W_n^{(0)}$ with $n\geq 3$ can be expressed in the quantities (3.26), (3.27) and (3.28). For the correlator $W_3^{(0)}$ this is certainly true. Then the above calculation in eqs. (3.30), (3.31) and (3.32) leads to the conclusion that also $W_{n+1}^{(0)}$ can be expressed in these quantities.

3.4 The correlator $W_4^{(0)}$

The application of the loop operator to the three point function results in

$$\begin{aligned} W_4^{(0)}(p_1,\ldots,p_4) &= \frac{\delta}{\delta V(p_4)} W_3^{(0)}(p_1,p_2,p_3) \\ &= \sum_{i,j=1}^{2s} \left(B_i^0(p_1) B_i^0(p_2) \left(\frac{1}{y_{1,i}}\right) B_{i,j}^{0,0} \left(\frac{1}{y_{1,j}}\right) B_j^0(p_3) B_j^0(p_4) \right. \\ &+ B_i^0(p_1) B_i^0(p_3) \left(\frac{1}{y_{1,i}}\right) B_{i,j}^{0,0} \left(\frac{1}{y_{1,j}}\right) B_j^0(p_2) B_j^0(p_4) \\ &+ \left. B_i^0(p_1) B_i^0(p_4) \left(\frac{1}{y_{1,i}}\right) B_{i,j}^{0,0} \left(\frac{1}{y_{1,j}}\right) B_j^0(p_3) B_j^0(p_2) \right) \\ &+ \sum_{i=1}^{2s} \left(-3\frac{y_{2,i}}{y_{1,i}^3}\right) \prod_{r=1}^{4} B_i^0(p_r) + \sum_{r=1}^{4} \sum_{i=1}^{2s} \left(\frac{1}{y_{1,i}^2}\right) B_i^1(p_r) \prod_{\substack{t=1 \\ t\neq r}}^{4} B_i^0(p_t). \end{aligned} \tag{3.33}$$

3.5 A field theory which describes the matrix model correlators $W_3^{(0)}$ and $W_4^{(0)}$

The terms calculated in eq. (3.33) are depicted in figure 3.2.

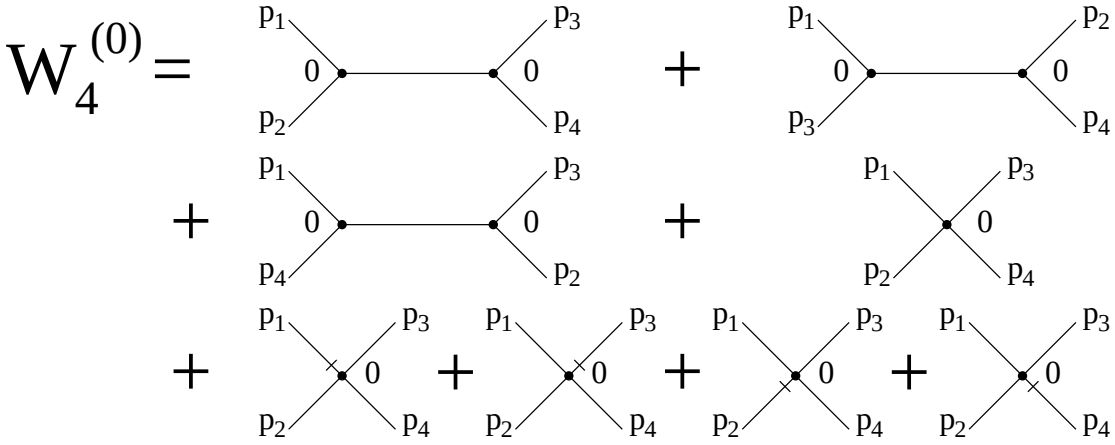

Figure 3.2: All contributions to the 4-point function $W_4^{(0)}(p_1,p_2,p_3,p_4)$. A derivative field $\partial^1\varphi$ is indicated by one bar on the propagator.

The calculation of the four point function of the field theory with the Lagrangian $\mathcal{L}_{\text{int}} = \mathcal{L}_3^{(0)}$, which was tailored to describe the matrix model three

point function, gives three diagrams. These three diagrams (the first three diagrams in figure 3.2) correspond to three contributions in eq. (3.33). The previously stated definition of the propagator for external legs (3.17) has to be generalized to derivatives and combined with a definition of the propagator for internal legs:

$$(\partial^f \overbrace{\varphi)_i\ \varphi(p)} \ = B_i^f(p) \qquad\qquad (\partial^f \overbrace{\varphi)_i\ (\partial^g \varphi)_j} \ = B_{i,j}^{f,g}. \tag{3.34}$$

Then the terms corresponding to the first three diagrams in 3.2 are described by $\mathcal{L}_{\text{int}} = \mathcal{L}_3^{(0)}$.
For the other parts of the correlator one has to add new terms to the Lagrangian. The contributions of the matrix model four point function can be inserted into the field theory as two different kinds of 4-point interaction terms:

$$\mathcal{L}_4^{(0)}(a_i) = \ \lambda^{(0)}_{(4,0),i}\frac{\varphi_i^4}{4!} + \lambda^{(0)}_{(3,1),i}\frac{\varphi_i^3(\partial\varphi)_i}{3!1!}. \tag{3.35}$$

The first subscript $\alpha = (\alpha_0, \alpha_1) = (4,0)$ or $\alpha = (3,1)$ of $\lambda^{(0)}$ denotes the structure of the legs of the interaction term. The interaction vertex consists of α_0 emanating legs with zero and α_1 emanating legs with one derivative. The coupling constants are

$$\lambda^{(0)}_{(3,1)} = \frac{1}{y_1^2} \ \text{ and } \ \lambda^{(0)}_{(4,0)} = -3\frac{y_2}{y_1^3}. \tag{3.36}$$

Thus a generalization of statement (3.23) holds for $k = 3$ and $k = 4$:

$$W_k^{(0)}(p_1,\ldots,p_k) = \left\langle 0\middle|\varphi(p_1)\ldots\varphi(p_k)\ e^{\sum_{i=1}^{2s}(\mathcal{L}_3^{(0)}(a_i)+\mathcal{L}_4^{(0)}(a_i))}\middle|0\right\rangle_{0\ \textit{loops}}. \tag{3.37}$$

3.6 A field theory which describes matrix model correlators in planar aproximation

We will first give a generalization of the method to calculate the contributions to the Lagrangian $\mathcal{L}_k^{(0)}$. The parts of the loop operator which produce new vertices of the kind $\mathcal{L}_3^{(0)}$, are $\Delta_4(q)$ and $\Delta_7(q)$. These parts do not have to be considered. Δ_5 and Δ_6 act like Δ_3, but to inner instead of outer legs. If a diagram has an internal line to which Δ_5 or Δ_6 could act, the diagram cannot have the maximal number of legs—k for a k-point function—at one single vertex. The new interactions, i.e. the terms for $\mathcal{L}_k^{(0)}$, develop only at such diagrams, i.e. at diagrams, which only consist of one vertex. The 1-vertex diagrams of $W_k^{(0)}$ emerge only from the action of Δ_1, Δ_2 and Δ_3. The

vertex has α_0 legs with 0 derivatives, α_1 legs with 1 derivative, etc., such that $\sum_{j=0}^{k-3}\alpha_j = k$. These derivatives are distributed arbitrarily to the external legs. From the symmetry of the correlators it follows that the vertex factor of such a diagram is independent of the exchange of the legs. One can explicitly check the commutativity of the loop operators $\delta/\delta V(q)$ and $\delta/\delta V(p)$. The legs are interchanged in such a way that eventually $p_1,\ldots,p_{\alpha_0}$ have no derivative, $p_{\alpha_0+1},\ldots,p_{\alpha_0+\alpha_1}$ have one derivative, $p_{\alpha_0+\alpha_1+1},\ldots,p_{\alpha_0+\alpha_1+\alpha_2}$ have two derivatives etc.. By this method Δ_3 is excluded. The vertex only emerges from the (α_0-3)-fold action of Δ_1 to $W_3^{(0)}$, followed by the $\alpha_1+\ldots\alpha_{k-3}$-fold application of Δ_2 to the result:

$$\sum_{i=1}^{2s}\lambda^{(0)}_{\alpha,i}B_i^0(p_1)\ldots B_i^0(p_{\alpha_0})B_i^1(p_{\alpha_0+1})\ldots B_i^1(p_{\alpha_0+\alpha_1})B_i^2(p_{\alpha_0+\alpha_1+1})\ldots B_i^2(p_{\alpha_0+\alpha_1+\alpha_2})\ldots$$

$$=\Delta_2(p_k)\Delta_2(p_{k-1})\ldots\Delta_2(p_{\alpha_0+1})\Delta_1(p_{\alpha_0})\ldots\Delta_1(p_4)\sum_{i=1}^{2s}\lambda^{(0)}_{(3),i}B_i^0(p_1)B_i^0(p_2)B_i^0(p_3). \quad (3.38)$$

From this, an equation for the vertex factors can be derived [3]:

$$\lambda^{(0)}_\alpha=\left(\prod_{f=1}^{k-3}\left(-\frac{\partial}{\partial y_f}\right)^{\alpha_f}\right)\left(\sum_{f=1}^{\infty}(2f+1)\frac{y_{f+1}}{y_1}\frac{\partial}{\partial y_f}\right)^{\alpha_0-3}\quad \lambda^{(0)}\equiv D^{(0)}_\alpha\ \lambda^{(0)}. \quad (3.39)$$

The above formalism is a generalization of the calculation of $\mathcal{L}_4^{(0)}$. The next terms are, for example,

$$\mathcal{L}_5^{(0)}=\left(27\frac{y_2^2}{y_1^5}-15\frac{y_3}{y_1^4}\right)\frac{\varphi^5}{5!}+\left(-9\frac{y_2}{y_1^4}\right)\frac{\varphi^4\,\partial\varphi}{4!1!}+\left(\frac{2}{y_1^3}\right)\frac{\varphi^3\,(\partial\varphi)^2}{3!2!}+\left(3\frac{1}{y_1^3}\right)\frac{\varphi^4(\partial^2\varphi)}{4!1!} \quad (3.40)$$

and

$$\begin{aligned}\mathcal{L}_6^{(0)} &= \left(-405\frac{y_2^3}{y_1^7}+450\frac{y_2y_3}{y_1^6}-105\frac{y_4}{y_1^5}\right)\frac{\varphi^6}{6!}+\left(135\frac{y_2^2}{y_1^6}-60\frac{y_3}{y_1^5}\right)\frac{\varphi^5\,\partial\varphi}{5!1!}\\ &+\left(-36\frac{y_2}{y_1^5}\right)\frac{\varphi^4(\partial\varphi)^2}{4!2!}+\left(-54\frac{y_2}{y_1^5}\right)\frac{\varphi^5(\partial^2\varphi)}{5!1!}+\left(6\frac{1}{y_1^4}\right)\frac{\varphi^3(\partial\varphi)^3}{3!3!}\\ &+\left(9\frac{1}{y_1^4}\right)\frac{\varphi^4(\partial\varphi)(\partial^2\varphi)}{4!1!1!}+\left(15\frac{1}{y_1^4}\right)\frac{\varphi^5(\partial^3\varphi)}{5!1!}. \quad (3.41)\end{aligned}$$

The general formula for the Lagrangian $\mathcal{L}_k^{(0)}$ for $k\geq 3$ is

$$\mathcal{L}_k^{(0)}(a_i)=\sum_{\alpha\in M_k^{(0)}}\lambda^{(0)}_{\alpha,i}\ \frac{\varphi_i^{\alpha_0}(\partial^1\varphi)_i^{\alpha_1}\cdots(\partial^{k+3h-3}\varphi)_i^{\alpha_{k+3h-3}}}{\alpha_0!\ \ \alpha_1!\ \ \cdots\ \ \alpha_{k+3h-3}!} \quad (3.42)$$

or, in short,

$$\mathcal{L}_k^{(0)} = \sum_{\alpha \in M_k^{(0)}} \lambda_\alpha^{(0)} \, \frac{\varphi^\alpha}{\alpha!}. \tag{3.43}$$

The set $M_k^{(0)}$ consists of all multi-indices $\alpha = (\alpha_0, \ldots, \alpha_{k-3}) \in (\mathbb{N}_0)^{k-2}$ which fulfill the conditions $\sum_{j=0}^{k-3} j\alpha_j \leq k-3$ and $\sum_{j=0}^{k-3} \alpha_j = k$. The complete Lagrangian at tree order is given by

$$\mathcal{L}^{(0)} = \mathcal{L}_3^{(0)} + \mathcal{L}_4^{(0)} + \mathcal{L}_5^{(0)} + \ldots \ . \tag{3.44}$$

The conjecture that the higher correlation functions of the matrix model are also described by a field theory, suggests itself. This is in analogy to (3.37). The proposed formula for all $k \geq 3$ is

$$W_k^{(0)}(p_1, \ldots, p_k) = \left\langle 0 \middle| \varphi(p_1) \ldots \varphi(p_k) \, e^{\sum_{i=1}^{2s} \mathcal{L}^{(0)}(a_i)} \middle| 0 \right\rangle_{0 \ \textit{loops}}. \tag{3.45}$$

Instead of the infinite sum $\mathcal{L}^{(0)}(a_i)$ in eq. (3.45), one could also insert $\mathcal{L}_3^{(0)}(a_i) + \ldots + \mathcal{L}_k^{(0)}(a_i)$. The r.h.s. of eq. (3.45) can be formulated as sum of diagrams as in figures 3.1 and 3.2. In the latter form, without definition of a Lagrangian, conjecture (3.45) was proved already in [3]. The proof used arguments which apply only to the tree diagrams of the $\frac{1}{N^0}$ approximation. We will prove conjecture (3.45) in chapter 9, together with similar conjectures for higher order corrections in $\frac{1}{N^2}$.

Chapter 4

First order radiative correction

4.1 The correlator $W_1^{(1)}$

The calculation in this subsection closely follows the arguments in [3], published in [4]. In the recursion formula (2.52) for the case $h = 1$, the function $W_2^{(0)}(x, x)$ is needed at coinciding arguments:

$$W_1^{(1)}(p) = \sum_{i=1}^{2s} \operatorname*{Res}_{x \to a_i} \frac{dS(p,x)}{dp} \frac{1}{y(x)} \, W_2^{(0)}(x,x). \tag{4.1}$$

To determine $W_2^{(0)}(x, x)$, the polynomials P_m are defined as

$$P_m(x) = -\sum_{j=1}^{s-1} L_j(x) \oint_{A_j} \frac{dz}{(z - a_m)\sqrt{\sigma(z)}} \qquad\qquad m = 1, \ldots, 2s.$$

The explicit form of $W_2^{(0)}(x, x)$ can be derived from the formulas (2.16) and (2.21):

$$\begin{aligned} W_2^{(0)}(x,x) &= \frac{1}{16} \sum_{i=1}^{2s} \frac{1}{(x-a_i)^2} - \frac{1}{16} \sum_{\substack{i,j=1 \\ i \neq j}}^{2s} \frac{1}{x-a_i} \frac{1}{x-a_j} + \frac{1}{4} \sum_{i=1}^{2s} \frac{P_i(x)}{x-a_i} \\ &= \frac{1}{16} \sum_{i=1}^{2s} \frac{1}{(x-a_i)^2} - \frac{1}{8} \sum_{\substack{i,j=1 \\ i \neq j}}^{2s} \frac{1}{a_i-a_j} \frac{1}{x-a_i} + \frac{1}{4} \sum_{i=1}^{2s} \frac{P_i(a_i)}{x-a_i} \\ &= \frac{1}{16} \sum_{i=1}^{2s} \frac{1}{(x-a_i)^2} + \frac{1}{4} \sum_{i=1}^{2s} \frac{B_{i,i}^{0,0}}{x-a_i}. \end{aligned} \tag{4.2}$$

For the second equality the asymptotic relation $W_2^{(0)}(p,p)|_{p\to\infty} \sim 1/p^2$ is utilised. The last equality is found by a direct evaluation of the two integrals in $B_{i,i}^{0,0}$.
To calculate the remaining constituents of the recursion (4.1), the definitions

$$dS(p,[x]_i) = 2\, dS(p,x)\frac{1}{\sqrt{x-a_i}}, \tag{4.3}$$

$$\widetilde{B}(p,[x]_i) = 2\, \widetilde{B}(p,x)\sqrt{x-a_i}, \tag{4.4}$$

the definition (3.19) and eq. (2.21) are used to obtain

$$\widetilde{B}(p,[x]_i) = \frac{1}{4}\frac{dS(p,[x]_i)}{dp} + \frac{1}{2}(x-a_i)\partial_x \frac{dS(p,[x]_i)}{dp}. \tag{4.5}$$

Eq. (4.5) is differentiated with respect to x. Then x is specified as $x = a_i$, leading to

$$\partial_x{}^k\big|_{x=a_i} \frac{dS(p,[x]_i)}{dp} = \frac{4k!}{2k+1} B_i^k(p). \tag{4.6}$$

By using eqs. (4.6) and (4.2) in eq. (4.1), the formula

$$W_1^{(1)}(p) = \sum_{i=1}^{2s} \left(\frac{1}{24}\frac{1}{y_{1,i}} B_i^1(p) - \frac{1}{8}\frac{y_{2,i}}{(y_{1,i})^2} B_i^0(p) + \frac{1}{2}\frac{1}{y_{1,i}} B_{i,i}^{0,0} B_i^0(p) \right) \tag{4.7}$$

is derived. The double pole in (4.2) leads to the first and second term in the r.h.s of (4.7) and the single pole leads to the third term.
Fortunately, the loop equation for $h = 1$ produces in conjunction with eq. (4.7) correlators of the $1/N^2$-correction, which, as the correlators in the planar approximation, can be expressed by the quantities (3.26), (3.27) and (3.28). This observation is a keystone in the construction of an effective field theory for the matrix model.

4.2 A field theory which describes the matrix model correlators $W_1^{(1)}$ and $W_k^{(0)}$ for $k \geq 3$

The three terms of eq. (4.7) can be translated into the three diagrams shown in figure 4.1. The field theory given by the Lagrangian $\mathcal{L}^{(0)}$ is compared to

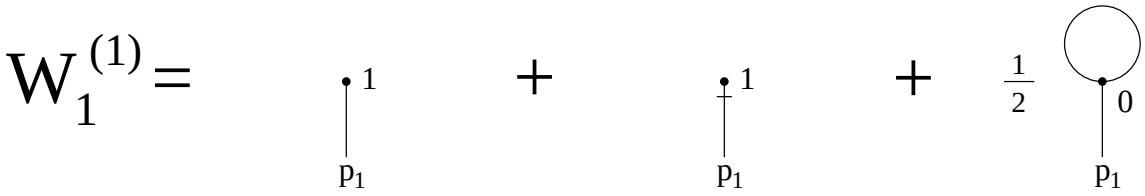

Figure 4.1: All contributions to $W_1^{(1)}(p_1)$. The number close to the vertex refers to the topological index of that vertex, i.e. the upper index h of the vertex factor $\lambda^{(h)}$. The fraction in front of the third diagram is the inverse symmetry factor, which weights the contributions according to their symmetry properties.

eq. (4.7).

$$\left\langle 0\middle|\varphi(p_1)\, e^{\sum_{i=1}^{2s}\mathcal{L}^{(0)}(a_i)}\middle|0\right\rangle_{1\text{ loop}}$$

$$= \left\langle 0\middle|\varphi(p_1)\sum_{i=1}^{2s}\lambda^{(0)}_{(3),i}\frac{\varphi_i\varphi_i\varphi_i}{3!}\middle|0\right\rangle_{1\text{ loop}} \tag{4.8}$$

$$= 3\,\overbrace{\varphi(p_1)\sum_{i=1}^{2s}\lambda^{(0)}_{(3),i}\frac{\varphi_i}{}\frac{\varphi_i}{}\frac{\varphi_i}{3!}} \tag{4.9}$$

$$= \frac{1}{2}\sum_{i=1}^{2s}\frac{1}{y_{1,i}}B_i^0(p)B_{i,i}^{0,0}. \tag{4.10}$$

This calculation reveals that the tadpole diagram (third diagram in figure 4.1) is already correctly described by the field theory tailored to describe the tree graphs. The symmetry factor of the tadpole diagram is 2 (as was calculated in eq. (4.10)) which reflects the prefactor 1/2 for the term in eq. (4.7). The only difference (which has to be inserted by hand) for this term is the $1/N^2$ by which the matrix model correlator $W_1^{(1)}$ is related to $W_3^{(0)}$. At this point, the definition of the Lagrangian in sections 3.2, 3.5 and 3.6 in conjunction with the field theory expressions (3.14), (3.37) and (3.45) pays off. In [3], without a definition of a Lagrangian, a closed formula for the k point correlator in the $1/N^2$ approximation could not be found, because the symmetry factor of a diagram was not recognized as an overall factor of the diagram. Instead, this factor was attached to one certain interaction vertex of the diagram. Note that the symmetry factor of a tree diagram, encountered in the planar approximation, is always 1.
The first two terms in eq. (4.7) are treated as new interactions in the effective Lagrangian:

$$\mathcal{L}_1^{(1)} = \sum_{i=1}^{2s} \lambda_{(1,0),i}^{(1)} \frac{\varphi_i}{1!} + \lambda_{(0,1),i}^{(1)} \frac{(\partial\varphi)_i}{1!} \tag{4.11}$$

$$\text{with } \lambda_{(1,0)}^{(1)} = -\frac{1}{8}\frac{y_2}{(y_1)^2} \quad \text{and} \quad \lambda_{(0,1)}^{(1)} = \frac{1}{24}\frac{1}{y_1}. \tag{4.12}$$

The first subscripts $(1,0)$ and $(0,1)$ for $\lambda^{(1)}$ again point to the number of legs with 0 and 1 derivatives in the interaction vertex. Under the assumption that eq. (3.45) holds, we conclude that the correlators $W_1^{(1)}$ and $W_k^{(0)}$ for $k \geq 3$ are described by the following expression:

$$\sum_{l=0}^{1} \frac{1}{N^{2l}} \left\langle 0 \middle| \varphi(p_1) \dots \varphi(p_k)\, e^{\sum_{i=1}^{2s} (\mathcal{L}^{(0)}(a_i) + \frac{1}{N^2}\mathcal{L}_1^{(1)}(a_i))} \middle| 0 \right\rangle_{l \text{ loops}}. \tag{4.13}$$

The evaluation of all terms in (4.13) for $k = 1$ which are proportional to $1/N^2$ gives all contributions of $W_1^{(1)}(p_1)$. If the conjecture (3.45) is true, then the evaluation of all terms in (4.13) for $k \geq 3$ which are proportional to $1/N^0$ gives all contributions of $W_k^{(0)}(p_1, \dots, p_k)$.

4.3 The coupling constant $\lambda^{(1)}$

The action of the loop operator to the two vertices of $\mathcal{L}_1^{(1)}$ is reminiscent of the action of the loop operator to the two vertices of $\mathcal{L}_4^{(0)}$. One can guess the form of $\lambda^{(1)} = \lambda_{(0)}^{(1)}$ which leads, by one application of $D_\alpha^{(0)}$ with $\alpha = (4,0)$ or $\alpha = (3,1)$, to one of the two mentioned vertices of $\mathcal{L}_1^{(1)}$. Since the number of outgoing legs with zero derivatives in this example is neither 4 nor 3, but 1 and 0, a new, shifted operator definition is useful:

$$D_\alpha = \left(\prod_{f=1}^{k-3} \left(-\frac{\partial}{\partial y_f} \right)^{\alpha_f} \right) \left(\sum_{f=1}^{\infty} (2f+1) \frac{y_{f+1}}{y_1} \frac{\partial}{\partial y_f} \right)^{\alpha_0}. \tag{4.14}$$

We require an expression $\lambda^{(1)}$ which fulfills the two conditions

$$D_{(1,0)}\lambda^{(1)} = \lambda_{(1,0)}^{(1)} \tag{4.15}$$

$$D_{(0,1)}\lambda^{(1)} = \lambda_{(0,1)}^{(1)}. \tag{4.16}$$

The correct guess is

$$\lambda^{(1)} = -\frac{1}{24} \log y_1, \tag{4.17}$$

which fulfills the requirements (4.15) and (4.16).

4.4 The correlator $W_2^{(1)}$

Action of the loop operator to $W_1^{(1)}$ gives, after a long calculation:

$$
\begin{aligned}
&W_2^{(1)}(p_1,p_2) = \\
&\quad \sum_{i=1}^{2s}\left(\frac{3}{4}\frac{y_{2,i}^2}{y_{1,i}^4}-\frac{5}{8}\frac{y_{3,i}}{y_{1,i}^3}\right)B_i^0(p_1)B_i^0(p_2)+\sum_{i=1}^{2s}\left(-\frac{1}{4}\frac{y_{2,i}}{y_{1,i}^3}\right)B_i^1(p_1)B_i^0(p_2)\\
&+\sum_{i=1}^{2s}\left(-\frac{1}{4}\frac{y_{2,i}}{y_{1,i}^3}\right)B_i^0(p_1)B_i^1(p_2)+\sum_{i=1}^{2s}\left(\frac{1}{8}\frac{1}{y_{1,i}^2}\right)B_i^2(p_1)B_i^0(p_2)\\
&+\sum_{i=1}^{2s}\left(\frac{1}{8}\frac{1}{y_{1,i}^2}\right)B_i^0(p_1)B_i^2(p_2)+\sum_{i=1}^{2s}\left(\frac{1}{24}\frac{1}{y_{1,i}^2}\right)B_i^1(p_1)B_i^1(p_2)\\
&+\sum_{i=1}^{2s}\sum_{j=1}^{2s}\left(-\frac{1}{8}\frac{y_{2,i}}{y_{1,i}^2}\right)\left(\frac{1}{y_{1,j}}\right)B_{i,j}^{0,0}B_j^0(p_1)B_j^0(p_2)\\
&+\sum_{i=1}^{2s}\sum_{j=1}^{2s}\left(\frac{1}{24}\frac{1}{y_{1,i}}\right)\left(\frac{1}{y_{1,j}}\right)B_{i,j}^{1,0}B_j^0(p_1)B_j^0(p_2)\\
&+\frac{1}{2}\sum_{i=1}^{2s}\left(-3\frac{y_{2,i}}{y_{1,i}^3}\right)B_{i,i}^{0,0}B_i^0(p_1)B_i^0(p_2)+\frac{1}{2}\sum_{i=1}^{2s}\left(\frac{1}{y_{1,i}^2}\right)B_{i,i}^{0,0}B_i^0(p_1)B_i^1(p_2)\\
&+\frac{1}{2}\sum_{i=1}^{2s}\left(\frac{1}{y_{1,i}^2}\right)B_{i,i}^{0,0}B_i^1(p_1)B_i^0(p_2)+\sum_{i=1}^{2s}\left(\frac{1}{y_{1,i}^2}\right)B_{i,i}^{1,0}B_i^0(p_1)B_i^0(p_2)\\
&+\frac{1}{2}\sum_{i=1}^{2s}\sum_{j=1}^{2s}\left(\frac{1}{y_{1,i}}\right)\left(\frac{1}{y_{1,j}}\right)B_{i,i}^{0,0}B_{i,j}^{0,0}B_j^0(p_1)B_j^0(p_2)\\
&+\frac{1}{2}\sum_{i=1}^{2s}\sum_{j=1}^{2s}\left(\frac{1}{y_{1,i}}\right)\left(\frac{1}{y_{1,j}}\right)B_i^0(p_1)B_{i,j}^{0,0}B_{i,j}^{0,0}B_j^0(p_2)
\end{aligned}
\tag{4.18}
$$

The reason to pull out the factor 1/2 in the terms number 9, 10, 11, 13 and 14 is to reproduce the known interaction terms for tree graphs (3.36) and (3.22).

4.5 A field theory which describes the matrix model correlator $W_k^{(1)}$ for $k = 1, 2$ and $W_k^{(0)}$ for $k \geq 3$

The search for further known terms in $W_2^{(1)}$ results in the identification of some factors in the terms 7 and 8 on the r.h.s. of eq. (4.18) as $\lambda^{(1)}_{(1,0),i}$ and $\lambda^{(1)}_{(0,1),i}$. The diagrams correponding to terms 1 to 6 in eq. (4.18) are not predicted by the two point function with the Lagrangian $\mathcal{L}^{(0)} + \frac{1}{N^2}\mathcal{L}_1^{(1)}$. These interactions, emerging from the action of the loop operator, have to be added to the Lagrangian:

$$\mathcal{L}_2^{(1)} = \left(\frac{3}{4}\frac{y_2^2}{y_1^4} - \frac{5}{8}\frac{y_3}{y_1^3}\right)\frac{\varphi^2}{2!} + \left(-\frac{1}{4}\frac{y_2}{y_1^3}\right)\frac{\varphi\,(\partial\varphi)}{1!1!} + \left(\frac{1}{24}\frac{1}{y_1^2}\right)\frac{(\partial\varphi)^2}{2!} + \left(\frac{1}{8}\frac{1}{y_1^2}\right)\frac{\varphi\,(\partial^2\varphi)}{1!1!}. \tag{4.19}$$

The evaluation of

$$\sum_{l=0}^{1}\frac{1}{N^{2l}}\left\langle 0\middle|\varphi(p_1)\ldots\varphi(p_k)\; e^{\sum_{i=1}^{2s}(\mathcal{L}^{(0)}(a_i)+\frac{1}{N^2}\mathcal{L}_1^{(1)}(a_i))+\frac{1}{N^2}\mathcal{L}_2^{(1)}(a_i))}\middle|0\right\rangle_{l\ loops}. \tag{4.20}$$

for $k = 2$ and the term proportional to $1/N^2$ exactly gives the terms noted in figure 4.2. The term for $k = 1$ in this expression which is proportional to $1/N^2$ is exactly $W_1^{(1)}(p_1)$, the terms which are proportional to $1/N^0$ for $k \geq 3$ are under the assumption of (3.45) $W_k^{(0)}(p_1, \ldots, p_k)$.

The term represented by the third diagram in the third line of figure 4.2, for example, is given by:

$$\frac{1}{2}\sum_{i=1}^{2s}\lambda^{(0)}_{(3,1),i}B_i^1(p_1)B_i^0(p_2)B_{i,i}^{0,0}.$$

The weights in front of the diagrams in the third and fourth line are determined as in eq. (4.10). These factors are the inverse symmetry factors of the diagrams.

A comparison of eq. (4.18) and terms of figure 4.2 leads to the result that the matrix model correlator $W_2^{(1)}$ is described by the field theory eq. (4.20).

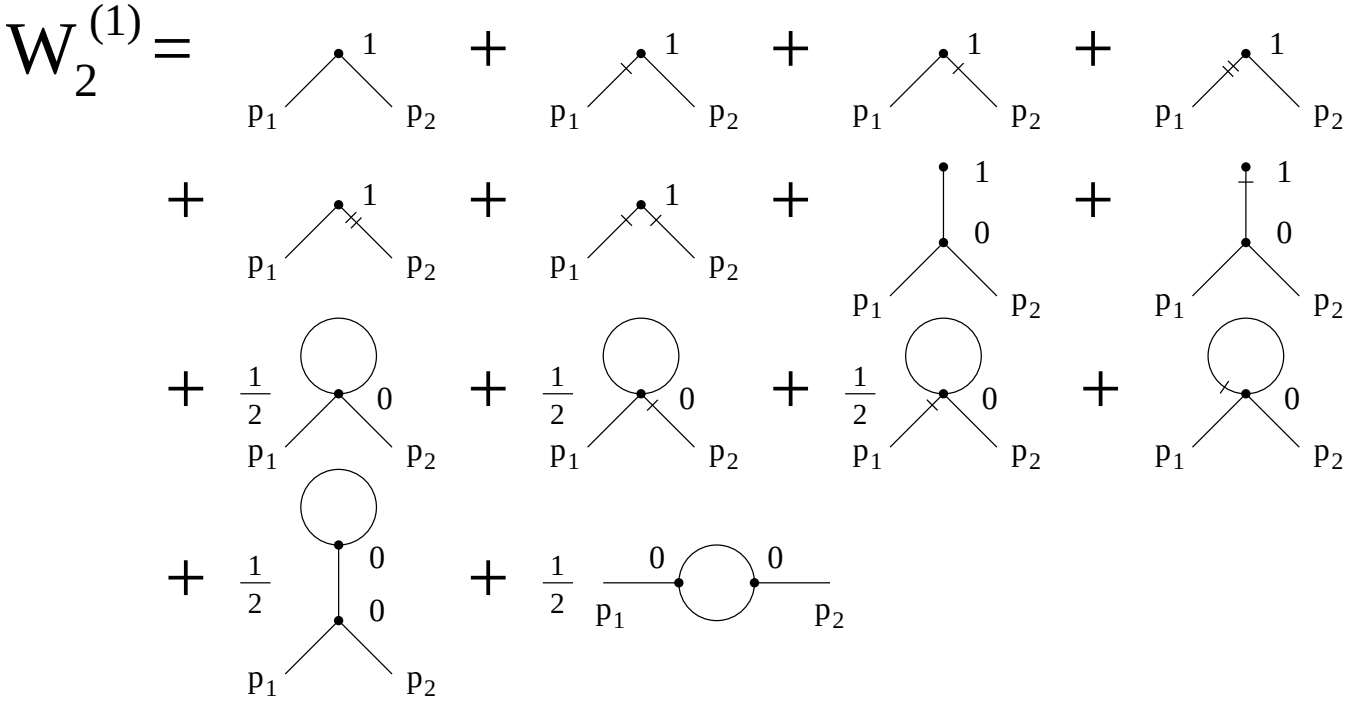

Figure 4.2: All contributions to $W_2^{(1)}(p_1, p_2)$.

4.6 A field theory which describes the matrix model correlators $W_k^{(1)}$ for $k \in \mathbb{N}$ and $W_k^{(0)}$ for $k \geq 3$

The new terms emerging in the Lagrangian can be traced back by the operator D_α from eq. (4.14) to only one constant which was already given in eq. (4.17). The general form of the Lagrangian is

$$\mathcal{L}_k^{(1)} = \sum_{\alpha \in M_k^{(1)}} \lambda_\alpha^{(1)} \frac{\varphi^\alpha}{\alpha!}, \tag{4.21}$$

where the set $M_k^{(1)}$ consists of all multi-indices $\alpha = (\alpha_0, \ldots, \alpha_k) \in (\mathbb{N}_0)^{k+1}$ which fulfill the conditions $\sum_{j=0}^k j\alpha_j \leq k$ and $\sum_{j=0}^k \alpha_j = k$. The coupling constants are given by

$$\lambda_\alpha^{(1)} = D_\alpha \lambda^{(1)}. \tag{4.22}$$

The complete Lagrangian at order 1 is

$$\mathcal{L}^{(1)} = \mathcal{L}_1^{(1)} + \mathcal{L}_2^{(1)} + \mathcal{L}_3^{(1)} + \ldots \ . \tag{4.23}$$

A natural conjecture is, that the expression

$$\sum_{l=0}^{1} \frac{1}{N^{2l}} \left\langle 0 \middle| \varphi(p_1) \dots \varphi(p_k)\ e^{\sum_{i=1}^{2s} (\mathcal{L}^{(0)}(a_i) + \frac{1}{N^2}\mathcal{L}^{(1)}(a_i))} \middle| 0 \right\rangle_{l\ loops} \tag{4.24}$$

describes with its terms proportional to $1/N^2$ for $k \geq 1$ the matrix model correlator $W_k^{(1)}$ and with its terms proportional to $1/N^0$ the matrix model correlator $W_k^{(0)}$ for $k \geq 3$. This conjecture will be proved in chapter 9.

Chapter 5

Higher order radiative corrections

5.1 Residue calculation

The residue calculation in eq. (4.7) for the correlator $W_1^{(1)}$ is generalized for higher orders in $1/N^2$. The calculation in this subsection closely follows [3]. It is assumed that for a certain order $h \geq 1$ the correlators can be written as

$$W_1^{(h)}(x) = \sum_{i,f} B_i^f(x)\omega_1^{(h)}(i,f) \tag{5.1}$$

and

$$W_k^{(h)}(x,x,\ldots,x) = \sum_{\substack{i_1,\ldots,i_k \\ f_1,\ldots,f_k}} B_{i_1}^{f_1}(x)\cdots B_{i_k}^{f_k}(x)\omega_k^{(h)}(i_1,f_1;\ldots;i_k,f_k) \text{ for } k \geq 2. \tag{5.2}$$

Note that $\omega_k^{(h)}$ does not depend on x. For the order $h = 1$ the assumption in eqs. (5.1) and (5.2) is true as shown by eq. (4.7), eq. (4.18) and the $(k-2)$-fold application of the loop operator to the r.h.s. of eq. (4.18). As the result at the end of this section will show, this assumption also holds for the higher order $h+1$. The integration in eq. (2.52) only concerns the x-dependent parts:

$$\operatorname*{Res}_{x\to a_i} \frac{dS(p,x)}{dp}\frac{1}{y(x)} B_j^f(x)B_k^g(x).$$

This integral is calculated for arbitrary integer values f and g and the special case $i = j = k$, which is the most complex case. The result for the less complex cases is given at the end of this subsection. From equations (3.26)

and Cauchy's integral representation, it follows that

$$\begin{aligned}\operatorname*{Res}_{x\to a_i} & \frac{dS(p,x)}{dp}\frac{1}{y(x)}B_i^f(x)B_i^g(x) \\ = & \oint\limits_{a_i}\frac{dx}{2\pi i}\frac{dS(p,x)}{dp\;y(x)}\;2\oint\limits_{a_i}\frac{dw}{2\pi i}\frac{\widetilde{B}(w,x)}{(w-a_i)^{f+1/2}}\;2\oint\limits_{a_i}\frac{dv}{2\pi i}\frac{\widetilde{B}(v,x)}{(v-a_i)^{g+1/2}}. \quad (5.3)\end{aligned}$$

By definition, the contour for x is positioned outside the contours for w and v. When the outer contour x is pushed through the contours for v and w, the double poles in $\widetilde{B}(w,x)$ and $\widetilde{B}(v,x)$ result in two additional terms:

$$\begin{aligned}(5.3) = & 4\oint\limits_{a_i}\frac{dw}{2\pi i}\frac{1}{(w-a_i)^{f+1/2}}\oint\limits_{a_i}\frac{dv}{2\pi i}\frac{1}{(v-a_i)^{g+1/2}}\oint\limits_{a_i}\frac{dx}{2\pi i}\frac{dS(p,x)}{dp\;y(x)}\widetilde{B}(w,x)\widetilde{B}(v,x) \\ & + 4\oint\limits_{a_i}\frac{dw}{2\pi i}\frac{1}{(w-a_i)^{f+1/2}}\oint\limits_{a_i}\frac{dv}{2\pi i}\frac{1}{(v-a_i)^{g+1/2}}\left(\frac{1}{2}\partial_w\left(\frac{dS(p,w)}{dp\;y(w)}\widetilde{B}(w,v)\right)\right. \\ & \left. + \frac{1}{2}\partial_v\left(\frac{dS(p,v)}{dp\;y(v)}\widetilde{B}(v,w)\right)\right). \quad (5.4)\end{aligned}$$

The first term on the r.h.s, denoted as (5.4a), contains an integration in x which can be solved easily because the integrand has a simple pole at $x = a_i$. By using (4.6) we obtain

$$(5.4\text{a}) = \frac{1}{2}\frac{B_i^0(p)B_{i,i}^{f,0}B_{i,i}^{g,0}}{y_{1,i}}.$$

The two further terms terms on the r.h.s. of (5.4), denoted (5.4b) and (5.4c), become after partial integration

$$(5.4\text{b}) = (2f+1)\oint\limits_{a_i}\frac{dw}{2\pi i}\frac{1}{(w-a_i)^{f+3/2}}\oint\limits_{a_i}\frac{dv}{2\pi i}\frac{1}{(v-a_i)^{g+1/2}}\frac{dS(p,w)}{dp}\frac{\widetilde{B}(w,v)}{y(w)} \quad (5.5)$$

and

$$(5.4\text{c}) = (2g+1)\oint\limits_{a_i}\frac{dw}{2\pi i}\frac{1}{(w-a_i)^{f+1/2}}\oint\limits_{a_i}\frac{dv}{2\pi i}\frac{1}{(v-a_i)^{g+3/2}}\frac{dS(p,v)}{dp}\frac{\widetilde{B}(v,w)}{y(v)}. \quad (5.6)$$

The integral in v in eq. (5.6) can be calculated with eq. (4.6) and gives

$$(5.6) = (g+\frac{1}{2})\sum_{k+r+t=g+1}\frac{1}{2k+1}B_i^k(p)B_{i,i}^{f,r}Z_{t,i} \quad (5.7)$$

where

$$Z_{t,i} = \frac{\partial_x{}^t}{t!} \frac{1}{y([x]_i)} \bigg|_{x=a_i} . \tag{5.8}$$

By interchanging the w and the v contours in (5.5) one obtains one term from the pole at $w = v$ and a term similar to (5.7):

$$\begin{aligned} (5.5) &= (f+\frac{1}{2}) \sum_{k+r+t=f+1} \frac{1}{2k+1} B_i^k(p) B_{i,i}^{g,r} Z_{t,i} \\ &+ \frac{1}{2}(2f+1)(2g+1) \sum_{k+l=f+g+2} \frac{1}{2k+1} B_i^k(p) Z_{l,i}. \end{aligned} \tag{5.9}$$

The result of the preceding calculations, i.e. eqs. (5.4a), (5.7) and (5.9) and the analogous calculations for the case of non-coinciding indices can be summarized as

$$\begin{aligned} &\operatorname*{Res}_{x \to a_i} \frac{dS(p,x)}{dp\; y(x)} B_j^f(x) B_k^g(x) \\ &= \frac{1}{2} B_{j,i}^{f,0} \frac{B_i^0(p)}{y_{1,i}} B_{i,k}^{0,g} \\ &+ \delta_{k,i}(g+\frac{1}{2}) \sum_{r+m+t=g+1} \frac{1}{2r+1} B_i^r(p) B_{j,i}^{f,m} Z_{t,i} \\ &+ \delta_{j,i}(f+\frac{1}{2}) \sum_{r+m+t=f+1} \frac{1}{2r+1} B_i^r(p) B_{k,i}^{g,m} Z_{t,i} \\ &+ \delta_{k,i}\delta_{j,i} \frac{1}{2}(2g+1)(2f+1) \sum_{r+l=f+g+2} \frac{1}{2r+1} B_i^r(p) Z_{l,i} \end{aligned} \tag{5.10}$$

with

$$Z_n = \sum_{\substack{k_1+\ldots+k_n=k \\ \sum_j j k_j = n}} \frac{(-)^k k!}{k_1! \cdots k_n!} \frac{1}{(y_1)^{k+1}} \prod_{l=1}^{n} (y_{1+l})^{k_l} = \sum_{k=0}^{n} \frac{Z_n^{[k]}}{(y_1)^{k+1}}. \tag{5.11}$$

The expression $Z_{n,i}$ can be obtained from the expression Z_n by substituting each y_f for $y_{f,i}$. This corresponds to specifying the general coordinate x as $x = a_i$.

Provided that eq. (5.1) and eq. (5.2) are valid for order h, eq. (5.10) shows that eq. (5.1) also holds for the higher order $h+1$. Then the $(k-1)$-fold action of the loop operator confirms that eq. (5.2) also holds for the higher order $h+1$. This method can be applied with these arguments to all orders.

5.2 Some diagrams of $W_1^{(2)}$

The field theory with the Lagrangian $\mathcal{L}_{\rm int} = \mathcal{L}^{(0)} + \frac{1}{N^2}\mathcal{L}^{(1)}$ predicts many diagrams at the order $1/N^4$ from equation

$$\sum_{l=0}^{2} \frac{1}{N^{2l}} \Big\langle 0 \Big| \varphi(p_1)\; e^{\sum_{i=1}^{2s} \mathcal{L}_{\rm int}(a_i)} \Big| 0 \Big\rangle_{l \;\; loops}. \tag{5.12}$$

All of them—judging by their form—appear in the matrix model correlator $W_1^{(2)}$ determined by the loop equation. The loop equation in addition gives more diagrams which are not predicted by the Lagrangian until now. How the Lagrangian will be enhanced by these contributions will be described in section 5.3. Now we concentrate on several examples of diagrams appearing in eq. (5.12) and in the correlator $W_1^{(2)}$.

The relevant loop equation (2.52) for the correlator $W_1^{(2)}$ is

$$W_1^{(2)}(p) = \sum_{i=1}^{2s} \operatorname*{Res}_{x \to a_i} \frac{dS(p,x)}{dp} \frac{1}{y(x)} \left(W_1^{(1)}(x) W_1^{(1)}(x) + W_2^{(1)}(x,x) \right). \tag{5.13}$$

In figures 5.1, 5.2 and 5.3 three diagrams are depicted which emerge from eq. (5.13) by the first term on the r.h.s., $\frac{1}{2} B_{j,i}^{f,0} \frac{B_i^0(p)}{y_{1,i}} B_{i,k}^{0,g}$, of equation (5.10). $W_1^{(1)}$ has three terms, so one can expect to obtain about nine diagrams from the first part of eq. (5.13) when restricting only to the first term on the r.h.s. of eq. (5.10). Three of these nine expected diagrams turn out to coincide with three other diagrams so that the number of different diagrams is only six. Three of them are depicted in figures 5.1, 5.2 and 5.3.

5.2.1 Matrix model calculation for diagram D_1

In figure 5.1, one diagram emerging from eq. (5.13) via the first term on the r.h.s. of eq. (5.10) is depicted. The diagram, D_1, arises from the multiplication of the first diagram in figure 4.1 with itself. As indicated in front of the diagram, the prefactor of this contribution is 1/2. The diagram, together with its prefactor, represents the contribution

$$q = \frac{1}{2} \sum_{i,j,k=1}^{2s} \lambda_{(3,0),i}^{(0)} \lambda_{(1,0),j}^{(1)} \lambda_{(1,0),k}^{(1)} B_i^0(p_1) B_{i,j}^{0,0} B_{i,k}^{0,0}. \tag{5.14}$$

The combination of the first diagram in figure 4.1 with itself appears once in the summation $\sum_{j=1}^{h-1} W_1^{(j)} W_1^{(h-j)}$ for $h = 2$. To obtain the prefactor of

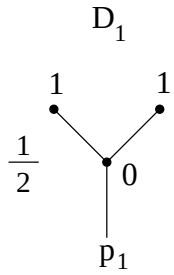

Figure 5.1: diagram D_1 from $W_1^{(2)}$.

D_1, one has to multiply the factor 1/2 from the first term on the r.h.s. of eq. (5.10) with the prefactors of the preimage diagrams from $W_1^{(1)}$, which are both 1, and with the number of occurences in the summation, which is 1, giving in total 1/2.

The vertex factor at the vertices with a topological index of one do not change in the procedure. The vertex factor of the newly created vertex is $1/y_1$, which is exactly the vertex factor of $\mathcal{L}_3^{(0)}$.

5.2.2 Field theory calculation for diagram D_1

Via the number of Wick contractions, the field theory with the Lagrangian $\mathcal{L}_{\text{int}} = \mathcal{L}^{(0)} + \frac{1}{N^2}\mathcal{L}^{(1)}$ predicts a certain inverse symmetry factor for diagram D_1. This inverse symmetry factor is calculated in the following. It can be compared to the prefactor of D_1 calculated in the previous subsection. The evaluation of expression (5.12) with respect to diagram D_1, i.e. the projection of (5.12) on the term belonging to diagram D_1, is denoted by the subscript D_1 in (5.15). In the Gell-Mann-Low series the exponential in (5.12) is expanded to receive a contribution from $\mathcal{L}_3^{(0)} \cdot \mathcal{L}_1^{(1)} \cdot \mathcal{L}_1^{(1)}$. This leads, since $\mathcal{L}_3^{(0)}$ appears once and $\mathcal{L}_1^{(1)}$ appears twice, to the factor $\frac{1}{1!2!}$. These factorials in eq. (5.16) are denoted Gell-Mann-Low factorials. The number of possible Wick contractions in this diagram is calculated in eq. (5.17). There are 3 possible ways to contract $\varphi(p_1)$ with one field from $\mathcal{L}_3^{(0)}$ and then, one can assign to φ_k one of the two remaining fields φ_i leading to a factor 2.

$$\left\langle 0 \middle| \varphi(p_1) e^{\sum_{i=1}^{2s} (\mathcal{L}^{(0)}(a_i) + \frac{1}{N^2}\mathcal{L}^{(1)}(a_i))} \middle| 0 \right\rangle_{D_1} \tag{5.15}$$

$$= \frac{1}{N^4}\frac{1}{1!2!} \left\langle 0 \middle| \varphi(p_1) \sum_{i,j,k=1}^{2s} \mathcal{L}_3^{(0)}(a_i)\mathcal{L}_1^{(1)}(a_j)\mathcal{L}_1^{(1)}(a_k) \middle| 0 \right\rangle_{D_1} \tag{5.16}$$

$$= \frac{1}{N^4}\frac{1}{1!2!} \sum_{i,j,k=1}^{2s} \lambda^{(0)}_{(3,0),i}\lambda^{(1)}_{(1,0),j}\lambda^{(1)}_{(1,0),k} \; \overbrace{\varphi(p_1)\frac{\varphi_i\,\varphi_i\,\varphi_i}{3!}\,\frac{\varphi_j}{1!}\,\frac{\varphi_k}{1!}} \cdot 3 \cdot 2 \tag{5.17}$$

$$= \frac{1}{N^4}\frac{1}{2} \sum_{i,j,k=1}^{2s} \lambda^{(0)}_{(3,0),i}\lambda^{(1)}_{(1,0),j}\lambda^{(1)}_{(1,0),k} \; \overbrace{\varphi(p_1)\,\varphi_i} \;\; \overbrace{\varphi_j\,\varphi_i} \;\; \overbrace{\varphi_k\,\varphi_i} \tag{5.18}$$

This results in an inverse symmetry factor 1/2 in eq. (5.18).

5.2.3 Matrix model calculation for diagram D_2

In figure 5.2, another diagram emerging from eq. (5.13) by the application of the first term on the r.h.s. of eq. (5.10) is depicted. The diagram, D_2, arises

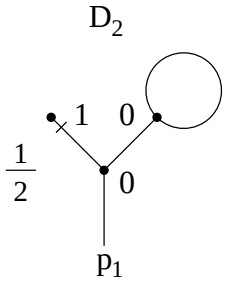

Figure 5.2: diagram D_2 from $W_1^{(2)}$.

from the multiplication of the first with the third diagram in figure 4.1. As indicated in front of the diagram, the prefactor of this contribution is 1/2. The combination of the first with the third diagram in figure 4.1 appears twice in the summation $\sum_{j=1}^{h-1} W_1^{(j)} W_1^{(h-j)}$ for $h = 2$. To obtain the prefactor of D_2, one has to multiply the factor 1/2 from the first term on the r.h.s. of eq. (5.10) with the prefactors of the preimage diagrams from $W_1^{(1)}$, which are 1 and 1/2, and with the number of occurences in the summation, which is 2, giving in total 1/2.

The vertex factors at the vertex with the loop and at the vertex with topological index one do not change in the procedure. The vertex factor of the newly created vertex is $1/y_1$, which is exactly the vertex factor of $\mathcal{L}_3^{(0)}$.

5.2.4 Field theory calculation for diagram D_2

This subsection is concerned with the following question: What is the inverse symmetry factor of diagram D_2? The expression (5.12) is evaluated with respect to diagram D_2 in (5.19). The exponential in the Gell-Mann-Low series is expanded to receive a contribution from $\mathcal{L}_3^{(0)} \cdot \mathcal{L}_3^{(0)} \cdot \mathcal{L}_1^{(1)}$. This leads, since $\mathcal{L}_3^{(0)}$ appears twice and $\mathcal{L}_1^{(1)}$ appears once, to the factor $\frac{1}{2!1!}$ in eq. (5.20). The number of possible Wick contractions in this diagram is calculated in eq. (5.21). There are $2 \cdot 3$ possible ways to contract $\varphi(p_1)$ with one field from one of the two $\mathcal{L}_3^{(0)}$. One can then contract one of the two remaining fields at this vertex with $\mathcal{L}_1^{(1)}$, which gives a factor 2. The other $\mathcal{L}_3^{(0)}$ can be connected in 3 different ways to this construction. The contraction belonging to the two fields of the loop is then fixed.

$$\left\langle 0 \middle| \varphi(p_1) e^{\sum_{i=1}^{2s} (\mathcal{L}^{(0)}(a_i) + \frac{1}{N^2}\mathcal{L}^{(1)}(a_i))} \middle| 0 \right\rangle_{D_2} \tag{5.19}$$

$$= \frac{1}{N^4}\frac{1}{2!1!} \left\langle 0 \middle| \varphi(p_1) \sum_{i,j,k=1}^{2s} \mathcal{L}_3^{(0)}(a_i)\mathcal{L}_1^{(1)}(a_j)\mathcal{L}_3^{(0)}(a_k) \middle| 0 \right\rangle_{D_2} \tag{5.20}$$

$$= \frac{1}{N^4}\frac{1}{2!1!} \sum_{i,j,k=1}^{2s} \lambda^{(0)}_{(3,0),i}\lambda^{(1)}_{(0,1),j}\lambda^{(0)}_{(3,0),k} \; \overbrace{\varphi(p_1)\frac{\varphi_i}{3!}}\; \overbrace{\varphi_i\varphi_i}\; \overbrace{\frac{(\partial\varphi)_j}{1!}\frac{\varphi_k}{3!}}\; \overbrace{\varphi_k\varphi_k} \cdot (2 \cdot 3) \cdot 2 \cdot 3 \tag{5.21}$$

$$= \frac{1}{N^4}\frac{1}{2} \sum_{i,j,k=1}^{2s} \lambda^{(0)}_{(3,0),i}\lambda^{(1)}_{(0,1),j}\lambda^{(0)}_{(3,0),k} \; \overbrace{\varphi(p_1)\,\varphi_i}\; \overbrace{(\partial\varphi)_j\,\varphi_i}\; \overbrace{\varphi_k\,\varphi_i}\; \overbrace{\varphi_k\,\varphi_k} \tag{5.22}$$

This results in an inverse symmetry factor 1/2 in eq. (5.22).

5.2.5 Matrix model calculation for diagram D_3

In figure 5.3, another diagram emerging from eq. (5.13) via the first term on the r.h.s. of eq. (5.10) is depicted. The diagram, D_3, arises from the multiplication of the third diagram in figure 4.1 with itself. As indicated in front of the diagram, the prefactor of this contribution is 1/8.
The combination of the third diagram in figure 4.1 with itself appears once in the summation $\sum_{j=1}^{h-1} W_1^{(j)} W_1^{(h-j)}$ for $h = 2$. To obtain the prefactor of

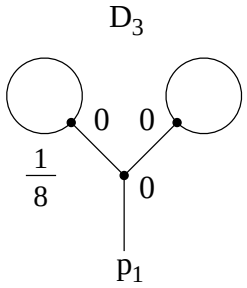

Figure 5.3: diagram D_3 from $W_1^{(2)}$.

D_3, one has to multiply the factor 1/2 from the first term on the r.h.s. of eq. (5.10) with the prefactors of the preimage diagrams from $W_1^{(1)}$, which are 1/2 and 1/2, and with the number of occurences in the summation, which is 1, giving in total 1/8.

The vertex factors at the vertices with the loops do not change in the procedure. The vertex factor of the newly created vertex is $1/y_1$, which is exactly the vertex factor of $\mathcal{L}_3^{(0)}$.

5.2.6 Field theory calculation for diagram D_3

The inverse symmetry factor of diagram D_3 is calculated in the following. The expression (5.12) is evaluated with respect to diagram D_3 in (5.23). The exponential in the Gell-Mann-Low series is expanded to receive a contribution from $\mathcal{L}_3^{(0)} \cdot \mathcal{L}_3^{(0)} \cdot \mathcal{L}_3^{(0)}$. This leads, since $\mathcal{L}_3^{(0)}$ appears three times, to the factor $\frac{1}{3!}$ in eq. (5.24). The number of possible Wick contractions is calculated in eq. (5.25). There are $3 \cdot 3$ possible ways to contract $\varphi(p_1)$ with one field from one of the three $\mathcal{L}_3^{(0)}$. Then, in each of the remaining two $\mathcal{L}_3^{(0)}$ one can choose one of 3 possiblilities to connect these vertices to the rest of the diagram. A factor 2 arises from choosing one of two remaining fields in the vertex connected to p_1. The two contractions belonging to the four fields of the loops are then fixed.

$$\left\langle 0 \middle| \varphi(p_1) e^{\sum_{i=1}^{2s} (\mathcal{L}^{(0)}(a_i) + \frac{1}{N^2}\mathcal{L}^{(1)}(a_i))} \middle| 0 \right\rangle_{D_3} \tag{5.23}$$

$$= \frac{1}{N^4}\frac{1}{3!}\left\langle 0 \middle| \varphi(p_1) \sum_{i,j,k=1}^{2s} \mathcal{L}_3^{(0)}(a_i)\mathcal{L}_3^{(0)}(a_j)\mathcal{L}_3^{(0)}(a_k) \middle| 0 \right\rangle_{D_3} \tag{5.24}$$

$$= \frac{1}{N^4}\frac{1}{3!}\sum_{i,j,k=1}^{2s} \lambda^{(0)}_{(3,0),i}\lambda^{(0)}_{(3,0),j}\lambda^{(0)}_{(3,0),k} \overbrace{\varphi(p_1)\frac{\varphi_i\varphi_i\varphi_i}{3!}\ \frac{\varphi_j\varphi_j\varphi_j}{3!}\ \frac{\varphi_k\varphi_k\varphi_k}{3!}} \cdot (3\cdot 3)\cdot 3\cdot 3\cdot 2 \tag{5.25}$$

$$= \frac{1}{N^4}\frac{1}{8}\sum_{i,j,k=1}^{2s} \lambda^{(0)}_{(3,0),i}\lambda^{(0)}_{(3,0),j}\lambda^{(0)}_{(3,0),k} \overbrace{\varphi_j\,\varphi_j}\ \ \overbrace{\varphi_j\,\varphi_i}\ \ \overbrace{\varphi(p_1)\,\varphi_i}\ \ \overbrace{\varphi_i\,\varphi_k}\ \ \overbrace{\varphi_k\,\varphi_k} \tag{5.26}$$

This results in an inverse symmetry factor 1/8 in eq. (5.26).

5.2.7 Matrix model calculation for diagram D_4

The three examples considered up to now, D_1, D_2 and D_3, have in common that they emerged from the first part of eq. (5.13) via the first term on the r.h.s. of eq. (5.10). In figure 5.4, another diagram, D_4, which is similar to D_3, is considered. Such a diagram, i.e. a contribution with these propagators, emerges from both parts of eq. (5.13) by the second and third term on the r.h.s. of eq. (5.10). The calculation of the vertex factor, which arises at

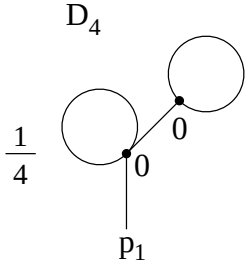

Figure 5.4: diagram D_4 from $W_1^{(2)}$.

the new vertex, is more complicated than in the previous examples. From the part $W_1^{(1)}W_1^{(1)}$ in eq. (5.13) (more precisely, from the combination of the third diagram in figure 4.1 with itself) a contribution q_1 to diagram D_4 arises due to the second and third term of eq. (5.10). The inverse symmetry factors of these preimage diagrams from $W_1^{(1)}$ are 1/2 and 1/2. Since the second and the third term on the r.h.s. of eq. (5.10) each give $\frac{1}{2}Z_1$, and the vertex factor

of the third diagram in figure 4.1 is equal to $1/y_1$, the contribution q_1 from this part is

$$q_1 = \frac{1}{2}\frac{1}{2}\left(\frac{1}{2}+\frac{1}{2}\right) Z_1 \frac{1}{y_1}. \tag{5.27}$$

From the part $W_2^{(1)}$ in eq. (5.13) (more precisely, from the first diagram in the fourth line of figure 4.2) a contribution q_2 to diagram D_4 arises due to the second and third term of eq. (5.10). The symmetry factor of this diagram is 1/2. Since the second and the third term of eq. (5.10) each give $\frac{1}{2}Z_1$, and the vertex factor of the first diagram in the fourth line of figure 4.2 is equal to $1/y_1$, the contribution q_2 from this part is

$$q_2 = \frac{1}{2}\left(\frac{1}{2}+\frac{1}{2}\right) Z_1 \frac{1}{y_1}. \tag{5.28}$$

The sum q of these contributions is the product of the prefactor of the diagram D_4 and the vertex factor of the vertex connected to p_1. One could define the prefactor of D_4 as 1, then the vertex factor at the new vertex would be

$$q = q_1 + q_2 = -\frac{3}{4}\frac{y_2}{(y_1)^3}. \tag{5.29}$$

However, since this vertex factor is related to a previously defined vertex factor from eq. (3.36) by

$$-\frac{3}{4}\frac{y_2}{(y_1)^3} = \frac{1}{4}\lambda^{(0)}_{(4,0)}, \tag{5.30}$$

we define the prefactor of D_4 as 1/4 and the vertex factor of the new vertex as $\lambda^{(0)}_{(4,0)}$. The fact that the known vertex factor $\lambda^{(0)}_{(4,0)}$ appears in this higher order correction is the crucial point in the construction of an effective field theory. The next subsection deals only with the prefactor of the diagram, because it has been shown by the above calculation that the vertex factor at the newly created vertex is given by $\mathcal{L}_4^{(0)}$. Note that the new vertex factor is not only identical to one of the previously calculated vertex factors, but, as demanded by the field theory, it exactly describes by its lower index $(\alpha_0, \alpha_1) = (4, 0)$ the diagram D_4 close to the vertex connected to p_1. 4 legs with zero derivatives and 0 legs with one derivative emanate from this vertex.

5.2.8 Field theory calculation for diagram D_4

Via the number of Wick contractions, the field theory predicts an inverse symmetry factor for diagram D_4. The expression (5.12) is evaluated with

respect to diagram D_4 in (5.31). The exponential in the Gell-Mann-Low series is expanded to receive a contribution from $\mathcal{L}_3^{(0)} \cdot \mathcal{L}_4^{(0)}$. This leads, since $\mathcal{L}_4^{(0)}$ and $\mathcal{L}_3^{(0)}$ appear only once, to the factor $\frac{1}{1!1!}$ in eq. (5.32). The number of possible Wick contractions is calculated in eq. (5.33). There are 4 possible ways to contract $\varphi(p_1)$ with one field from $\mathcal{L}_4^{(0)}$. From the remaining 3 fields in $\mathcal{L}_4^{(0)}$, one is chosen for the connection to $\mathcal{L}_3^{(0)}$. For the same contraction, there are 3 possibilities to chose a field from $\mathcal{L}_3^{(0)}$. The two contractions representing the loops are then fixed.

$$\left\langle 0 \middle| \varphi(p_1) e^{\sum_{i=1}^{2s} (\mathcal{L}^{(0)}(a_i) + \frac{1}{N^2}\mathcal{L}^{(1)}(a_i))} \middle| 0 \right\rangle_{D_4} \tag{5.31}$$

$$= \frac{1}{N^4} \frac{1}{1!1!} \left\langle 0 \middle| \varphi(p_1) \sum_{i,k=1}^{2s} \mathcal{L}_3^{(0)}(a_i) \mathcal{L}_4^{(0)}(a_k) \middle| 0 \right\rangle_{D_4} \tag{5.32}$$

$$= \frac{1}{N^4} \frac{1}{1!1!} \sum_{i,k=1}^{2s} \lambda^{(0)}_{(3,0),i} \lambda^{(0)}_{(4,0),k} \; \overbrace{\varphi(p_1) \frac{\varphi_i \varphi_i \varphi_i \varphi_i}{4!} \; \frac{\varphi_k \varphi_k \varphi_k}{3!}} \cdot 4 \cdot 3 \cdot 3 \tag{5.33}$$

$$= \frac{1}{N^4} \frac{1}{4} \sum_{i,k=1}^{2s} \lambda^{(0)}_{(3,0),i} \lambda^{(0)}_{(4,0),k} \; \overbrace{\varphi(p_1) \varphi_i} \; \overbrace{\varphi_i \varphi_i} \; \overbrace{\varphi_i \varphi_k} \; \overbrace{\varphi_k \varphi_k}. \tag{5.34}$$

This results in an inverse symmetry factor 1/4 in eq. (5.34).

5.2.9 Matrix model calculation for diagram D_5

In figure 5.5 another diagram emerging from eq. (5.13) by the first term on the r.h.s. of eq. (5.10) is depicted. This diagram, D_5, receives, contrary to the previous examples, no contribution from the part $W_1^{(1)} W_1^{(1)}$ in eq. (5.13). The sole contribution to D_5 arises from the part $W_2^{(1)}$ in eq. (5.13) (more

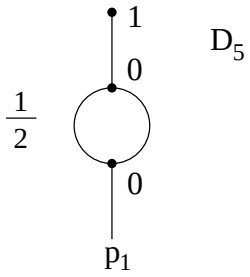

Figure 5.5: diagram D_5 from $W_1^{(2)}$.

precisely, from the third diagram in the second line of figure 4.2).
As indicated in front of diagram D_5 in figure 5.5, the prefactor of this contribution is 1/2. This prefactor results from the multiplication of the factor 1/2 in front of the first term on the r.h.s. of eq. (5.10) with the prefactor of the third diagram in the second line of figure 4.2 from $W_2^{(1)}$, which is 1, giving in total 1/2.
The vertex factor at the vertex with topological index one does not change in the procedure. The vertex factor of the newly created vertex is $1/y_1$, which is exactly the vertex factor of $\mathcal{L}_3^{(0)}$.

5.2.10 Field theory calculation for diagram D_5

This subsection deals with the following question: What is the inverse symmetry factor of diagram D_5? The expression (5.12) is evaluated with respect to diagram D_5 in (5.35). The exponential in the Gell-Mann-Low series is expanded to receive a contribution from $\mathcal{L}_3^{(0)} \cdot \mathcal{L}_3^{(0)} \cdot \mathcal{L}_1^{(1)}$. This leads, since $\mathcal{L}_3^{(0)}$ appears twice and $\mathcal{L}_1^{(1)}$ appears once, to the factor $\frac{1}{2!1!}$ in eq. (5.36). The number of possible Wick contractions is calculated in eq. (5.37). There are $2 \cdot 3$ possible ways to contract $\varphi(p_1)$ with one field from one of the two $\mathcal{L}_3^{(0)}$. Then, there are 3 possible ways to contract the other $\mathcal{L}_3^{(0)}$ with $\mathcal{L}_1^{(1)}$. The remaining two contractions can now be chosen in 2 different ways.

$$\left\langle 0 \middle| \varphi(p_1) e^{\sum_{i=1}^{2s} (\mathcal{L}^{(0)}(a_i) + \frac{1}{N^2} \mathcal{L}^{(1)}(a_i))} \middle| 0 \right\rangle_{D_5} \tag{5.35}$$

$$= \frac{1}{N^4} \frac{1}{2!1!} \left\langle 0 \middle| \varphi(p_1) \sum_{i,j,k=1}^{2s} \mathcal{L}_3^{(0)}(a_i) \mathcal{L}_3^{(0)}(a_j) \mathcal{L}_1^{(1)}(a_k) \middle| 0 \right\rangle_{D_5} \tag{5.36}$$

$$= \frac{1}{N^4} \frac{1}{2!1!} \sum_{i,j,k=1}^{2s} \lambda^{(0)}_{(3,0),i} \lambda^{(0)}_{(3,0),j} \lambda^{(1)}_{(1,0),k} \; \overbrace{\varphi(p_1) \frac{\varphi_i \varphi_i \varphi_i}{3!} \; \frac{\varphi_j \varphi_j \varphi_j}{3!} \; \frac{\varphi_k}{1!}} \cdot (2 \cdot 3) \cdot 3 \cdot 2 \tag{5.37}$$

$$= \frac{1}{N^4} \frac{1}{2} \sum_{i,j,k=1}^{2s} \lambda^{(0)}_{(3,0),i} \lambda^{(0)}_{(3,0),j} \lambda^{(1)}_{(1,0),k} \; \overbrace{\varphi(p_1) \varphi_i} \; \overbrace{\varphi_i \varphi_j} \; \overbrace{\varphi_i \varphi_j} \; \overbrace{\varphi_j \varphi_k} \tag{5.38}$$

This results in an inverse symmetry factor 1/2 in eq. (5.38).

5.2.11 Matrix model calculation for diagram D_6

The examples considered up to now have in common that they only used the first, second and third term on the r.h.s. of eq. (5.10). In figure 5.6

the diagram D_6 is depicted. As indicated by the absence of a fraction in front of D_6 in figure 5.6, the prefactor of this diagram is 1. Such a diagram (i.e. a contribution with these propagators) emerges from eq. (5.13) by the application of the second, third and fourth term on the r.h.s. of eq. (5.10). The calculation of the vertex factor, which arises at the new vertex, is more

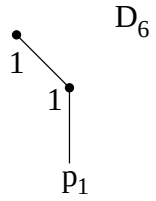

Figure 5.6: diagram D_6 from $W_1^{(2)}$.

complicated than in the examples D_1, D_2, D_3 and D_5.
Three contributions to diagram D_6 arise from the part $W_1^{(1)}W_1^{(1)}$ in eq. (5.13). The first, denoted q_1, emerges from the combination of the first diagram of figure 4.1 with itself. The contribution q_2 emerges from the combination of the first diagram with the second diagram of figure 4.1, whereas q_3 arises from the combination of the second diagram with the first diagram of figure 4.1. A fourth contribution, denoted q_4, emerges from the third diagram in the second line of figure 4.2.
In the following calculation we will concentrate on the contribution q_1:

$$\begin{aligned}
W_1^{(2)}(p_1) &= \left(\sum_{i=1}^{2s} \operatorname*{Res}_{x \to a_i} \frac{dS(p,x)}{dp} \frac{1}{y(x)} W_1^{(1)}(x) W_1^{(1)}(x) \right) + \dots \\
&= \left(\left[\sum_{i=1}^{2s} \operatorname*{Res}_{x \to a_i} \frac{dS(p,x)}{dp} \frac{1}{y(x)} \sum_{j=1}^{2s} \lambda_{(1,0),j}^{(1)} B_j^0(x) \sum_{k=1}^{2s} \lambda_{(1,0),k}^{(1)} B_k^0(x) \right] + \dots \right) + \dots \\
&= \left(\left[\sum_{i,j} \frac{1}{2} B_i^0(p_1) B_{j,i}^{0,0} Z_{1,i} \lambda_{(1,0),j}^{(1)} \lambda_{(1,0),i}^{(1)} \right. \right. \\
&\quad \left. \left. + \sum_{i,k} \frac{1}{2} B_i^0(p_1) B_{k,i}^{0,0} Z_{1,i} \lambda_{(1,0),i}^{(1)} \lambda_{(1,0),k}^{(1)} + \dots \right] + \dots \right) + \dots \quad . \qquad (5.39)
\end{aligned}$$

The third line of eq. (5.39) only evaluates the second and third term on the r.h.s. of eq. (5.10), because only these terms lead to diagram D_6. Then the contribution q_1 to the product of the prefactor and the vertex factor is

$$q_1 = \frac{1}{2} Z_1 \lambda_{(1,0)}^{(1)} \cdot 2. \qquad (5.40)$$

In a similar way, we determine

$$q_2 = \frac{3}{2} Z_2 \lambda^{(1)}_{(0,1)} = q_3. \tag{5.41}$$

For q_2 and q_3, either the second or the third term on the r.h.s. of eq. (5.10) is used. In the following calculation we will concentrate on the contribution q_4:

$$\begin{aligned} W_1^{(2)}(p_1) &= \left(\sum_{i=1}^{2s} \operatorname*{Res}_{x \to a_i} \frac{dS(p,x)}{dp} \frac{1}{y(x)} W_2^{(1)}(x,x) \right) + \dots \\ &= \left(\left[\sum_{i=1}^{2s} \operatorname*{Res}_{x \to a_i} \frac{dS(p,x)}{dp} \frac{1}{y(x)} \sum_{j=1}^{2s} \sum_{m=1}^{2s} \lambda^{(0)}_{(3,0),j} \lambda^{(1)}_{(1,0),m} B^{0,0}_{j,m} B^0_j(x) B^0_j(x) \right] + \dots \right) + \dots \\ &= \left(\left[\sum_{i,m} \frac{1}{2} B^0_i(p_1) Z_{2,i} \lambda^{(0)}_{(3,0),i} \lambda^{(1)}_{(1,0),m} B^{0,0}_{i,m} + \dots \right] + \dots \right) + \dots \quad . \end{aligned} \tag{5.42}$$

The last identity in eq. (5.42) only evaluates the fourth term on the r.h.s. of eq. (5.10), because only this term leads to diagram D_6. Then the contribution q_4 to the product of the prefactor and the vertex factor is

$$q_4 = \frac{1}{2} Z_2 \lambda^{(0)}_{(3,0)}. \tag{5.43}$$

The total contribution q is given by

$$q = q_1 + q_2 + q_3 + q_4 = \frac{3}{4} \frac{(y_2)^2}{(y_1)^4} - \frac{5}{8} \frac{y_3}{(y_1)^3}. \tag{5.44}$$

This expression is related to a previously defined coupling constant from eq. (4.19):

$$\frac{3}{4} \frac{(y_2)^2}{(y_1)^4} - \frac{5}{8} \frac{y_3}{(y_1)^3} = 1 \cdot \lambda^{(1)}_{(2,0)}. \tag{5.45}$$

The fact that the known vertex factor $\lambda^{(1)}_{(2,0)}$ appears in this higher order correction is the crucial point in the construction of an effective field theory. The next subsection deals only with the prefactor of the diagram, because it has been shown by the above calculation that the vertex factor at the newly created vertex is given by $\mathcal{L}_2^{(1)}$. Note that the new vertex factor is not only identical to one of the previously calculated vertex factors, but, as demanded by the field theory, it exactly describes by its lower index $(\alpha_0, \alpha_1) = (2, 0)$ the diagram D_6 close to the vertex connected to p_1. 2 legs with zero derivatives and 0 legs with one derivative emanate from this vertex. The calculated multiplicity of this vertex factor, which is 1 in this case, is the prefactor of the diagram.

5.2.12 Field theory calculation for diagram D_6

We shall now calculate the inverse symmetry factor of diagram D_6. The expression (5.12) is evaluated with respect to diagram D_6 in (5.46). The exponential in the Gell-Mann-Low series is expanded to receive a contribution from $\mathcal{L}_2^{(1)} \cdot \mathcal{L}_1^{(1)}$. This leads, since $\mathcal{L}_2^{(1)}$ and $\mathcal{L}_1^{(1)}$ appear once, to the factor $\frac{1}{1!1!}$ in eq. (5.47). The number of possible Wick contractions is calculated in eq. (5.48). There are 2 possible ways to contract $\varphi(p_1)$ with one field from $\mathcal{L}_2^{(1)}$. The contraction $\mathcal{L}_2^{(1)}$ with $\mathcal{L}_1^{(1)}$ is then fixed.

$$\left\langle 0 \middle| \varphi(p_1) e^{\sum_{i=1}^{2s} (\mathcal{L}^{(0)}(a_i) + \frac{1}{N^2}\mathcal{L}^{(1)}(a_i))} \middle| 0 \right\rangle_{D_6} \tag{5.46}$$

$$= \frac{1}{N^4} \frac{1}{1!1!} \left\langle 0 \middle| \varphi(p_1) \sum_{i,k=1}^{2s} \mathcal{L}_2^{(0)}(a_i) \mathcal{L}_1^{(1)}(a_k) \middle| 0 \right\rangle_{D_6} \tag{5.47}$$

$$= \frac{1}{N^4} \frac{1}{1!1!} \sum_{i,k=1}^{2s} \lambda^{(1)}_{(2,0),i} \lambda^{(1)}_{(1,0),k} \; \overbrace{\varphi(p_1) \frac{\varphi_i \varphi_i}{2!}} \; \overbrace{\frac{\varphi_k}{1!}} \cdot 2 \tag{5.48}$$

$$= \frac{1}{N^4} \sum_{i,k=1}^{2s} \lambda^{(1)}_{(2,0),i} \lambda^{(1)}_{(1,0),k} \; \overbrace{\varphi(p_1) \, \varphi_i} \; \overbrace{\varphi_i \, \varphi_k} \tag{5.49}$$

This results in an inverse symmetry factor 1 in eq. (5.49).

5.2.13 Summary

In the examples D_1, D_2, ..., D_6 we have seen that the vertex factors which emerge by the matrix model calculation are those predicted by the field theory with the Lagrangian $\mathcal{L}_{\text{int}} = \mathcal{L}^{(0)} + \frac{1}{N^2}\mathcal{L}^{(1)}$. In addition, the prefactor of each of these example diagrams, determined by matrix model calculations, is equal to the inverse symmetry factor calculated by field theory methods. From this, we can conjecture that this equality of inverse symmetry factors and prefactors holds for all diagrams of $W_1^{(2)}$. This conjecture will be proved in chapters 8 and 9.

In addition to this important observation, we can learn more from these examples. The first term on the r.h.s. of eq. (5.10) leads to simple prefactor calculations as was the case for diagrams D_1, D_2, D_3 and D_5. These diagrams can be directly associated either to a combination of two diagrams from $W_1^{(1)}$ or to one diagram from $W_2^{(1)}$. The first term on the r.h.s. of eq. (5.10) merges two diagrams from $W_1^{(1)}$ or the two free ends of a diagram from $W_2^{(1)}$ into a new diagram by an additional vertex of topological index 0 with 3 emanating

lines.
On the other hand, the second and third term on the r.h.s. of eq. (5.10) lead to a complex prefactor calculation as was the case for diagrams D_4 and D_6. These diagrams are associated with several contributions. In the creation of a diagram via the second and third term on the r.h.s. of eq. (5.10) one edge shrinks to zero compared to the creation of a diagram via the first term. The two vertices of that edge are fused into one new vertex. This can be observed in the comparison of diagram D_3 in figure 5.3 with diagram D_4 in figure 5.4. It can also be observed in the comparison of diagram D_1 in figure 5.1 with diagram D_6 in figure 5.6.
The fourth term on the r.h.s. of eq. (5.10), as in diagram D_6, also leads to a complex prefactor calculation. D_6 is associated with several contributions. In the creation of a diagram via the fourth term on the r.h.s. of eq. (5.10) two edges shrink to zero compared to the creation of a diagram via the first term. This can be observed in the comparison of diagram D_5 in figure 5.5 with diagram D_6 in figure 5.6.

5.3 The Lagrangian $\mathcal{L}_1^{(2)}$

The Lagrangian $\mathcal{L}_1^{(2)}$ is constructed in analogy to the construction of the Lagrangian $\mathcal{L}_1^{(1)}$ in eq. (4.11). Many diagrams, in particular all diagrams from the previous section, are correctly described by the field theory with $\mathcal{L}_{\text{int}} = \mathcal{L}^{(0)} + \frac{1}{N^2}\mathcal{L}^{(1)}$. These diagrams are reminiscent of the tadpole diagram in $W_1^{(1)}$ (third diagram in figure 4.1) which is correctly described by the field theory with $\mathcal{L}_{\text{int}} = \mathcal{L}^{(0)}$. However, in the case of the two other diagrams in $W_1^{(1)}$ (first and second diagram in figure 4.1), the new part of the Lagrangian $\mathcal{L}_1^{(1)}$ had to be introduced, whereas now a Lagrangian $\mathcal{L}_1^{(2)}$ has to be introduced. There are two diagrams on the level of the $1/N^2$ correction which only consist of one external edge and the vertex (the first two diagrams in figure 4.1). A careful look on the recursion equation (5.13) reveals that there are five such diagrams on the level of the $1/N^4$ correction. These five diagrams are summarized as $\widehat{W}_1^{(2)}$ in figure 5.7.
One of these diagrams is calculated in the following. The fifth diagram in figure 5.7 arises via the fourth term on the r.h.s. of eq. (5.10) from four different origins: (1) from the combination of the second diagram in figure 4.1 with itself, (2) from the fourth diagram in the first line of figure 4.2, (3) from the first diagram in the second line of figure 4.2 and (4) from the second diagram in the second line of figure 4.2. The first contribution, denoted q_1,

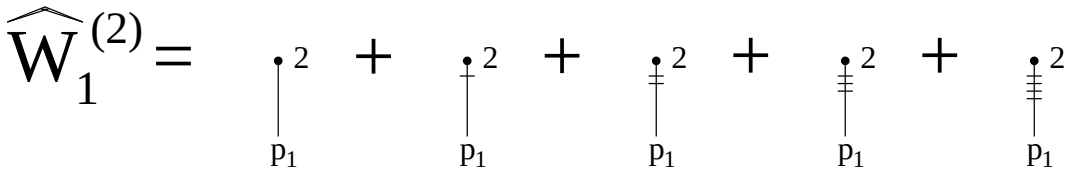

Figure 5.7: Five diagrams of the one point function $W_1^{(2)}(p_1)$. These five diagrams correspond to the first two diagrams of figure 4.1. The interactions with the maximal topological index 2 are added to the Lagrangian as $\mathcal{L}_1^{(2)}$.

is given by

$$q_1 = \frac{1}{2}\cdot 3\cdot 3\cdot \frac{1}{9}\cdot Z_0\lambda^{(1)}_{(0,1)}\lambda^{(1)}_{(0,1)} = \frac{1}{1152}\frac{1}{(y_1)^3}. \tag{5.50}$$

The second, third and fourth contributions, denoted q_2, q_3 and q_4 respectively, are

$$q_2 = \frac{1}{2}\cdot 5\cdot \frac{1}{9}\cdot Z_0\lambda^{(1)}_{(1,0,1)} = \frac{5}{144}\frac{1}{(y_1)^3} = q_3 \tag{5.51}$$

$$q_4 = \frac{1}{2}\cdot 3\cdot 3\cdot \frac{1}{9}\cdot Z_0\lambda^{(1)}_{(0,2,0)} = \frac{1}{48}\frac{1}{(y_1)^3}. \tag{5.52}$$

This results in the definition of the vertex factor

$$\lambda^{(2)}_{(0,0,0,0,1)} = \left(\frac{1}{1152}+\frac{5}{144}+\frac{5}{144}+\frac{1}{48}\right)\frac{1}{(y_1)^3} = \frac{35}{384}\frac{1}{(y_1)^3}. \tag{5.53}$$

The result of the calculation of the other diagrams is given below:

$$\begin{aligned}
\widehat{W}_1^{(2)}(p_1) \;=\; & \sum_{i=1}^{2s}\left(\frac{63}{32}\frac{y_2^4}{y_1^7}-\frac{75}{16}\frac{y_2^2y_3}{y_1^6}+\frac{77}{32}\frac{y_2y_4}{y_1^5}+\frac{145}{128}\frac{y_3^2}{y_1^5}-\frac{105}{128}\frac{y_5}{y_1^4}\right)_i B_i^0(p_1)\\
& +\sum_{i=1}^{2s}\left(-\frac{21}{32}\frac{y_2^3}{y_1^6}+\frac{29}{32}\frac{y_2y_3}{y_1^5}-\frac{35}{128}\frac{y_4}{y_1^4}\right)_i B_i^1(p_1)\\
& +\sum_{i=1}^{2s}\left(\frac{63}{160}\frac{y_2^2}{y_1^5}-\frac{29}{128}\frac{y_3}{y_1^4}\right)_i B_i^2(p_1)\\
& +\sum_{i=1}^{2s}\left(-\frac{29}{128}\frac{y_2}{y_1^4}\right)_i B_i^3(p_1)\\
& +\sum_{i=1}^{2s}\left(\frac{35}{384}\frac{1}{y_1^3}\right)_i B_i^4(p_1).
\end{aligned} \tag{5.54}$$

This leads to five new terms for the Lagrangian:

$$\begin{aligned}\mathcal{L}_1^{(2)} &= \left(\frac{63}{32}\frac{y_2^4}{y_1^7} - \frac{75}{16}\frac{y_2^2 y_3}{y_1^6} + \frac{77}{32}\frac{y_2 y_4}{y_1^5} + \frac{145}{128}\frac{y_3^2}{y_1^5} - \frac{105}{128}\frac{y_5}{y_1^4}\right)\frac{\varphi}{1!} \\ &+ \left(-\frac{21}{32}\frac{y_2^3}{y_1^6} + \frac{29}{32}\frac{y_2 y_3}{y_1^5} - \frac{35}{128}\frac{y_4}{y_1^4}\right)\frac{(\partial\varphi)}{1!} \\ &+ \left(\frac{63}{160}\frac{y_2^2}{y_1^5} - \frac{29}{128}\frac{y_3}{y_1^4}\right)\frac{(\partial^2\varphi)}{1!} \\ &+ \left(-\frac{29}{128}\frac{y_2}{y_1^4}\right)\frac{(\partial^3\varphi)}{1!} \\ &+ \left(\frac{35}{384}\frac{1}{y_1^3}\right)\frac{(\partial^4\varphi)}{1!}. \end{aligned} \tag{5.55}$$

These five new coupling constants are now abbreviated as $\lambda_\alpha^{(2)}$ in the following way:

$$\mathcal{L}_1^{(2)} = \lambda_{(1,0,0,0,0)}^{(2)}\frac{\varphi}{1!} + \lambda_{(0,1,0,0,0)}^{(2)}\frac{(\partial\varphi)}{1!} + \lambda_{(0,0,1,0,0)}^{(2)}\frac{(\partial^2\varphi)}{1!} \tag{5.56}$$

$$+\lambda_{(0,0,0,1,0)}^{(2)}\frac{(\partial^3\varphi)}{1!} + \lambda_{(0,0,0,0,1)}^{(2)}\frac{(\partial^4\varphi)}{1!} = \sum_{\alpha\in M_1^{(2)}}\lambda_\alpha^{(2)}\frac{\varphi^\alpha}{\alpha!}. \tag{5.57}$$

The set $M_1^{(2)}$ consists of all multi-indices $\alpha = (\alpha_0, \ldots, \alpha_4) \in \mathbb{N}^5$ which fulfill the conditions $\sum_{j=0}^4 j\alpha_j \leq 4$ and $\sum_{j=0}^4 \alpha_j = 1$.

5.4 First method to determine diagrams from the free energy $\mathcal{F}^{(2)}$ and the coupling constant $\lambda^{(2)}$

5.4.1 The operator H

In [7], Chekhov and Eynard found an operator which gives $\mathcal{F}^{(h)}$ for $h \geq 2$ as 'integral' of $W_1^{(h)}$. The details of this integration operator, which is called H, are irrelevant for the application to the effective field theory. The important part is that H, applied to the Bergmann kernel, gives the algebraic curve:

$$H \cdot \frac{B(\cdot, p)}{dp} = -\frac{1}{2}y(p). \tag{5.58}$$

Using the formula [7]

$$\mathcal{F}^{(h)} = -\frac{1}{2h-2} H_q \cdot W_1^{(h)}(q) \tag{5.59}$$

for $h \geq 2$ and the eq. (5.1) we arrive at

$$\mathcal{F}^{(h)} = \frac{1}{2h-2} \sum_{\substack{i \\ l \geq 1}} \omega_1^{(h)}(i,l) y_{l,i}, \tag{5.60}$$

where the $l = 0$ part of eq. (5.1) drops out since it leads to a vanishing residuum.
This equation, translated into diagrams, states that the external legs of a diagram are cut: B_i^f is replaced by $-y_{f,i}$ for $f \geq 1$ and by 0 for $f = 0$. That leads to the fact that diagrams from $W_1^{(1)}$ which only differ by the number of derivatives at the external leg are related to one sole diagram in $\mathcal{F}^{(2)}$. The free energies in the zeroth and the first order approximation, $\mathcal{F}^{(0)}$ and $\mathcal{F}^{(1)}$, are special cases. Regarding the calculation of these free energies we refer to [13] and [33].
The fact that a direct calculation of $\mathcal{F}^{(1)}$ in the formalism of Chekhov and Eynard [7] is impossible can immediately be seen in eq. (5.59). This equation contains a factor $\frac{1}{h-1}$, which prevents an application to the case $h = 1$.
The fact that a direct calculation of $\mathcal{F}^{(1)}$ in the field theory formalism is impossible can be seen in the following case: To obtain the tadpole diagram (third diagram from figure 4.1) from the free energy at order one by Δ_1, a vertex with a topological index 0 and only two emanating legs is necessary. Such a vertex factor did not appear up to now in the formalism. The existence of such a vertex would lead to field theory correlators in the planar approximation which are different from the matrix model correlators. Assuming this vertex factor has been calculated somehow, and neglecting the problem with the planar approximation, one problem still remains. The action of Δ_7 on the constructed diagram from $\mathcal{F}^{(1)}$, which gives the tadpole diagram by Δ_1, leads to a diagram with two vertices, whereas all diagrams in $W_1^{(1)}$ have only one vertex.
Contrary to the free energy at planar order and in the $1/N^2$-correction, these obstacles are not present at the second or higher order corrections.

5.4.2 Matrix model calculation for diagram A_1

The application of eq. (5.60) to the diagrams of the correlator $W_1^{(2)}$ significantly reduces the number of diagrams. All diagrams in $W_1^{(2)}$ which differ

only by the number of derivatives at the external leg, correspond to one sole diagram in $\mathcal{F}^{(2)}$. In figure 5.8, the diagram D_6 from $W_1^{(2)}$ and two diagrams from $W_1^{(2)}$, D_7 and D_8, which differ from D_6 only in the number of derivatives at the external leg, are depicted. They lead by eq. (5.60) to diagram A_1 from $\mathcal{F}^{(2)}$. The equation replaces the external legs with l derivatives $B_i^l(p_1)$

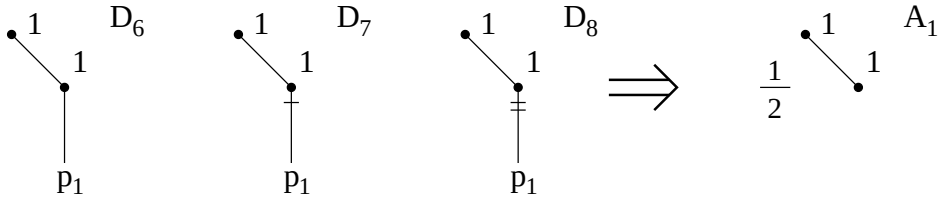

Figure 5.8: diagram D_6 and two further diagrams of $W_1^{(2)}$, lead by eq. (5.60) to a diagram A_1 of $\mathcal{F}^{(2)}$. The prefactor and the new vertex factor of the diagram from $\mathcal{F}^{(2)}$, which are indicated as $\frac{1}{2}$ and by a small 1 close to the lower vertex, are not known a priori, but are calculated by eq. (5.61).

by $(-y_{l,i})$ for $l \geq 1$ and by 0 for $l = 0$. Diagrammatically, this corresponds to cutting the external legs.
The product of the vertex factor and the prefactor of A_1 is calculated by eq. (5.60) to be

$$-\frac{1}{2 \cdot 2 - 2}\left(\lambda^{(1)}_{(2,0)} \cdot 0 + \lambda^{(1)}_{(1,1)}(-y_1) + \lambda^{(1)}_{(1,0,1)}(-y_2)\right) = -\frac{1}{16}\frac{y_2}{(y_1)^2}. \qquad (5.61)$$

The r.h.s. of eq. (5.61) is related to a previously defined coupling constant from eq. (4.12) by

$$-\frac{1}{16}\frac{y_2}{(y_1)^2} = \frac{1}{2}\lambda^{(1)}_{(1,0)}. \qquad (5.62)$$

The fact that the known coupling constant $\lambda^{(1)}_{(1,0)}$ appears in this calculation of $\mathcal{F}^{(2)}$, which is based on the operator H, is a cornerstone in the construction of the effective field theory. Eq. (5.62) leads to a prefactor 1/2 for diagram A_1.

5.4.3 Field theory calculation for diagram A_1

The field theory with the Lagrangian $\mathcal{L}_{\text{int}} = \mathcal{L}^{(0)} + \frac{1}{N^2}\mathcal{L}^{(1)}$ predicts an inverse symmetry factor of diagram A_1. Adapting (5.12) to the free energy by

omitting the field $\varphi(p_1)$ we evaluate the expression

$$\sum_{l=0}^{2} \frac{1}{N^{2l}} \left\langle 0 \middle| e^{\sum_{i=1}^{2s} (\mathcal{L}^{(0)}(a_i) + \frac{1}{N^2}\mathcal{L}^{(1)}(a_i))} \middle| 0 \right\rangle_{l \ loops} \tag{5.63}$$

with respect to diagram A_1 in (5.64). The exponential in the Gell-Mann-Low series is expanded to receive a contribution from $\mathcal{L}_1^{(1)} \cdot \mathcal{L}_1^{(1)}$. This leads, since $\mathcal{L}_1^{(1)}$ appears twice, to the factor $\frac{1}{2!}$ in eq. (5.65). The number of possible Wick contractions in this diagram is calculated in eq. (5.66). There is only 1 possible way to contract $\mathcal{L}_1^{(1)}$ with the other $\mathcal{L}_1^{(1)}$:

$$\left\langle 0 \middle| e^{\sum_{i=1}^{2s} (\mathcal{L}^{(0)}(a_i) + \frac{1}{N^2}\mathcal{L}^{(1)}(a_i))} \middle| 0 \right\rangle_{A_1} \tag{5.64}$$

$$= \frac{1}{N^4} \frac{1}{2!} \left\langle 0 \middle| \sum_{i,k=1}^{2s} \mathcal{L}_1^{(1)}(a_i) \mathcal{L}_1^{(1)}(a_k) \middle| 0 \right\rangle_{A_1} \tag{5.65}$$

$$= \frac{1}{N^4} \frac{1}{2} \sum_{i,k=1}^{2s} \lambda_{(1,0),i}^{(1)} \lambda_{(1,0),k}^{(1)} \overbrace{\varphi_i \, \varphi_k}. \tag{5.66}$$

This results in an inverse symmetry factor 1/2 in eq. (5.66).

5.4.4 Calculation of $\lambda^{(2)}$

Applying the above method to the five diagrams from $\widehat{W}_2^{(1)}$ results in one diagram with a topological index 2. It is a one-vertex diagram without internal and external legs, i.e. it only consists of the vertex factor $\lambda^{(2)} = \lambda_{(0,0,\ldots)}^{(2)}$:

$$\begin{aligned} \lambda^{(2)} &= -\frac{1}{2 \cdot 2 - 2} \Big(\lambda_{(1,0,0,0,0)}^{(2)} \cdot 0 + \lambda_{(0,1,0,0,0)}^{(2)}(-y_1) + \lambda_{(0,0,1,0,0)}^{(2)}(-y_2) \\ &\quad + \lambda_{(0,0,0,1,0)}^{(2)}(-y_3) + \lambda_{(0,0,0,0,1)}^{(2)}(-y_4) \Big) \qquad (5.67) \\ &= -\frac{21}{160} \frac{y_2^3}{y_1^5} + \frac{29}{128} \frac{y_2 y_3}{y_1^4} - \frac{35}{384} \frac{y_4}{y_1^3}. \qquad (5.68) \end{aligned}$$

5.5 Second method to determine diagrams from the free energy $\mathcal{F}^{(2)}$ and the coupling constant $\lambda^{(2)}$

5.5.1 Matrix model calculation for diagram A_1

The action of Δ_7 (eq. (3.32)) on diagram A_1 leads to the diagram D_1, depicted in figure 5.9. The aim is to determine the prefactor of the diagram A_1 from $\mathcal{F}^{(2)}$. The prefactor $1/2$ of diagram D_1 from $W_1^{(2)}$ was calculated in eq. (5.14). Since Δ_7 can only be applied to D_1 on one edge to obtain A_1,

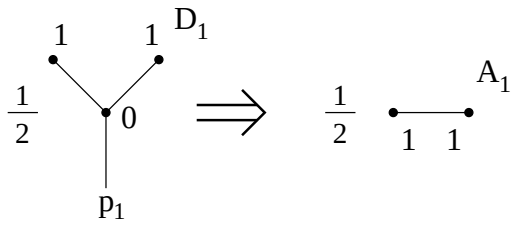

Figure 5.9: To calculate the prefactor of the diagram A_1 from the free energy we apply Δ_7 to it.

the prefactor of diagram A_1 must be $1/2$ as the prefactor of diagram D_1.
It was already shown in eq. (5.66), that the field theory reproduces this prefactor as an inverse symmetry factor.

5.5.2 Calculation of $\lambda^{(2)}$

The loop operator is inverted by this method directly in the form of the seven terms $\Delta_1, \ldots, \Delta_7$. Starting from the diagram of the free energy without any edges, we apply the loop operator term Δ_2. Acting on the loop operator, this gives, as already was noted in eqs. (3.39) and (4.14), the negative of the derivative with respect to y_f, $f = 1, 2, 3, \ldots$. For the order two, we have four

equations:

$$-\frac{\partial}{\partial y_1}\lambda^{(2)} = \lambda^{(2)}_{(0,1,0,0,0)} \tag{5.69}$$

$$-\frac{\partial}{\partial y_2}\lambda^{(2)} = \lambda^{(2)}_{(0,0,1,0,0)} \tag{5.70}$$

$$-\frac{\partial}{\partial y_3}\lambda^{(2)} = \lambda^{(2)}_{(0,0,0,1,0)} \tag{5.71}$$

$$-\frac{\partial}{\partial y_4}\lambda^{(2)} = \lambda^{(2)}_{(0,0,0,0,1)}. \tag{5.72}$$

$\lambda^{(2)}$ is a function of four variables y_1, y_2, y_3 and y_4. Since there are four conditions to determine a function of four variables, a solution, which is unique up to a constant, exists. However, it is not possible to solve this coupled system of equations in general. Fortunately, we can use the fact that in $\lambda^{(2)}_{\alpha'}$ with $\alpha'_j = \delta_{j,k'}$ and $k' = 0, \ldots, 4$ there are no y_1 independent terms. Therefore the system of equations can be solved easily by:

$$\lambda^{(2)} = \text{antiderivative of } (-\lambda^{(2)}_{(0,1,0,0,0)}) \text{ with respect to } y_1 \tag{5.73}$$

$$= \text{antiderivative of } \left(\frac{21}{32}\frac{y_2^3}{y_1^6} - \frac{29}{32}\frac{y_2 y_3}{y_1^5} + \frac{35}{128}\frac{y_4}{y_1^4}\right) \text{ with respect to } y_1$$

$$= -\frac{21}{160}\,\frac{y_2^3}{y_1^5} + \frac{29}{128}\,\frac{y_2 y_3}{y_1^4} - \frac{35}{384}\,\frac{y_4}{y_1^3}. \tag{5.74}$$

5.5.3 Advantages of the second method

As regards the coupling constant $\lambda^{(2)}$, the second method requires less computations, because it only needs as an input $\lambda^{(2)}_{(0,1,0,0,0)}$, whereas the complicated computation of of all five $\lambda^{(2)}_{\alpha'}$ with $\alpha'_j = \delta_{j,k'}$ and $k' = 0, \ldots, 4$, is a necessary precondition for the first method.
As regards the other diagrams of the free energy, the second method is better for the following two reasons. To calculate one diagram from $\mathcal{F}^{(2)}$ by the second method, it suffices, as exemplified in figure 5.9, to calculate one diagram from $W_1^{(2)}$. Using the first method, exemplified in figure 5.8, requires the calculation of several diagrams from $W_1^{(2)}$.
The most important advantage of the second method is that the vertex factor, because it is always $1/y_1$, drops from the discussion and the prefactors can be calculated without interference by the different vertex factors. For the first method, on the other hand, one or more vertex factors of diagrams from $W_1^{(2)}$ and one vertex factor of the diagram from $\mathcal{F}^{(2)}$ must be calculated. In the example of diagram A_1, these calculations include the determination

of a vertex factor of D_6 in eq. (5.44), D_7, D_8 (not displayed) and A_1 in eq. (5.61).

5.6 The free energy $\mathcal{F}^{(2)}$

By the above described methods now all terms of $\mathcal{F}^{(2)}$ can be calculated. First of all, all diagrams of the correlator $W_1^{(2)}$, created by eq. (5.13), are drawn. There are 70 diagrams. In practise, it is not necessary to actually calculate the vertex factors and the prefactor by eq. (5.13). It is sufficient to know all propagator combinations.

Then, by the first method, we restrict ourselves to 25 of these 70 diagrams which have at least one derivative at the external leg. Among them are D_7 and D_8 from figure 5.8 and the last four diagrams from figure 5.7. These 25 diagrams are calculated by eq. (5.13) including their vertex factor and prefactor. From these 25 diagrams now emerge by the cutting procedure, which was visualized in figure 5.8, all diagrams of the free energy.
Included in this list is the diagram with no internal and no external lines. This diagram just consists of one vertex without any emerging lines. The vertex has the vertex factor $\lambda^{(2)} = \lambda^{(2)}_{(0,0,\ldots)}$ which was already calculated by the first method in eq. (5.68). This gives the result depicted in figure 5.10. Despite the use of the field theory notation, note that figure 5.10 represents the matrix model calculation.

The calculation of the complete free energy $\mathcal{F}^{(2)}$ by the second method works as follows. Every diagram of the free energy $\mathcal{F}^{(2)}$ with the exception of the already calculated one vertex diagram with topological index 2 and vertex factor $\lambda^{(2)}$ (eq. (5.74)) has at least one internal edge. To each of these internal edges of each diagram of the free energy the loop operator term Δ_7 is applied. This results in a certain number of diagrams of $W_1^{(2)}$. These are 17 of the 70 diagrams of $W_1^{(2)}$, which have to be calculated including the vertex factor and the prefactor. Fortunately, these 17 diagrams are very easy to calculate since the new vertex factor is always $1/y_1$ and emerges entirely from the first term on the r.h.s. of eq. (5.10). However, there is an even simpler way to perform the calculation. For this way, it is not necessary to draw all 70 diagrams of $W_1^{(2)}$. Taking as an input all maximally possible $3 \cdot 3$ combinations of diagrams from $W_1^{(1)} \cdot W_1^{(1)}$ and all 14 diagrams of $W_2^{(1)}$ suffices to determine all diagams of the free energy. Only 6 of the $3 \cdot 3$ combinations of diagrams from $W_1^{(1)} \cdot W_1^{(1)}$ lead to different diagrams in $W_1^{(2)}$. Only 11 of 14

diagrams from $W_2^{(1)}$ lead to different diagrams in $W_1^{(2)}$. We will not reduce the number of diagrams further, although it would be possible, because one diagram from the free energy which has two or more edges (which are not all pairwise equivalent to each other) leads by the application of Δ_7 to different diagrams of $W_1^{(2)}$. To calculate the prefactor of the diagram from the free energy, one of these diagrams from $W_1^{(2)}$ suffices. As in example A_1 in figure 5.9 the prefactors for all $6+11$ diagrams are calculated. This gives the result depicted in figure 5.10 Despite the use of the field theory notation, note that figure 5.10 represents the matrix model calculation.

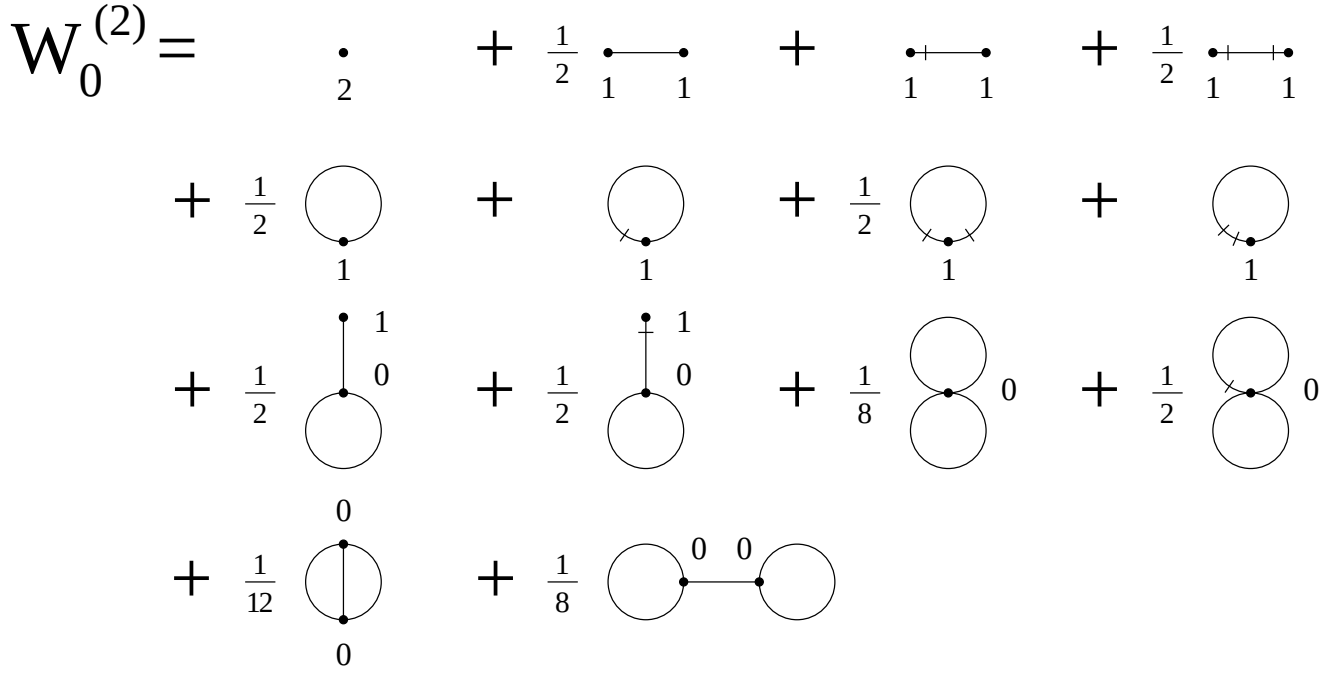

Figure 5.10: Free energy $W_0^{(2)} = \mathcal{F}^{(2)}$.

The contribution to $\mathcal{F}^{(2)}$ from diagram A_1, which is the second diagram in the first line of figure 5.10, is given by:

$$\frac{1}{2}\sum_{i,j=1}^{2s} \lambda^{(1)}_{(1,0),i}\lambda^{(0)}_{(1,0),j}B^{0,0}_{i,j}.$$

5.7 A field theory which describes the free energy $\mathcal{F}^{(2)}$

The result of the matrix model calculation is already displayed in figure 5.10 in diagrams. The vertex factors emerging from the matrix model calculation have already been calculated to coincide with the vertex factors produced by different terms of the Lagrangian. This leaves only two tasks: Firstly, it must be shown that these diagrams and no more are generated by the field theory description, and, secondly, the prefactors noted in figure 5.10 must match the inverse symmetry factors for all these diagrams.
The first diagram in the first line of figure 5.10 is not predicted by the Lagrangian $\mathcal{L}^{(0)} + \frac{1}{N^2}\mathcal{L}^{(1)}$. For this diagram, a new term, emerging from the action of the loop equation, has to be added to the Lagrangian:

$$\mathcal{L}_0^{(2)} = \left(-\frac{21}{160}\,\frac{y_2^3}{y_1^5} + \frac{29}{128}\,\frac{y_2 y_3}{y_1^4} - \frac{35}{384}\,\frac{y_4}{y_1^3} \right) = \lambda^{(2)}. \tag{5.75}$$

The evaluation of

$$\sum_{l=0}^{2} \frac{1}{N^{2l}} \left\langle 0 \middle| e^{\sum_{i=1}^{2s} (\mathcal{L}^{(0)}(a_i) + \frac{1}{N^2}\mathcal{L}^{(1)}(a_i) + \frac{1}{N^4}\mathcal{L}_0^{(2)}(a_i))} \middle| 0 \right\rangle_{l \ loops} \tag{5.76}$$

with respect to the term proportional to $1/N^4$ exactly gives the same 14 diagrams, which are noted in figure 5.10. It remains to show that the symmetry factors of these diagrams correspond to the prefactors noted in 5.10. This was already done for the second diagram in the first line of figure 5.10, A_1, in eq. (5.66). The calculation for the other 13 diagrams is similar. It reveals that all of the inverse symmetry factors are equal to the prefactors.
We conclude this section by the statement that the free energy $\mathcal{F}^{(2)}$ is described by the field theory eq. (5.76).

Chapter 6

The loop equation of the effective field theory

6.1 Derivation

The first two coupling constants, $\lambda^{(0)}$ and $\lambda^{(1)}$, are functions of y_1. The coupling constant $\lambda^{(2)}$ is a function of y_1, y_2, y_3 and y_4. An inspection of eq. (2.52) and eq. (5.10) reveals that $\lambda^{(h)}$ for $h \geq 2$ is a function of $y_1, \ldots, y_{3h-2}$. The coupling constants $\lambda^{(h)}$ of higher order $h \geq 2$ are determined in the following by the second method in analogy to the case $h = 2$ from eq. (5.73). The loop equation for the correlators (eq. (2.52)) can be transformed in an equation for the coupling constants:

$$\begin{aligned}\lambda_{\alpha'}^{(h)} = &\sum_{m=1}^{h-1} \sum_{\alpha \in M_1^{(h-m)}} \sum_{\beta \in M_1^{(m)}} \frac{2A_\alpha A_\beta}{2k'+1} Z_{n(\alpha,\beta,m)-k'+1} \lambda_\alpha^{(h-m)} \lambda_\beta^{(m)} \\ &+ \sum_{\alpha \in M_2^{(h-1)}} \left(2 - \sum_{f=0}^{3h-4} \delta_{\alpha_f,2}\right) \frac{2A_\alpha}{2k'+1} Z_{n(\alpha)-k'+1} \lambda_\alpha^{(h-1)} \end{aligned} \tag{6.1}$$

where $A_\alpha = \prod_{f=0}^{\infty} (f+1/2)^{\alpha_f}$, the first index $n(\alpha) = 1 + \sum_{j=0}^{3h-4} j\alpha_j$,
the second index $n(\alpha, \beta, m) = 1 + \sum_{j=0}^{3(h-m)-2} j\alpha_j + \sum_{j=0}^{3m-2} j\beta_j$
and $\alpha'_j = \delta_{j,k'}$ with $k' = 0, \ldots, 3h-2$.
The set $M_k^{(h)}$ consists of all multi-indices $\alpha = (\alpha_0, \ldots, \alpha_{k+3h-3}) \in (\mathbb{N}_0)^{k+3h-2}$ which fulfill the conditions $\sum_{j=0}^{k+3h-3} j\alpha_j \leq k + 3h - 3$ and $\sum_{j=0}^{k+3h-3} \alpha_j = k$.
Note that only the fourth term on the r.h.s. of eq. (5.10) contributes to $\lambda_{\alpha'}^{(h)}$.
The integration in eq. (5.73) for $h = 2$ can be generalized for $h \geq 2$. Since

there are no y_1 independent parts of $\lambda^{(h)}_{\alpha'}$, one can deduce by induction over $h \geq 2$:

$$\lambda^{(h)} = \text{ antiderivative of } (-\lambda^{(h)}_{(0,1,0,0,\cdots,0)}) \text{ with respect to } y_1. \tag{6.2}$$

One can also eliminate the elementary integration in the equation.
We obtain, after integration for $h \geq 2$,

$$\begin{aligned}\lambda^{(h)} = &\sum_{m=1}^{h-1} \sum_{\alpha \in M_1^{(h-m)}} \sum_{\beta \in M_1^{(m)}} \sum_{k,r,r'=0}^{\infty} \frac{2A_\alpha A_\beta}{3(k+r+r')} \frac{Z^{[k]}_{n(\alpha,\beta,m)}}{(y_1)^k} (P_r D_\alpha \lambda^{(h-m)})(P_{r'} D_\beta \lambda^{(m)}) \\ &+ \sum_{\alpha \in M_2^{(h-1)}} \sum_{k,r=0}^{\infty} \left(2 - \sum_{f=0}^{3h-4} \delta_{\alpha_f,2}\right) \frac{2A_\alpha}{3(k+r)} \frac{Z^{[k]}_{n(\alpha)}}{(y_1)^k} (P_r D_\alpha \lambda^{(h-1)}) \end{aligned} \tag{6.3}$$

where P_r is a projection operator: $P_r \sum_{f=0}^{\infty} c_f / y_1^f = c_r / y_1^r$.

There are only notational reasons to introduce infinite sums. For all sums in this equation an upper bound can easily be given. The vertex factor of the free energy of order h can be determined with this equation recursively. Note that only differential operators and simple projection operators are used in this procedure, but no integration has to be performed. Therefore no operator inversion in any sense is necessary to solve the equation recursively. In that sense the equation is remarkably simple.

6.2 Solution

Usually the explicit solutions of loop equations are given up to the second order correction ($\sim 1/N^4$) (eq. (4.8) (alias eq. (54)) in [7] or eq. (4-49) in [13]). The solution of eq. (6.3) is written down up to the fifth order correction ($\sim 1/N^{10}$). Even higher order corrections up to the tenth order ($\sim 1/N^{20}$) were calculated (table 6.1) but could not be displayed due to the large number of terms.

h	0	1	2	3	4	5	6	7	8	9	10
# of terms in $\lambda^{(h)}$	1	-	3	11	30	77	176	385	792	1575	3010

Table 6.1: number of terms in $\lambda^{(h)}$

The explicit solution of the loop equation (6.3) for the coupling constant of the orders three to five is given. For completeness, also the lower orders, zero

to two, which were calculated in eqs. (3.22), (4.17), (5.68) and (5.74), are stated in the following list.

$$\begin{aligned}
\lambda^{(0)} &= \frac{1}{y_1} \\
\lambda^{(1)} &= -\frac{1}{24}\log y_1 \\
\lambda^{(2)} &= -\frac{21}{160}\,\frac{y_2^3}{y_1^5} + \frac{29}{128}\,\frac{y_2 y_3}{y_1^4} - \frac{35}{384}\,\frac{y_4}{y_1^3}.
\end{aligned}$$

$$\lambda^{(3)} = \frac{2205}{256}\frac{y_2^6}{y_1^{10}} - \frac{8685}{256}\frac{y_2^4 y_3}{y_1^9} + \frac{15375}{512}\frac{y_2^2 y_3^2}{y_1^8} + \frac{5565}{256}\frac{y_2^3 y_4}{y_1^8} - \frac{72875}{21504}\frac{y_3^3}{y_1^7}$$
$$-\frac{5605}{256}\frac{y_2 y_3 y_4}{y_1^7} - \frac{3213}{256}\frac{y_2^2 y_5}{y_1^7} + \frac{21245}{9216}\frac{y_4^2}{y_1^6} + \frac{2515}{512}\frac{y_3 y_5}{y_1^6} + \frac{5929}{1024}\frac{y_2 y_6}{y_1^6} - \frac{5005}{3072}\frac{y_7}{y_1^5}$$

$$\begin{aligned}
\lambda^{(4)} = &-\frac{8437275}{32768}\frac{y_5 y_6}{y_1^8} + \frac{1511055}{2048}\frac{y_2 y_5^2}{y_1^9} - \frac{12677665}{32768}\frac{y_2 y_9}{y_1^8} - \frac{32418925}{24576}\frac{y_3^3 y_4}{y_1^{10}} \\
&+\frac{11532675}{16384}\frac{y_3^2 y_6}{y_1^9} - \frac{10156575}{32768}\frac{y_3 y_8}{y_1^8} - \frac{8913905}{32768}\frac{y_4 y_7}{y_1^8} + \frac{4456305}{512}\frac{y_2^6 y_4}{y_1^{13}} \\
&-\frac{12829887}{1024}\frac{y_2^7 y_3}{y_1^{14}} + \frac{98342775}{4096}\frac{y_2^5 y_3^2}{y_1^{13}} - \frac{12093543}{2048}\frac{y_2^5 y_5}{y_1^{12}} + \frac{15411627}{4096}\frac{y_2^4 y_6}{y_1^{11}} \\
&-\frac{16200375}{1024}\frac{y_2^3 y_3^3}{y_1^{12}} - \frac{44207163}{20480}\frac{y_2^3 y_7}{y_1^{10}} + \frac{83895625}{32768}\frac{y_2 y_3^4}{y_1^{11}} - \frac{578655}{128}\frac{y_2 y_3^2 y_5}{y_1^{10}} \\
&+\frac{13024935}{1024}\frac{y_2^3 y_3 y_5}{y_1^{11}} + \frac{12367845}{2048}\frac{y_2^3 y_4^2}{y_1^{11}} + \frac{21023793}{10240}\frac{y_2^9}{y_1^{15}} - \frac{26413065}{1024}\frac{y_2^4 y_3 y_4}{y_1^{12}} \\
&+\frac{7503125}{36864}\frac{y_4^3}{y_1^9} + \frac{4297293}{4096}\frac{y_2^2 y_8}{y_1^9} + \frac{2642325}{2048}\frac{y_3 y_4 y_5}{y_1^9} - \frac{5472621}{1024}\frac{y_2^2 y_3 y_6}{y_1^{10}} \\
&-\frac{10050831}{2048}\frac{y_2^2 y_4 y_5}{y_1^{10}} + \frac{8083075}{98304}\frac{y_{10}}{y_1^7} - \frac{17562825}{4096}\frac{y_2 y_3 y_4^2}{y_1^{10}} + \frac{6968247}{4096}\frac{y_2 y_3 y_7}{y_1^9} \\
&+\frac{68294625}{4096}\frac{y_2^2 y_3^2 y_4}{y_1^{11}} + \frac{6242775}{4096}\frac{y_2 y_4 y_6}{y_1^9}
\end{aligned}$$

$$\lambda^{(5)} = -\frac{30087162105}{32768}\frac{y_2^2y_3y_9}{y_1^{12}} + \frac{20308307985}{8192}\frac{y_2^2y_4^2y_5}{y_1^{13}} - \frac{26135514405}{32768}\frac{y_2^2y_4y_8}{y_1^{12}} + \frac{1336297095}{512}\frac{y_2^2y_3y_5^2}{y_1^{13}}$$
$$+\frac{739690835625}{32768}\frac{y_2^4y_3^2y_5}{y_1^{15}} + \frac{10981859175}{512}\frac{y_2^4y_3y_4^2}{y_1^{15}} - \frac{179984279475}{32768}\frac{y_2^4y_3y_7}{y_1^{14}} - \frac{357630901425}{32768}\frac{y_2^2y_3^2y_4^2}{y_1^{14}}$$
$$+\frac{98590152375}{32768}\frac{y_2^2y_3^2y_7}{y_1^{13}} - \frac{24241354137}{32768}\frac{y_2^2y_5y_7}{y_1^{12}} + \frac{40226430195}{4096}\frac{y_2^5y_4y_5}{y_1^{15}} - \frac{1632433564125}{32768}\frac{y_2^5y_3^2y_4}{y_1^{16}}$$
$$+\frac{350207643555}{32768}\frac{y_2^5y_3y_6}{y_1^{15}} + \frac{261787425795}{8192}\frac{y_2^7y_3y_4}{y_1^{17}} - \frac{9732778965}{512}\frac{y_2^6y_3y_5}{y_1^{16}} - \frac{37121844375}{4096}\frac{y_2^3y_3^2y_6}{y_1^{14}}$$
$$+\frac{11830867475}{8192}\frac{y_2y_3y_4^3}{y_1^{13}} - \frac{8775042255}{8192}\frac{y_2^{12}}{y_1^{20}} - \frac{877489930625}{262144}\frac{y_2y_3^4y_4}{y_1^{14}} + \frac{12359275929}{65536}\frac{y_2y_6y_7}{y_1^{11}}$$
$$+\frac{3222490635}{16384}\frac{y_2y_5y_8}{y_1^{11}} + \frac{33732646101}{16384}\frac{y_2^3y_5y_6}{y_1^{13}} - \frac{26915796875}{262144}\frac{y_3^6}{y_1^{14}} + \frac{217019504625}{131072}\frac{y_2y_3^3y_6}{y_1^{13}}$$
$$+\frac{12983424025}{131072}\frac{y_3^2y_9}{y_1^{11}} - \frac{5553643095}{4096}\frac{y_2^5y_8}{y_1^{14}} - \frac{2109682575}{65536}\frac{y_4y_{10}}{y_1^{10}} - \frac{136426972815}{8192}\frac{y_2^3y_3y_4y_5}{y_1^{14}}$$
$$-\frac{12753475735}{262144}\frac{y_2y_{12}}{y_1^{10}} + \frac{35383072725}{16384}\frac{y_2^6y_7}{y_1^{15}} - \frac{52671571029}{16384}\frac{y_2^7y_6}{y_1^{16}} + \frac{1122904568025}{32768}\frac{y_2^6y_3^3}{y_1^{17}}$$
$$+\frac{74926833597}{16384}\frac{y_2^8y_5}{y_1^{17}} + \frac{20420786925}{262144}\frac{y_3y_6^2}{y_1^{11}} + \frac{8203397345}{32768}\frac{y_2y_3y_{10}}{y_1^{11}} - \frac{37992975405}{65536}\frac{y_2y_4^2y_6}{y_1^{12}}$$
$$-\frac{250975486125}{32768}\frac{y_2^2y_3^3y_5}{y_1^{14}} + \frac{144886833945}{16384}\frac{y_2^{10}y_3}{y_1^{19}} - \frac{147985547535}{16384}\frac{y_2^6y_4^2}{y_1^{16}} + \frac{10137152025}{4096}\frac{y_2^3y_3y_8}{y_1^{13}}$$
$$+\frac{21786582125}{32768}\frac{y_3^3y_4^2}{y_1^{13}} - \frac{3611933325}{131072}\frac{y_6y_8}{y_1^{10}} - \frac{161462697165}{32768}\frac{y_2^4y_4y_6}{y_1^{14}} - \frac{9188135775}{16384}\frac{y_2y_4y_5^2}{y_1^{12}}$$
$$+\frac{5226845715}{32768}\frac{y_3y_5y_7}{y_1^{11}} + \frac{91746650625}{262144}\frac{y_3^4y_5}{y_1^{13}} - \frac{21601719825}{8192}\frac{y_2^3y_4^3}{y_1^{14}} + \frac{176853471795}{32768}\frac{y_2^2y_3y_4y_6}{y_1^{13}}$$
$$-\frac{2481504025}{65536}\frac{y_3y_{11}}{y_1^{10}} + \frac{951059690625}{262144}\frac{y_2^2y_3^5}{y_1^{15}} - \frac{12688164489}{32768}\frac{y_2^3y_{10}}{y_1^{12}} - \frac{26018510375}{131072}\frac{y_3^3y_7}{y_1^{12}}$$
$$-\frac{19518799797}{8192}\frac{y_2^4y_5^2}{y_1^{14}} + \frac{4685481675}{32768}\frac{y_4y_5y_6}{y_1^{11}} + \frac{17861648805}{8192}\frac{y_2^3y_4y_7}{y_1^{13}} - \frac{16063796175}{32768}\frac{y_3y_4^2y_5}{y_1^{12}}$$
$$-\frac{47335422519}{131072}\frac{y_2^2y_6^2}{y_1^{12}} - \frac{625336273125}{32768}\frac{y_2^4y_3^4}{y_1^{16}} - \frac{430379379675}{16384}\frac{y_2^8y_3^2}{y_1^{18}} - \frac{24057537075}{32768}\frac{y_2y_3^2y_8}{y_1^{12}}$$
$$+\frac{7044102065}{32768}\frac{y_2y_4y_9}{y_1^{11}} - \frac{20008618245}{16384}\frac{y_2y_3y_5y_6}{y_1^{12}} + \frac{74747945475}{16384}\frac{y_2y_3^2y_4y_5}{y_1^{13}} - \frac{42370573245}{32768}\frac{y_2y_3y_4y_7}{y_1^{12}}$$
$$-\frac{69991007625}{131072}\frac{y_3^2y_4y_6}{y_1^{12}} + \frac{5635204575}{32768}\frac{y_3y_4y_8}{y_1^{11}} - \frac{104068152405}{16384}\frac{y_2^9y_4}{y_1^{18}} + \frac{861719557125}{32768}\frac{y_2^3y_3^3y_4}{y_1^{15}}$$
$$-\frac{1909423425}{65536}\frac{y_5y_9}{y_1^{10}} + \frac{25370560215}{32768}\frac{y_2^4y_9}{y_1^{13}} + \frac{5234922693}{32768}\frac{y_2^2y_{11}}{y_1^{11}} - \frac{5081656475}{131072}\frac{y_4^4}{y_1^{12}}$$
$$-\frac{3545717175}{262144}\frac{y_7^2}{y_1^{10}} + \frac{6506875375}{786432}\frac{y_{13}}{y_1^9} + \frac{4154848425}{180224}\frac{y_5^3}{y_1^{11}} - \frac{8459871525}{32768}\frac{y_3^2y_5^2}{y_1^{12}}$$
$$+\frac{4958959005}{65536}\frac{y_4^2y_7}{y_1^{11}}$$

Chapter 7

Main Results

The different terms of the Lagrangian with the topological index h read

$$\mathcal{L}_k^{(h)}(a_i) = \sum_{\alpha \in M_k^{(h)}} \lambda_{\alpha,i}^{(h)} \frac{\varphi_i^{\alpha_0} (\partial^1 \varphi)_i^{\alpha_1} \cdots (\partial^{k+3h-3} \varphi)_i^{\alpha_{k+3h-3}}}{\alpha_0! \;\; \alpha_1! \quad \cdots \quad \alpha_{k+3h-3}!} = \sum_{\alpha \in M_k^{(h)}} \lambda_{\alpha,i}^{(h)} \frac{\varphi_i^{\alpha}}{\alpha!}.$$

The set $M_k^{(h)}$ consists of all multi-indices $\alpha = (\alpha_0, \ldots, \alpha_{k+3h-3}) \in (\mathbb{N}_0)^{k+3h-2}$ which fulfill the conditions $\sum_{j=0}^{k+3h-3} j\alpha_j \leq k + 3h - 3$ and $\sum_{j=0}^{k+3h-3} \alpha_j = k$. A formula for the number of terms in $\mathcal{L}_k^{(h)}$, i.e. the number of elements of the set $M_k^{(h)}$, is given in appendix A. In analogy to eqs. (3.39), (4.14) and (4.22) we define the operator

$$D_\alpha^{(h)} = \left(\prod_{f=1}^{k+3h-3} \left(-\frac{\partial}{\partial y_f} \right)^{\alpha_f} \right) \left(\sum_{f=1}^{\infty} (2f+1) \frac{y_{f+1}}{y_1} \frac{\partial}{\partial y_f} \right)^{\alpha_0 - 3\,\delta_{h,0}}. \tag{7.1}$$

The two parts of this operator can be associated with Δ_1 and Δ_2 (eq. (3.30)). The coupling constant of a vertex of topological index h which contains α_i emanating legs with i derivatives, is given by

$$\lambda_\alpha^{(h)} = D_\alpha^{(h)} \lambda^{(h)}. \tag{7.2}$$

By definition, $D_\alpha^{(h)} = D_\alpha$ for all $h \in \mathbb{N}$ (cf. eq. (4.14)). This operator, as was discussed in section 3.6, is sufficient to describe the action of the loop operator on the level of the Lagrangian for the 1-vertex diagrams with exclusively external legs. The discussion in section 3.6 extends to all orders. The calculation of the coupling constants $\lambda^{(h)}$ is described in chapter 6. The

lowest orders are

$$\begin{aligned}\lambda^{(0)} &= \frac{1}{y_1}\\ \lambda^{(1)} &= -\frac{1}{24}\log y_1\\ \lambda^{(2)} &= -\frac{21}{160}\,\frac{y_2^3}{y_1^5}+\frac{29}{128}\,\frac{y_2y_3}{y_1^4}-\frac{35}{384}\,\frac{y_4}{y_1^3}.\end{aligned}$$

The expression $\lambda_{\alpha,i}^{(h)}$ can be obtained from the expression $\lambda_\alpha^{(h)}$ by substituting each y_f for $y_{f,i}$.

$$\begin{aligned}\mathcal{L}^{(0)} &= \mathcal{L}_3^{(0)}+\mathcal{L}_4^{(0)}+\dots\\ \mathcal{L}^{(1)} &= \mathcal{L}_1^{(1)}+\mathcal{L}_2^{(1)}+\mathcal{L}_3^{(1)}+\mathcal{L}_4^{(1)}+\dots\\ \mathcal{L}^{(h)} &= \mathcal{L}_0^{(h)}+\mathcal{L}_1^{(h)}+\mathcal{L}_2^{(h)}+\mathcal{L}_3^{(h)}+\mathcal{L}_4^{(h)}+\dots \text{ for } h\geq 2\end{aligned}$$

We would like to exclude four special cases from the correlators and define

$$\overline{W}_k = W_k-\delta_{k,0}(\mathcal{F}^{(0)}+\frac{1}{N^2}\mathcal{F}^{(1)})-\delta_{k,1}W_1^{(0)}-\delta_{k,2}W_2^{(0)}.$$

For the two special free energies, we refer to [13] and [33]. The two special correlators are described directly by the spectral curve and the Bergmann kernel [6]. The expression $\langle 0|\dots|0\rangle_{l \text{ loops}}$ denotes the sum of all l loop diagrams of $\langle 0|\dots|0\rangle_{conn}$.

Theorem 1

With the Lagrangian $\mathcal{L}=\mathcal{L}^{(0)}+\frac{1}{N^2}\mathcal{L}^{(1)}+\frac{1}{N^4}\mathcal{L}^{(2)}+\dots$ the Hermitean 1-matrix model correlation functions and the free energy ($\mathcal{F}^{(h)}\equiv W_0^{(h)}$) are given by

$$\overline{W}_k(p_1,\dots,p_k)=\sum_{l=0}^{\infty}\frac{1}{N^{2l}}\left\langle 0\,\middle|\,\varphi(p_1)\cdots\varphi(p_k)e^{\sum_{i=1}^{2s}\mathcal{L}(a_i)}\,\middle|\,0\right\rangle_{l \text{ loops}}.$$

This theorem implies that the correlation function $W_k^{(h)}$ consists of all connected diagrams with k external legs where the sum of topological indices h_j of the vertices plus the number of loops l in the diagram is equal to h: $l+\sum_j h_j=h$.

To proof theorem 1, the following equivalent formulation as theorem 1a is more appropriate. The structure μ of a vertex is defined by $\mu = (h, \alpha)$, where h is the topological index of the vertex and $\alpha = (\alpha_0, \alpha_1, \alpha_2, \ldots)$ determines with α_j the number of emanating lines with a j-th derivative. In a given diagram D, with n vertices, the vertex j has a vertex structure $\mu_j = (h_j, \alpha(\mu_j))$. The internal line x connects vertex $i(x)$ with $k(x)$ derivatives to vertex $j(x)$ with $l(x)$ derivatives. The external line v connects p_v to vertex $d(v)$ with $m(v)$ derivatives. Then we define

$$S_D := \sum_{i_1,\ldots,i_n=1}^{2s} \Big(\prod_{\substack{\text{external} \\ \text{line } v=1}}^{k} B^{m(v)}_{i_{d(v)}}(p_v) \Big) \Big(\prod_{\substack{\text{internal} \\ \text{line } x}} B^{k(x),l(x)}_{i_{i(x)},i_{j(x)}} \Big) \Big(\prod_{\substack{\text{vertex} \\ j=1}}^{n} \lambda^{(h_j)}_{\alpha(\mu_j),i_j} \Big).$$

Π_D is the inverse symmetry factor of diagram D ([19], [20]).
The summation $\sum_{\text{diagrams } D}$ consists of all diagrams with k external lines fulfilling $l + \sum_{j=1}^{n} h_j = h$, where l is the number of loops.

Theorem 1a

For $(k, h) \in \mathbb{N}_0 \times \mathbb{N}_0 \setminus \{(0,0), (1,0), (2,0), (0,1)\}$, the Hermitean 1-matrix model correlation functions of order h and the free energy of order h are given by

$$W^{(h)}_k(p_1, \ldots, p_k) = \sum_{\text{diagrams } D} \Pi_D S_D.$$

Chapter 8

Deriving the correlator $W_0^{(h)}$ from lower order correlators

It is assumed that the statement of theorem 1*a* is true for $W_2^{(h-1)}$ and for all $W_1^{(j)}$ with $j = 1, \ldots, h-1$. The assertion is that the prefactors of the diagrams resulting from the loop equation are equal to the symmetry factors of the diagrams. The main idea of the proof is to avoid all complicated diagrams of $W_1^{(h)}$ generated in the loop equation (2.52) by the second, third or fourth term on the r.h.s. of eq. (5.10) and, instead, to prove theorem 1*a* directly for the free energy $\mathcal{F}^{(h)} = W_0^{(h)}$. Since $\mathcal{F}^{(h)}$ contains less diagrams than $W_1^{(h)}$, only some diagrams of $W_1^{(h)}$ generated by the first term on the r.h.s. of eq. (5.10) have to be inspected to obtain all diagrams of $\mathcal{F}^{(h)}$ (with the exception of the diagram with one vertex of topological index h).

In the following, the field theory method for calculating symmetry factors, used in eqs. (4.10), (5.18), (5.22), (5.26), (5.34) (5.38), (5.49) and (5.66), is generalized. Let $m_\mu(D)$ be the multiplicity of vertices with structure μ in diagram D. Let $R(D)$ be the set of all vertex structures in a diagram D. $\alpha_i(\mu)$ is the number of emanating lines with a i-th derivative in a vertex with the structure μ. The inverse symmetry factor Π_D can be calculated by

$$\Pi_D = \frac{1}{c_D d_D}\, \pi_D$$

$$\text{with} \quad c_D = \prod_{\mu \in R(D)} m_\mu(D)!, \qquad\qquad d_D = \prod_{j=1}^{n} \alpha(\mu_j)!$$

$$\text{and} \quad \pi_D = \left\langle 0 \left| \varphi(p_1) \ldots \varphi(p_k) \sum_{i_1,\ldots,i_n=1}^{2s} \prod_{j=1}^{n} \left(\lambda^{(h_j)}_{\alpha(\mu_j),i_j} \varphi_{i_j}^{\alpha(\mu_j)} \right) \right| 0 \right\rangle_D \quad \frac{1}{S_D}. \tag{8.1}$$

$\langle 0|\ldots|0\rangle_D$ only contains the part of $\langle 0|\ldots|0\rangle$ belonging to diagram D. π_D as defined above denotes the number of possible pairings of the fields in eq. (8.1) which lead to diagram D. The product of the Gell-Mann-Low factorials c_D applies in this general form also to the case where two different couplings of the same $\mathcal{L}_k^{(h)}$ appear in the diagram. Within the diagram D, one edge could be equivalent to another edge and therefore the number of equivalence classes of edges in D could be smaller than the number of edges.

An example of the method used to assure that the field theory produces the same weights of the diagrams as those produced by the matrix model is given in figure 8.1.
Consider the diagram A from $\mathcal{F}^{(h)} = \mathcal{F}^{(5)}$, which is depicted on the l.h.s. of figure 8.1. Its prefactor, $\frac{1}{144}$, is determined via the matrix model method and via the field theory method. One of the several diagrams or diagram pairs from $W_1^{(4)}$ corresponding to diagram A is chosen by cutting one edge of A. This diagram, where p_1 is attached to the left free end and p_2 to the right free end, is denoted B. The diagram resulting from the interchange of p_1 and p_2 in B is denoted B'. A calculation of the symmetry factor of the diagram by the field theory method, i.e. counting the number of possible Wick contractions of the expression

$$\left\langle 0\left|\varphi(p_1)\varphi(p_2)e^{\sum_{i=1}^{2s}\mathcal{L}(a_i)}\right|0\right\rangle \tag{8.2}$$

leading to diagram B, results in $\frac{1}{36}$. By the induction assumption, the matrix model correlator at order $h-1=4$ has the same prefactor. The application of the loop equation from the matrix model in form of eqs. (2.52) and (5.10) to the contributions of B and B' leads to a prefactor of $\frac{1}{36}$ of the diagram C from $W_1^{(4)}$. By taking into account the fact that the loop operator can act on 4 equivalent edges in A to obtain C, the prefactor of A is determined to be $\frac{1}{144}$ by the matrix model method. For the field theory method, the counting of possible Wick contractions in the expression

$$\left\langle 0\left|e^{\sum_{i=1}^{2s}\mathcal{L}(a_i)}\right|0\right\rangle \tag{8.3}$$

leading to diagram A gives $\frac{1}{144}$. Another example, where a different edge of diagram A is cut, is represented in figure 8.3. The procedure demonstrated in these examples is generalized for the proof.
In $\mathcal{F}^{(h)}$ there is only one diagram with a vertex of topological index h (e.g., the first diagram in the first line of figure 5.10). This diagram of the field theory gives a priori by eq. (6.3) the correct matrix model contribution.

Consider a diagram A from $\mathcal{F}^{(h)}$ which does not contain a vertex of topological index h. Choose one edge of A which is cut.

8.1 Case 1

The cutting procedure produces one diagram B from $W_2^{(h-1)}$ which is transformed into A by connecting the two external legs.

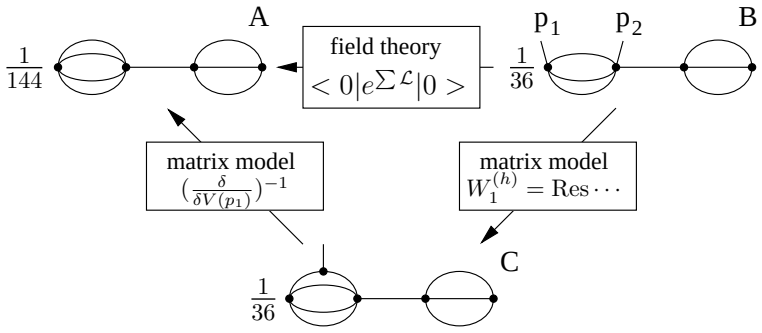

Figure 8.1: Example 1 for determining the prefactor of diagram A. All vertices are of topological index 0.

The prefactor Π_B of diagram B is known according to the induction assumption. It is possible that the exchange of external legs creates a second diagram B' which is different to B. In this case, $u = 2$. However, if B' is identical to B, then $u = 1$. The loop equation (eq. (2.52)) is applied to diagram B (and diagram B'). Then the first term on the r.h.s. of eq. (5.10), $1/2 \cdot B_{j,i}^{f,0} \cdot (B_i^0(p)/y_{1,i}) \cdot B_{i,k}^{0,g}$, gives rise to a diagram C from $W_1^{(h)}$. Since C cannot be created from other diagrams and, in the recursion formula, a multiplication with $1/2$ occurs, the prefactor of C is given by $\Pi_C = \frac{1}{2} u \Pi_B$.
The external leg of C is rooted in a vertex of index zero with 3 emanating lines. C can only have been created by Δ_7 from a diagram of $\mathcal{F}^{(h)}$. This diagram must have been A. Let v be the number of edges in the equivalence class of the edge which is cut. Then C can be created by Δ_7 from A in v different ways. The matrix model calculation yields $\Pi_C = v \Pi_A$ and hence $\Pi_A = \frac{u}{2v} \Pi_B$.
In the following, the quotient Π_A / Π_B is investigated in the field theory language. The specific example of figure 8.1 is generalized for the proof. In

figure 8.2 one special contraction of diagram A is given and compared to four corresponding special contractions from diagram B.

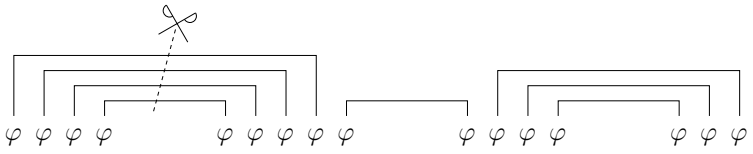

Figure 8.2: One contraction of A corresponds to four contractions of B, i. e. $\pi_B = 4\pi_A$. Each of the four equivalent edges can be cut and replaced by contracting the left open end to $\varphi(p_1)$ and the right open end to $\varphi(p_2)$.

In this way, each of the π_A contractions of A corresponds to 4 contractions of B: $\pi_B = 4\pi_A$. The generalization of this formula for v equivalent edges in A is $\pi_B = v\pi_A$.
If the interchange $\varphi(p_1) \leftrightarrow \varphi(p_2)$ in B does not give a new diagram B' different from B, then for every contraction in A there are two in B: $\pi_B = 2\pi_A$. Combining both equations leads to $\pi_B = \frac{2}{u}v\pi_A$. $c_B = c_A$ and $d_B = d_A$ imply that $\Pi_B = \frac{1}{c_B d_B}\pi_B = \frac{1}{c_A d_A}\frac{2}{u}v\pi_A = \frac{2}{u}v\Pi_A$.

8.2 Case 2

The cutting procedure produces two diagrams B_1 and B_2.

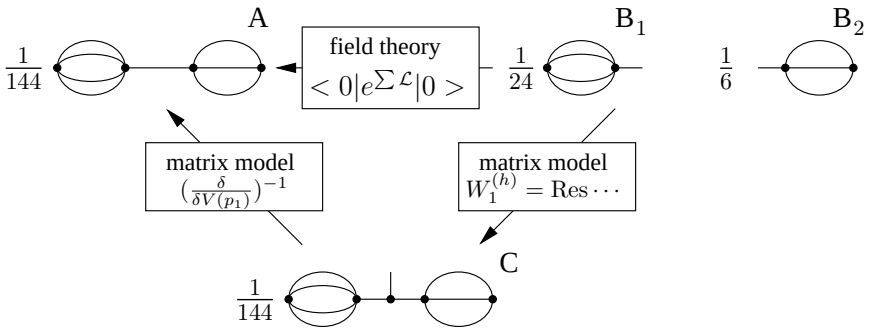

Figure 8.3: Example 2 for determining the prefactor of diagram A for the case where the diagram splits in two parts.

There is a $j \in \{1, \ldots, h-1\}$, such that B_1 is a diagram from $W_1^{(j)}$ and

B_2 is a diagram from $W_1^{(h-j)}$. The loop equation (eq. (2.52)) is applied to the diagrams B_1 and B_2. Then the first term on the r.h.s. of eq. (5.10), $1/2 \cdot B^{f,0}_{j,i} \cdot (B^0_i(p)/y_{1,i}) \cdot B^{0,g}_{i,k}$, gives rise to a diagram C from $W_1^{(h)}$. The diagram C does not receive additional contributions from $W_2^{(h-1)}$ in eq. (2.52) for the following reasons. The diagrams generated by the first term on the r.h.s. of eq. (5.10) do not break in two parts in the cutting procedure, whereas the other terms on the r.h.s. of eq. (5.10) produce a non-zero topological index at the external leg.
For $j \neq h/2$, the diagram C appears twice in the loop equation summation $\sum_{m=1}^{h-1} W_1^{(m)} W_1^{(h-m)}$. For $j = h/2$ and $B_1 \neq B_2$, the situation does not change. However, for $B_1 = B_2$, the diagram C only appears once. Let $u = 2$ for $B_1 \neq B_2$ and $u = 1$ for $B_1 = B_2$. Since in the first term of the recursion formula (eq. (5.10)) one multiplies with $1/2$, this gives $\Pi_C = \frac{u}{2} \Pi_{B_1} \Pi_{B_2}$. The external leg of C is connected to a vertex of topological index zero with 3 emanating lines. C can only have been created by the action of Δ_7 on a diagram of $\mathcal{F}^{(h)}$. This diagram must be diagram A. Let v be the number of elements in the equivalence class of the edge which is cut. Then C can be deduced from A in v different ways. This matrix model calculation yields $\Pi_C = v \Pi_A$ and hence $\Pi_A = \frac{u}{2v} \Pi_{B_1} \Pi_{B_2}$.
In the following, the quotient between Π_A and $\Pi_{B_1} \Pi_{B_2}$ is investigated in the field theory language.
The specific example of figure 8.3 is generalized for the proof.
Since in A two vertices of the same vertex structure (topological index zero and four emanating edges without derivatives) appear and only one is part of B_1, there are $\binom{2}{1}$ more possible ways to contract in B than in B_1 and B_2. In general, this factor is $\Pi_{\mu \in R(A)} \binom{m_\mu(A)}{m_\mu(B_1)}$. If $B_1 = B_2$ then this number is reduced by $\frac{1}{2}$ because the assignment of vertices to B_1 gives the same contractions in A as the assignment of the complementary vertices to B_1. If the edge which is cut in A is one of v equivalent edges in A then the number of contractions $\pi_{B_1} \cdot \pi_{B_2}$ is enhanced by a factor v. This gives in total $v \pi_A = \frac{u}{2} \Pi_{\mu \in R(A)} \binom{m_\mu(A)}{m_\mu(B_1)} \pi_{B_1} \pi_{B_2}$. The relation of the Gell-Mann-Low factorials is $\frac{c_A}{c_{B_1} c_{B_2}} = \Pi_{\mu \in R(A)} \binom{m_\mu(A)}{m_\mu(B_1)}$ and hence $\Pi_A = \frac{u}{2v} \Pi_{B_1} \Pi_{B_2}$.

This closes the proof by induction on h.

Chapter 9

Deriving the $(k+1)$-point correlator $W_{k+1}^{(h)}$ from the k-point correlator $W_k^{(h)}$

It is assumed that the statement of theorem $1a$ is correct for a certain h and k. In this chapter, we show that theorem $1a$ is also true for h and $k+1$.

To prove the induction step from k to $k+1$, two assertions have to hold: the prefactor of any diagram A from $W_{k+1}^{(h)}$ arising from the action of the loop operator must be equal to the inverse symmetry factor of diagram A which is determined by counting Wick contractions. Secondly, the vertex factor emerging at the new vertex from the action of the loop operator must be equal to the coupling constant of the field theory defined in eq. (7.1). Provided the induction assumption holds for any diagram B from $W_k^{(h)}$, the former assertion is true if the ratio Π_A/Π_B calculated with the field theory method is equal to the ratio Π_A/Π_B calculated with the loop operator method.

Let A be a diagram of $W_{k+1}^{(h)}$.

9.1 Case 1

The leg p_{k+1} emanates in diagram A from a vertex with a vertex structure $\mu = (0,(3,0))$.

Only the action of Δ_7 or Δ_4 on diagrams of $W_k^{(h)}$ with the same number of loops as in A and one vertex less than A can have generated this diagram. The multiplicity of the edge in the preimage diagram B, which is cut, is denoted v, i.e. the equivalence class of such an edge in B contains v elements. Let m_A be the number of vertices with $\alpha = (3, 0)$ and topological index 0 in A.
The number of contractions π_A in diagram A is larger than the number of contractions π_B in diagram B. One of the m_A vertices can be chosen for the new vertex, then 3 possibilities exist to choose one leg of that vertex for the connection to $\varphi(p_{k+1})$ and 2 more possibilities to assign the remaining two free legs of the new vertex to the contraction which is cut in diagram B. Eventually, since the new vertex can be inserted in each of the v equivalent individual contractions of the considered complete contraction of B we have

$$\frac{\pi_A}{\pi_B} = m_A \cdot 3 \cdot 2 \cdot v. \tag{9.1}$$

The quotient of the Gell-Mann-Low factorials $c_B/c_A = 1/m_A$ and the quotient of the factorials from the definition of the Lagrangian $d_B/d_A = 1/3!$ result in

$$\Pi_A = v\Pi_B, \tag{9.2}$$

which is also predicted by the action of Δ_7 or Δ_4 in the matrix model calculation.
The emerging vertex factor at the new vertex is $1/y_1$, which is exactly the definition of $\lambda^{(0)}_{(3,0)}$ in eq. (7.1).

9.2 Case 2

The leg p_{k+1} has at least one derivative.

Only the action of Δ_2 on diagrams of $W_k^{(h)}$ with the same number of loops as in A and the same number of vertices can have generated the diagram A. The structure of the vertex connected to p_{k+1} is denoted $\mu_A = (h_0, \alpha)$ and the number of derivatives at the leg p_{k+1} is $r > 0$. Let m_A be the number of vertices with structure μ_A in A. Let m_B be the number of preimage vertices in B with the same structure, of which v are equivalent.

The number of contractions π_A in diagram A is compared to the number of contractions π_B in diagram B. The interchange of one of the m_B vertices in

B with the structure of the preimage vertex leads to m_B different complete contractions which give rise (for $m_A = \alpha_r = v = 1$) to only one contraction for diagram A. Similarly, if $m_A > 1$ then the number of contractions in A is reduced by the factor m_A in comparison to the contractions of B. Additionally, the number of contractions in A is enhanced by choosing one of v equivalent vertices and one of α_r legs for p_{k+1}:

$$\frac{\pi_A}{\pi_B} = \frac{m_A}{m_B} \cdot \alpha_r \cdot v. \tag{9.3}$$

The quotient of the Gell-Mann-Low factorials $c_B/c_A = m_B/m_A$ and the quotient of the factorials from the definition of the Lagrangian $d_B/d_A = 1/\alpha_r$ result in

$$\Pi_A = v\Pi_B, \tag{9.4}$$

which is also predicted by the action of Δ_2 in the matrix model calculation.

The vertex factor of the new vertex emerges from the action of Δ_2 on the diagram with the old vertex. Since in the definition of $\lambda_\alpha^{(h_0)}$ the remnants of Δ_1 and Δ_2 are used, this gives the correct vertex factor of eq. (7.1).

9.3 Case 3

The leg p_{k+1} in diagram A has no derivative and is rooted at a vertex with vertex structure $\mu \neq (0, (3, 0))$.

In contrast to the other cases, in this case, the new diagram emerges from different parts (Δ_1, Δ_3 and $\Delta_{5/6} = \Delta_5 + \Delta_6$) of the loop operator. Therefore the assertion that the new vertex factor is described by eq. (7.1) is closely related to the different symmetry factors of the preimage diagrams.
There is at most one preimage diagram which becomes diagram A after action of Δ_1. This is denoted as B_0. Each external or internal line (apart from the leg p_{k+1} itself) emanating from the vertex connected with p_{k+1} gives possibly one further preimage diagram, which transforms under the action of Δ_3 or $\Delta_{5/6}$ to diagram A. In A, the outgoing external and internal legs emanating from the vertex connected to p_{k+1} are named arbitrarily, with $f = 1, \ldots, n$, and their derivatives are denoted as $r_1, \ldots, r_n$ respectively.
If $r_f = 0$ then no preimage diagram B_f associated to leg f exists. This kind of 'missing diagram' does not present large difficulties in the computation of the new vertex factor of A, because in the consideration of a vertex consisting exclusively of external legs, Δ_3 can not act on such a leg without derivative

as $\Delta_{5/6}$ can not act on f. To describe the second kind of 'misssing diagrams' we define δ to be the number of diagrams from $B_1, \ldots, B_n$ which are equal to B_f. If $\delta > 1$, there is only one preimage diagram for δ legs, rather than one for each leg.

The following notation will be used. The number of vertices in A with the same structure as the vertex connected to p_{k+1} is denoted m_A. The structure of the vertex connected to p_{k+1} is defined as $\mu_A = (h_0, \alpha)$ and γ is defined as the number of possible ways to apply Δ_5 or Δ_3 to B_f to obtain A.

9.3.1 Symmetry factors of the diagrams B_0 and A

Let the number of possible ways to apply $\Delta_1(p_{k+1})$ to B_0 to obtain A be v. This is the number of equivalent preimage vertices. Let m_B be the number of vertices with the structure $(h_0, (\alpha_0 - 1, \alpha_1, \alpha_2, \ldots))$ in B_0.
The number of contractions π_A in diagram A is compared to the number of contractions π_{B_0} in diagram B_0. The interchange of one of the m_B vertices in B with the structure of the preimage vertex leads to m_B different complete contractions which give rise (for $m_A = \alpha_0 = v = 1$) to only one contraction for diagram A. Similarly, if $m_A > 1$ then the number of contractions in A is reduced by the factor m_A relative to the number of contractions of B_0. Additionally, the number of contractions in A in enhanced by choosing one of v equivalent vertices and one of α_0 legs for p_{k+1}:

$$\frac{\pi_A}{\pi_{B_0}} = \frac{m_A}{m_B} \cdot \alpha_0 \cdot v. \tag{9.5}$$

The quotient of the Gell-Mann-Low factorials $c_B/c_A = m_B/m_A$ and the quotient of the factorials from the definition of the Lagrangian $d_B/d_A = 1/\alpha_0$ result in

$$\Pi_A = v\Pi_{B_0} \tag{9.6}$$

which is also predicted by the action of Δ_1 in the matrix model calculation.

9.3.2 Symmetry factors of the diagrams B_f with $f > 0$ and A

Let v_A be the number of elements in the equivalence class of edge f in A. The number of derivatives at edge f in diagram A is r (also denoted r_f) at the end of edge oriented towards p_{k+1}. The vertex structure of the vertex

connected to p_{k+1} is denoted μ_A and the structure of the preimage vertex in B_f is $\mu_B = (h_0, \beta)$ with $\beta_i = \alpha_i - \delta_{i,0} + \delta_{i,r-1} - \delta_{i,r}$. Then we define $m_A = m_{\mu_A}(A)$ and $m_B = m_{\mu_B}(B_f)$. Let $\hat{f}$ be one edge in B_f with $r_f - 1$ derivatives which transforms under the action of Δ_3 or $\Delta_{5/6}$ to the edge f in diagram A. The number of elements in the equivalence class of edge $\hat{f}$ in B_f is denoted v_B.

The number of contractions π_A in diagram A is compared to the number of contractions π_B in diagram B_f. The vertex connected to p_{k+1} in diagram A is one out of a total of m_A vertices. In diagram B_f, this vertex is replaced by a vertex with the structure μ_B, which is one out of a total of m_B vertices. From the choice of the vertex in A or B_f the factor m_A/m_B appears in the relation of π_A to π_B. At this vertex, the leg p_{k+1} can be connected to one of α_0 legs without derivatives, which gives rise to the factor α_0 in the comparison of the contractions. For the same reason, the connection of the edge f to the vertex leads to a factor α_r. On the other hand, the connection of the edge $\hat{f}$ to the preimage vertex with the structure μ_B leads to a factor $1/\beta_{r-1}$.

If the edge f in A is equivalent to another edge in A or the edge $\hat{f}$ is equivalent to another edge in B_f or the edge f connects a vertex with itself then the relation γ/δ is also part of the comparison of contractions. γ, as can be read from the definition, is equal to v_B or $2v_B$, where the latter occurs if and only if the edge f connects a vertex with itself and the number of derivatives at the other end of this edge is equal to $r - 1$. δ, as can be read from the definition, is equal to v_A or $2v_A$, where the latter occurs if and only if edge f connects a vertex with itself and the number of derivatives at the other end of this edge is equal to r. The enlargement of the number of equivalent edges by a factor 2 in these special examples reflects the fact that, in the contractions for each equivalent edge, 2 legs instead of 1 leg of that vertex are affected. This gives, in total,

$$\frac{\pi_A}{\pi_{B_f}} = \frac{m_A}{m_B} \frac{\alpha_0 \alpha_r}{\beta_{r-1}} \frac{\gamma}{\delta}. \tag{9.7}$$

The quotient of the Gell-Mann-Low factorials $c_B/c_A = m_B/m_A$ and the quotient of the factorials from the definition of the Lagrangian $d_B/d_A = \beta_{r-1}/(\alpha_0 \alpha_r)$ result in

$$\Pi_A = \frac{\gamma}{\delta} \Pi_{B_f}. \tag{9.8}$$

In the loop operator determination of the relation of $\frac{\Pi_{B_f}}{\Pi_A}$, one has to consider, on the one hand, that there are γ possible ways to apply Δ_3 or Δ_5 to

the diagram B_f and on the other hand that the number of diagrams in comparison to a one-vertex calculation with exclusively external legs is lowered by a factor $1/\delta$. The matrix model calculation therefore yields

$$\Pi_A = \frac{\gamma}{\delta}\Pi_{B_f}, \tag{9.9}$$

which coincides with the field theory calculation from eq. (9.8).

9.3.3 New vertex factor

The definition of the vertex factor is based on Δ_1 and Δ_2, but it was shown in section 3.6 that the vertex factors of the diagrams with only 1 vertex without internal lines are correctly described by eq. (7.1)—this includes the action of Δ_3. We compare the action of the loop operator on the preimage diagrams leading to the vertex connected to p_{k+1} in A to the case in which the loop operator acts on a vertex of the same structure with solely external legs. No difference occurs for the action of Δ_3 to the external lines. The action of $\Delta_{5/6}$ on the internal lines can be regarded as an action of Δ_3 on additional external lines. The contribution of B_0 to the new vertex factor is—relative to the corresponding 1-vertex diagram—enhanced by a factor $v\Pi_{B_0}$. The contribution of B_f to the new vertex factor is—relative to the corresponding contribution to the 1-vertex diagram—enhanced by a factor $\gamma\Pi_{B_f}$, where γ is equal to the number of possible ways to apply Δ_3 or Δ_5 to B_f to obtain A. Instead of δ preimage diagrams for the 1-vertex diagram there is only one. Consequently, the new vertex factor arises in this complicated vertex in exactly the same way as in 1-vertex diagrams if the equation $v\Pi_{B_0} = \gamma\Pi_{B_f}/\delta$ is valid. The combination of eqs. (9.6) and (9.9) from the previous paragraph establishes this condition and hence the new vertex is described by eq. (7.1).

This closes the proof by induction on k.

9.4 Combining the induction on h with the induction on k to obtain correlators of all orders

Starting from $W_3^{(0)}$ and $W_1^{(1)}$ (shown in (3.23) and (4.13) to be described by the field theory) one applies the induction on k from this chapter to prove

that theorem $1a$ holds for $W_k^{(0)}$ with $k \geq 3$ and $W_k^{(1)}$ with $k \in \mathbb{N}$. From the application of the induction on h from chapter 8, it follows that theorem $1a$ also holds for $W_0^{(2)} = \mathcal{F}^{(2)}$. The application of the induction on k reveals that theorem $1a$ holds for all $W_k^{(2)}$ with $k \in \mathbb{N}_0$. The $(h-2)$-fold alternating use of the inductions on h and k proofs that $W_k^{(h)}$ with $h \geq 3$ and $k \in \mathbb{N}_0$ is described by a field theory. This concludes the proof of theorem $1a$, and, thereby, the proof of theorem 1.

Chapter 10

Conclusion

We have found a reformulation of the Hermitean 1-matrix model as an effective field theory. The reformulation was proved to be valid to all orders in the genus expansion. This was achieved by comparing the prefactors of all terms arising from the loop operator with the symmetry factors of the corresponding diagrams and finding full agreement. The spectral curve of the matrix model is associated with a Riemann surface. The scalar field propagates on this hyperelliptic Riemann surface with multiple self-interactions of the scalar field taking place at the branch points.
In addition to the correlation functions, the free energy was calculated and incorporated into the statement of the theorem. Furthermore, the procedure to obtain coupling constants of a given topological index from the coupling constants of lower indices, was condensed into one equation. This is the loop equation of the effective field theory.
It was solved to the tenth order and explicit expressions were given to the fifth order. Two methods of determining the free energy from the one point function were found. The second method inverts a part of the loop operator and gives rise to a simple integration. This second method does not, contrary to the first method, rely on results for the properties of the operator H obtained in [7].

There remain open questions. The effective field theory for the Hermitean 1-matrix model is found. Is there a similar effective field theory for other, more general matrix models? We believe the answer is yes.
If one could apply this field theory scheme to Complex Matrix Models one would perhaps gain the benefit of calculating the number of links of higher genus surfaces easily because the loop equation in the approach is relatively easy and one can explicitly calculate higher free energies [23].

The propagators and the vertex factors for a special number of cuts, e.g. two, can be determined.
The Weil-Petersson volumes ([22], [30]) can be calculated in terms of the field theory.

Appendix A

This paragraph contains a formula for the number of terms in the Lagrangian $\mathcal{L}_k^{(h)}$:

$$N(k,h) := |M_k^{(h)}| = \text{number of terms in } \mathcal{L}_k^{(h)}.$$

The number $P(m,r)$ of multi-indices $\alpha = (\alpha_1, \ldots, \alpha_m) \in (\mathbb{N}_0)^m$ fulfilling $\sum_{j=1}^m j\alpha_j = m$ and $\sum_{j=1}^m \alpha_j = r$ can be computed [23] with

$$\sum_{m=0}^{\infty}\sum_{r=0}^{\infty} P(m,r) q^m x^r = \prod_{n=1}^{\infty}\left(\frac{1}{1-xq^n}\right). \tag{1}$$

Comparing to the conditions for $M_k^{(h)}$ (chapter 7) one finds a summation over m and a summation over $r = k - \alpha_0$:

$$N(k,h) = \sum_{m=0}^{k+3h-3}\sum_{r=0}^{k} P(m,r) = \sum_{m=0}^{k+3h-3}\sum_{r=0}^{k}\left(\frac{1}{m!}\frac{\partial^m}{\partial q^m}\Big|_{q=0}\right)\left(\frac{1}{r!}\frac{\partial^r}{\partial x^r}\Big|_{x=0}\right)\prod_{n=1}^{\infty}\left(\frac{1}{1-xq^n}\right).$$

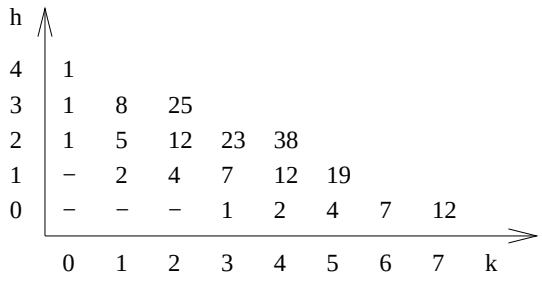

Figure 1: Number of terms in the Lagrangian $\mathcal{L}_k^{(h)}$

Bibliography

[1] E. P. Wigner, *On the statistical distribution of the width and spacings of nuclear resonance levels,* Proc. Cambridge Phil. Soc. 47 (1951) 790

[2] E. Brezin, C. Itzykson, G. Parisi and J.B. Zuber, *Planar Diagrams,* Comm. Math. Phys. 59 (1978) 35

[3] J. Grossehelweg, *Rechnungen am 1-Matrixmodell,* diploma thesis, Bonn IB-2006-12 (2006)

[4] R. Flume, J. Grossehelweg, A. Klitz, *A Lagrangean formalism for Hermitean matrix models,* Nucl. Phys. B812 (2009) 322, arXiv:0805.3078 [hep-th]

[5] G. Akemann, *Higher genus correlators for the hermitian matrix model with multiple cuts,* Nucl. Phys. B482 (1996) 403

[6] B. Eynard, *Topological expansion for the 1-hermitian matrix model correlation functions,* JHEP 0411 (2004) 031

[7] L. Chekhov and B. Eynard, *Hermitian matrix model free energy: Feynman graph technique for all genera,* JHEP 0603 (2006) 014

[8] B. Eynard and N. Orantin, *Topological expansion of the 2-matrix model correlation functions: diagrammatic rules for a residue formula,* JHEP 0512 (2005) 034

[9] R. Dijkgraaf and C. Vafa, *Two Dimensional Kodaira-Spencer Theory and Three Dimensional Chern-Simons Gravity,* arXiv:0711.1932 [hep-th]

[10] L. Chekhov, A. Marshakov, A. Mironov and D. Vasiliev, *Complex Geometry of Matrix Models,* arXiv:hep-th/0506075

[11] H.E. Rauch, *Weierstrass points, branch points, and moduli of Riemann sufaces,* Comm. Pure Appl. Math. 12 (1959) 543

[12] L. Chekhov, B. Eynard, and N. Orantin, *Free energy topological expansion for the 2-matrix model,* JHEP 0612 (2006) 053

[13] B. Eynard and N. Orantin, *Invariants of algebraic curves and topological expansion,* arXiv:math-ph/0702045

[14] B. Eynard and N. Orantin, *Algebraic methods in random matrices and enumerative geometry,* arXiv:0811.3531 [math-ph]

[15] E. Brézin and J. Zinn-Justin, *Renormalization Group Approach to Matrix Models,* Phys. Lett. B288 (1992) 54

[16] S. Higuchi, C. Itoi, S. Nishigaki, N. Sakai, *Nonlinear Renormalization Group Equation for Matrix Models,* Phys. Lett. B318 (1993) 63-72

[17] S. Higuchi, C. Itoi, S. Nishigaki, N. Sakai, *Renormalization group flow in one- and two-matrix models,* Nucl. Phys. B 434 (1995) 283-318

[18] S. Higuchi, C. Itoi, S. M. Nishigaki, N. Sakai, *Renormalization group approach to multiple-arc random matrix models,* Phys. Lett. B398 (1997) 123-129

[19] M. Peskin, D. Schroeder, *An Introduction to Quantum Field Theory,* Westview Press, Boulder (1995)

[20] G. Sterman, *An introduction to quantum field theory,* Cambridge University Press, Cambridge (1993)

[21] W.T. Tutte, *A census of planar maps,* Can. J. Math. 15 (1963) 249

[22] B. Eynard, N. Orantin, *Weil-Petersson volume of moduli spaces, Mirzakhani's recursion and matrix models* arXiv:0705.3600 [math-ph]

[23] J.B. Zuber, private communication

[24] P. Di Francesco, P. Ginsparg and J. Zinn-Justin, *2D gravity and random matrices,* Phys. Rept. 254 (1995) 1

[25] B. Eynard, *Large N expansion of the 2-matrix model, multicut case,* arXiv:math-ph/0307052

[26] M. Kontsevich, *Intersection theory on the moduli space of curves and the matrix Airy function,* Comm. Math. Phys. 147 (1992) 1

[27] M. Mariño, *Open string amplitudes and large order behavior in topological string theories,* JHEP 0803 (2008) 060

[28] B. Eynard, M. Mariño and N. Orantin, *Holomorphic anomaly and matrix models,* JHEP 0706 (2007) 058

[29] V. Bouchard, A. Klemm, M. Mariño and Sara Pasquetti, *Remodeling the B-model,* arXiv:0709.1453 [hep-th]

[30] B. Eynard, *Recursion between Mumford volumes of moduli spaces,* arXiv:0706.4403 [math.AG]

[31] V. Bouchard and M. Mariño, *Hurwitz numbers, matrix models and enumerative geometry,* arXiv:0709.1458 [math.AG]

[32] A. Klitz, in preparation

[33] L. Chekhov, *Genus one correlation to multi-cut matrix model solutions,* Theor. Math. Phys. 141 (2004) 1640

[34] T. Guhr, A. Müeller-Groeling, H. A. Weidenmüller, *Random matrix theories in quantum physics: common concepts,* Phys. Rep. 299 (1998) 189 [arXiv:cond-math/9707301]

[35] M. L. Mehta, *Random Matrices, Third Edition,* Elsevier Academic Press, Amsterdam (2004)

[36] A. A. Migdal, *Loop Equations and 1/N expansion,* Phys. Rep. 102 (1983) 195

[37] J. Ambjørn, J. Jurkiewicz, Y. Makeenko, *Multiloop correlators for two-dimensional quantum gravity,* Phys. Lett. B 251 (1990) 517

[38] J. Ambjørn, L. Chekhov, Y. Makeenko, *Higher Genus Correlators from the Hermitian One-Matrix Model,* Phys. Lett. B282 (1992) 341 [arXiv:hep-th/9203009]

[39] J. Ambjørn, L. Chekhov, C. F. Kristjansen, Y. Makeenko, *Matrix Model Calculations beyond the spherical limit,* Nucl. Phys. B 404 (1993) 127 [arXiv:hep-th/9302014]

[40] I. K. Kostov, Conformal Field Theory Techniques in Random Matrix models, arXiv:hep-th/9907060

[41] J. Ambjørn, *Quantization of geometry,* Lectures presented at the 1994 Les Houches Summerschool 'Fluctuating Geometries in Statistical Mechanics and Field Theory', [arXiv:hep-th/9411179]

[42] J. Jurkiewicz, *Regularisation of one-matrix models,* Phys. Lett. B245 (1990) 178